



UFRGS
UNIVERSIDADE FEDERAL
DO RIO GRANDE DO SUL



**INSTITUTO DE BIOCIÊNCIAS
PROGRAMA DE PÓS-GRADUAÇÃO EM BIOLOGIA ANIMAL**

DARIO RUBEN FAUSTINO FUSTER

Revisão taxonômica de *Heptapterus mustelinus* (Valenciennes, 1835) (Siluriformes:
Heptapteridae)

PORTO ALEGRE
2017

DARIO RUBEN FAUSTINO FUSTER

Revisão taxonômica de *Heptapterus mustelinus* (Valenciennes, 1835) (Siluriformes:
Heptapteridae)

Dissertação apresentada ao Programa de Pós-graduação em Biologia Animal, Instituto de Biociências, Universidade Federal do Rio Grande do Sul, como requisito para obtenção do título de Mestre em Biologia Animal.

Área de Concentração: Biologia Comparada

Orientador: Prof. Dr. Luiz Roberto Malabarba

Co-orientador: Prof. Dr. Flavio A. Bockmann

PORTE ALEGRE
2017

DARIO RUBEN FAUSTINO FUSTER

Revisão taxonômica de *Heptapterus mustelinus* (Valenciennes, 1835) (Siluriformes:
Heptapteridae)

Aprovada em ____ de _____ de ____.

BANCA EXAMINADORA

Dr/a. Avaliador/a 1

Dr/a. Avaliador/a 2

Dr/a. Avaliador/a 3

Se andarmos apenas por caminhos já traçados, chegaremos apenas aonde os outros chegaram (A. G.Bell)

Agradecimentos

Em primeiro lugar gostaria de agradecer a meu orientador, Luiz R. Malabarba pela oportunidade e apoio de realizar o mestrado na Universidade Federal do Rio Grande do Sul, pelas sugestões, recomendações, correções, opiniões e comentários na realização do meu projeto. Ao meu coorientador Flavio A. Bockmann, pelas críticas e apoio que apesar da distância sempre estava disposição para resolver minhas dúvidas. A Vanessa Meza parceira, amiga e cúmplice pelo seu carinho e por sempre estar presente apoiando-me incondicionalmente.

Ao Conselho Nacional de Desenvolvimento Científico e Tecnológico pela bolsa de mestrado.

Aos meus colegas do Laboratório de Ictiologia, pela acolhida, convivência e troca de experiência durante estes dois anos que fizeram meus dias fáceis com suas recomendações, sugestões e apoio na UFRGS e fora dela. Ao Junior meu amigo e parceiro da vida Ictiológica, obrigado pela ajuda, sugestões, críticas, intercâmbio de informações e largas conversas. A Juliana e Juliano pela assistência na coleção e as caronas para ir a casa. Ao Rafael, Tiago e Priscilla pelo auxílio e ensino durante a aprendizagem na Molecular e peixes. Aos amigos do laboratório de peixes do MCP, pela acolhida e convivência durante minha visita.

Aos curadores e técnicos das coleções ictiológicas pela disponibilidade do material examinado que esta sob seus cuidados. Ao Carlos Lucena (MCP); Mario de Pinna, Aléssio Datovo e Oswaldo Oyakawa (MZUSP); Paulo Buckup e Marcelo Brito (MNRJ), Flavio Bockmann (LIRP). Ao Gastón Aguilera e Juan Marcos Mirante (CIFML).

Aos professores e colegas do Programa de Pós-graduação em Biologia Animal por fazer as disciplinas amenas.

Aos colegas e amigos do departamento de Ictiologia do Museo de Historia Nacional de San Marcos-Lima. Ao Professor Hernán Ortega pelos conselhos e incentivo para fazer o mestrado.

A minha família, pela compreensão durante minha ausência e apoio incondicional dos meus pais e irmãos.

SUMÁRIO

SUMÁRIO.....	- 5 -
RESUMO.....	- 6 -
ABSTRACT	- 6 -
INTRODUÇÃO	- 7 -
OBJETIVOS	- 11 -
Geral.....	- 11 -
Específico.....	- 11 -
Referências Bibliográficas	- 12 -
TÍTULO – Taxonomic revision of the <i>Heptapterus mustelinus</i> species complex (Siluriformes: Heptapteridae).....	- 14 -
Abstract.....	- 15 -
Introduction	- 17 -
Material and Methods.....	- 18 -
Results	- 23 -
Key to species of <i>Heptapterus</i>	- 23 -
Discussion	- 48 -
References	- 53 -
ANEXOS	- 58 -
CONSIDERAÇÕES FINAIS	82

RESUMO

As populações de *Heptapterus mustelinus* do rio Uruguai, sistema da Laguna dos Patos e os rios dos sistemas costeiros do sul do Brasil e Uruguai foram revisados com dados morfológicos e moleculares. Duas novas espécies de *Heptapterus* foram reconhecidas. *Heptapterus* sp.n.A com distribuição restrita para o rio Pelotas na bacia do alto rio Uruguai. *Heptapterus* sp.n.B endêmica de tributários do rio Ibicuí na bacia do baixo rio Uruguai. As novas espécies distinguem-se do seu congênero mais próximo *H. mustelinus* pelo menor número de vértebras. Dados morfométricos e moleculares são congruentes no reconhecimento das duas espécies novas.

Palavras chaves: rio Uruguai, endemismo, *Heptapterus*, bagre, taxonomia.

ABSTRACT

The populations of *Heptapterus mustelinus* from the Uruguay River, laguna dos Patos system and the coastal streams of southern Brazil were reviewed with morphological and molecular data. Two new species of *Heptapterus* were recognized. *Heptapterus* sp.n.A with a restricted distribution to rio Pelotas, in the upper Uruguay River basin. *Heptapterus* sp.n.B endemic to tributaries of rio Ibicuí, in the lower Uruguay River basin. The new species are distinguished from its closest congener *H. mustelinus* by the lower number of vertebrae. Morphometric and molecular data are congruent to recognize the two new species.

Key words: Uruguay River, endemism, *Heptapterus*, catfish, taxonomy.

INTRODUÇÃO

A família Heptapteridae representa a quinta de maior riqueza dentro da ordem Siluriformes, com 211 espécies válidas distribuídas em 24 gêneros (Eschmeyer & Fong, 2017). A situação taxonômica da família foi confusa dentro da família Pimelodidae por muito tempo sendo que o primeiro trabalho que reconhece o grupo como monofilético foi realizado por Lundberg & McDade (1986), que trataram como um clado não nomeado dentro de Pimelodidae. Posteriormente, Lundberg *et al.* (1991a) formalmente denominaram o grupo como subfamília Rhamdiinae Bleeker (1862), ainda pertencente à família Pimelodidae. Esta subfamília foi elevada ao nível de família por de Pinna (1993), na tese de doutorado não publicada, sendo retificada por Silfvergrip (1996), que demonstrou a prioridade do nome Heptapterinae Gill (1861) sobre Rhamdiinae Bleeker (1862). Sob a denominação de Heptapteridae, Bockmann (1998) realizou uma análise filogenética da família, redefinindo e sugerindo 11 novos gêneros. No entanto, nenhum dos gêneros propostos foi formalmente descrito, apesar de alguns nomes serem usados inapropriadamente em inventários biológicos de fauna (e.g. Pitman *et al.*, 2011) ou por aquaristas.

Segundo Bockmann & Guazzelli (2003), a família Heptapteridae pode ser diagnosticada pela combinação dos seguintes caracteres: tamanho do corpo pequeno, geralmente 200 mm ou menor (exceto *Goeldiella*, *Pimelodella*, *Rhamdia*, *Rhamdioglanis*); pele desprovida de escamas ou escudos; canal láterosensorial cutâneo simples; narinas separadas e não portando barbillões; três pares de barbillões (maxilar e mentonianos interno e externo); nadadeira adiposa bem desenvolvida; nadadeira caudal extremamente bifurcada, recortada, arredondada ou lanceolada; membranas branquiais livres; margem orbital livre ou não e primeiro raio das nadadeiras dorsal e peitoral variando entre possuindo espinhos agudos até completamente flexível ou principalmente segmentados.

O gênero *Heptapterus*

O gênero *Heptapterus* foi proposto com a espécie tipo *Pimelodus mustelinus* por Bleeker (1858). Mees (1967) incluiu o gênero *Chasmocranus* como sinônimo júnior de *Heptapterus*. Mees (1974) definiu o gênero *Heptapterus* de acordo com os seguintes caracteres: corpo alongado e delgado, cabeça deprimida, ausência do espinho nas nadadeiras dorsal e peitoral, superfície superior da cabeça completamente coberta com

capa de tecido conectivo e pele grossa; comprimento dos barbillões curtos ou moderados, atingindo no máximo a base das nadadeiras ventrais, geralmente muito mais curto; olhos pequenos, em posição dorsal, sem bordas orbitais livres; dentes em bandas nas mandíbulas, com ou sem projeções pôstero-lateral, ausência de dentes no vómer e palatinos; nadadeira dorsal curta, sete raios da nadadeira dorsal (oito em uma espécie); nadadeira anal variando de oito para mais de 30 raios; nadadeira pélvica com seis raios, origem da nadadeira pélvica anterior ou posteriores da origem da nadadeira dorsal; nadadeira adiposa longa, amplamente ou estreitamente ligada com a nadadeira caudal, ou claramente separada da nadadeira caudal; nadadeira caudal de qualquer formato; baseado nessa diagnose ao gênero *Heptapterus* foram adicionados os gêneros *Imparales*, *Nemuroglanis*, *Medemichthys*, (sinônimo júnior de *Nemuroglanis*), *Nannoglanis*, *Pariolius* e *Phenacorhamdia*. *Heptapterus* foi reconhecido filogeneticamente pela primeira vez como um clado dentro da família Pimelodidae por Stewart (1986a). *Heptapterus* foi considerado como membro do clado *Nemuroglanis* por Ferraris (1988) baseado em quatro sinapomorfias: (1) *laminar portion of complex centrum transverse process, posterior to branched segment, is triangular and extends nearly to the lateral tip of fifth vertebral transverse process*; (2) *first dorsal-fin basal pterygiophore is inserted behind Weberian complex, usually above vertebrae 7 to 10*; (3) “*dorsal-fin spine*” is thin and flexible; (4) *dorsal-fin lock (= first dorsal spine or spinelet) absent*. Como resultado das considerações de Mees, *Heptapterus* continuava sendo não diagnosticável segundo Buckup (1988), que introduziu *Phreatobius* na sinonímia de *Heptapterus*. A posição do gênero *Heptapterus* como membro da subfamília Rhamdiinae e dentro do clado *Nemuroglanis* foi corroborado por Bockmann (1994) fornecendo mais 12 sinapomorfias para o subclado: (5) *pectoral-fin “spine” is thin and flexible for its distal half, rather than pungent*; (6) *mesocoracoid arch modified into a wide band*; (7) *two posterior proximal radials of pectoral fin are enlarged and flattened*; (8) *pectoral girdle delicate, with a short mesial contact line comprising only three weakly joined scapulo-coracoid dentations*; (9) *pointed process projected posteroventrally from the coracoid keel absent*; (10) *posterior chambers of swimbladder atrophied, conforming a bilobed, transversely aligned structure*; (11) *nasal bone long and weakly ossified*; (12) *ridges of neural arch of the fourth vertebra absent (which is more properly defined as neural arch of the fourth vertebra approximately straight, not covering the neural arch of the fifth vertebra and not giving rise to two divergent ridges that reach the anterior limbs of the transverse process of*

the fourth vertebra); (13) presence of a distinct deep medial notch which divides the posterior limb of the fourth transverse process into two divergent, approximately symmetrical, long arms; (14) tips of the parapophyses of anterior free vertebrae distally expanded and ventrally concave; (15) hemal and neural spines of the caudal vertebrae oriented at about 35° to the vertebral column axis; and (16) hemal and neural spines of the last free precaudal vertebrae robust.

O gênero *Heptapterus* atualmente apresenta 12 espécies válidas segundo Eschmeyer & Fong (2017), a saber: *Heptapterus bleekeri* Boeseman, 1953, *H. fissipinnis* Miranda Ribeiro, 1911, *H. mandimbusu* Aguilera, Benitez, Terán, Alonso & Mirande 2017, *H. mbya* Azpelicueta, Aguilera & Mirande, 2011, *H. multiradiatus* Ihering, 1907, *H. mustelinus* (Valenciennes, 1835), *H. ornaticeps* Ahl, 1936, *H. panamensis* (Bussing, 1970), *H. qenqo* Aguilera, Mirande & Azpelicueta, 2011, *H. stewarti* Haseman, 1911, *H. sympterygium* Buckup, 1988, e *H. tapanahoniensis* Mees, 1967.

Heptapterus mustelinus descrito por Valenciennes (1835) originalmente descrito como *Pimelodus mustelinus* tem a localidade tipo na bacia do rio da Prata e o material tipo não conhecido (Bockmann & Guazzelli, 2003) ou possivelmente no Muséum national d'Histoire naturelle (MNHN) sem especificar o lote (Ferraris, 2007).

Eigenmann & Eigenmann (1890 e 1891) identificaram dois espécimes de Maldonado, Uruguai, como *H. mustelinus*. Baseado somente na descrição publicada, Steindachner (1907) propõe uma nova espécie *H. eigenmanni* aos dois espécimes identificados por Eigemann & Eigenmann, considerando o alto número de raios na nadadeira anal (24) e o comprimento dos barbillões em relação ao comprimento da nadadeira peitoral como caracteres diagnósticos. Eigenmann (1917) cita os dois espécimes provisoriamente como *H. mustelinus*. Devincenzi (1942) questiona a validade do caráter comprimento do barbillão como diagnose, mas não consegue demonstrar a sinonímia das espécies com esse caráter, considerando o alto número de raios na nadadeira anal caráter que diagnostica *H. eigenmanni*. Os síntipos de *H. eigenmanni* foram examinados por Buckup (1988) mostrando que a população de Maldonado exibia algumas peculiaridades para ser *H. mustelinus*. Como Steindachner não selecionou o holótipo para *H. eigenmanni*; Buckup 1988 designou como lectótipo o lote MCZ 7597, espécime com 24 raios na nadadeira anal, citado erroneamente como MCZ 7579 (Buckup, 1988), e como paralectótipo o lote MCZ 6330, espécime com 23 raios na nadadeira anal, também erroneamente citado como MCZ 63330.

Após os aportes realizados por Buckup (1988), a maioria dos estudos com *H. mustelinus* baseia-se em comparações morfológicas com as espécies descritas recentemente para o gênero: *Heptapterus qenqo* Aguilera *et al.* (2011) e *Heptapterus mbya* Azpelicueta *et al.* (2011).

No presente trabalho foi realizada uma revisão taxonômica de *Heptapterus mustelinus* distribuídos amplamente no rio Uruguai, Sistema da Laguna dos Patos e rios costeiros do sul do Brasil, baseado *em* dados morfológicos e moleculares. Duas espécies novas são descritas, *Heptapterus* sp.n.A com distribuição restrita para o rio Pelotas e *Heptapterus* sp.n.B endêmica para o rio Ibicuí.

OBJETIVOS

Geral

- Revisão taxonômica de *Heptapterus mustelinus* com distribuição nas principais bacias do sul do Brasil (rio Uruguai, Sistema Laguna dos Patos e rios costeiros da região sul do Brasil).

Específicos

- Descrever as possíveis espécies novas do gênero com dados morfológicos e moleculares.
- Elaborar uma chave de identificação para as espécies do gênero *Heptapterus* nas bacias do sul do Brasil.

Referências Bibliográficas

- Aguilera, G., J. M. Mirande and M. de las M. Azpelicueta. (2011) A new species of *Heptapterus* Bleeker 1858 (Siluriformes: Heptapteridae) from the Río Salí basin, north-western Argentina. *Journal of Fish Biology*, 78 (1), 240–250.
- Azpelicueta, M. de las M., Aguilera G. and Mirande J. M. (2011) *Heptapterus mbya* (Siluriformes: Heptapteridae), a new species of catfish from the Paraná River basin, in Argentina. *Revue Suisse de Zoologie*, 118 (2): 319–327.
- Bockmann, F.A. (1994) Description of *Mastiglanis asopos*, a new pimelodid catfish from northern Brazil, with comments on phylogenetic relationships inside the subfamily Rhamdiinae (Siluriformes: Pimelodidae). *Proc. Biol. Soc. Wash.*, 107 (4), 760–777.
- Bockmann, F.A. (1998) Análise filogenética da família Heptapteridae (Teleostei: Ostariophysi: Siluriformes) e redefinição de seus gêneros. Unpublished Doctoral Dissertation. São Paulo, Universidade de São Paulo, 599.
- Bockmann, F. A., & Guazzelli, G. M. (2003). Family Heptapteridae (Heptapterids). *Checklist of the freshwater fishes of South and Central America. Porto Alegre: Editora da Pontifícia Universidade Católica do Rio Grande do Sul-EDIPUCRS*, 406-431.
- Buckup, P. A. (1988) The genus *Heptapterus* (Teleostei: Pimelodidae) in southern Brazil and Uruguay, with the description of a new species. *Copeia*, 1988 (3), 641–653.
- Devincenzi, G.J. (1942). Peces del Uruguay. II. Nuestra fauna ictiologica segun nuestras colecciones (continuaci6n). *An. Mus. Nac. Montevideo, Ser. 2*, 1(5): 139-294.
- Eigenmann, C. H. (1917) *Pimelodella* and *Typhlobagrus*. Memoirs of the Carnegie Museum, 5: 229-258.
- Eigenmann, C. H. & Eigenmann R. S. (1890) Preliminary notes on South American Nematognathi. II. *Proc. Calif. Acad. Sci., Ser. 2*, 2:28-58.
- Eigenmann, C. H. & Eigenmann R. S. (1891) A catalogue of the freshwater fishes of South America. *Proc. U.S. Nat. Mus.* 14:1-81.
- Eschmeyer, W. N., & Fong, J. (2017). Species by family/subfamily in the Catalog of fishes, electronic version (June 2017). San Francisco (California Academy of Sciences).

- Ferraris Jr, C. J. (1988). Relationships of the neotropical catfish genus *Nemuroglanis*, with a description of a new species (Osteichthyes: Siluriformes: Pimelodidae). *Proceedings of the Biological Society of Washington*, 101(3), 509-516.
- Ferraris, C. J. Jr. (2007) Checklist of catfishes, recent and fossil (Osteichthyes: Siluriformes), and catalogue of siluriform primary types. *Zootaxa*, 1418, 1–628.
- Gill, T. N. (1861). Synopsis of the genera of the sub-family of Pimelodinae. In *Proceedings of the Boston Society of Natural History* (Vol. 8, pp. 46-55).
- Lundberg, J.G., Bornbusch A.H. & Mago-Leccia F. (1991) *Gladioglanis conquistador* n. sp., from Ecuador with diagnoses of the subfamilies Rhamdiinae Bleeker and Pseudopimelodinae n. subf. (Siluriformes, Pimelodidae). *Copeia*, 1991(1), 190–209.
- Lundberg, J. G. & L. A. McDade. 1986. On the South American catfish *Brachyrhamdia imitator* Myers (Siluriformes, Pimelodidae), with phylogenetic evidence for a large intrafamilial lineage. *Notulae Naturae*, 463: 1-24.
- Mees, G. F. 1967. Freshwater fishes of Suriname: the genus *Heptapterus* (Pimelodidae). *Zoologische Mededelingen*, 42 (20): 215-229.
- Mees, G.F. 1974. The Auchenipteridae and Pimelodidae of Suriname (Pisces, Nematognathi). *Zool. Verh.* (Leiden), (132): 1–256, 1–15.
- Pinna, M. C. C. 1993. Higher-level phylogeny of Siluriformes, with a new classification of the order (Teleostei, Ostariophysi). New York, The City University of New York. 482 p. [Tese de doutorado não publicada]
- Pitman, N., Vriesendorp, C., Moskovits, D. K., Von May, R., Alvira, D., Wachter, T., ... & del Campo, Á. (Eds.). (2011). *Perú: Yaguas-Cotuhé*. Field Museum, Environment, Culture, and Conservation.
- Silvergrip, A. M. C. (1996). *A systematic revision of the Neotropical catfish genus Rhamdia (Teleostei, Pimelodidae)*. M. Sci (Doctoral dissertation, Thesis in Zoology, Stockholm University, Stockholm).
- Steindachner, F. (1907). Über einige Fischarten aus dem Flusse Cubatão in Staate Santa Catharina, bei Therezopolis (Brasilien). *Sitzungsberichte der Akademie der Wissenschaften, Wien*, 116(1), 475-92.
- Stewart, D. J. (1986). Revision of Pimelodina and description of a new genus and species from the Peruvian Amazon (Pisces: Pimelodidae). *Copeia*, 653-672.
- Valenciennes, A. (1834–39) Poissons [plates]. In: A. d'Orbigny. *Voyage dans l'Amérique méridionale*. 1–16.

**TÍTULO – Taxonomic revision of the *Heptapterus mustelinus* species complex
(Siluriformes: Heptapteridae)**

(Manuscrito a ser submetido para o periódico Zootaxa)

Taxonomic revision of *Heptapterus mustelinus* (Siluriformes: Heptapteridae)

Dario R. Faustino-Fuster¹, Flavio A. Bockmann² and Luiz R. Malabarba¹

¹UFRGS – Universidade Federal do Rio Grande do Sul, Programa de Pós-Graduação em Biologia Animal, Departamento de Zoologia.

² FFCLRP–LIRP – Universidade de São Paulo, Laboratório de Ictiologia de Ribeirão Preto, Departamento de Biologia.

Abstract

Neotropical freshwater catfish *Heptapterus mustelinus* from laguna dos Patos system, rio Uruguay drainage and Atlantic coastal streams of south Brazil and Uruguay are reviewed. *Heptapterus mustelinus* group is herein recognized based on morphological analyses, being represented by *H. mbya*, *H. qenqo*, *H. mustelinus*, and two new species *Heptapterus* sp.n.A and *Heptapterus* sp.n.B. *Heptapterus mustelinus* group can be distinguished from *H. bleekeri* and *H. tapanahoniensis* by the position of the adipose-fin origin, located anterior to anal-fin origin (vs. adipose-fin origin, posterior to anal-fin origin); from *H. panamensis* by the confluence of the adipose and caudal fins (vs. adipose and caudal fins separated); from *Heptapterus fissipinnis* and *H. panamensis* by having the caudal-fin truncate (vs. caudal-fin bifurcate); from *H. multiradiatus*, *H. stewarti* and *H. sympterygium* by having 15–23 anal-fin rays (vs. 36, 30, 22-29 respectively); additionally differs from *H. sympterygium* by having the anal-fin not continuous with the caudal-fin (vs. anal-fin continuous with the caudal-fin). Two new species are described based on molecular and morphological data. *Heptapterus* sp.n.A is distinguished from *H. mbya* and *H. qenqo* by having 18-21 anal-fin rays (vs. 15-17 rays); from *Heptapterus* sp.n.B by having 20–43 lateral line pores (vs. 8–19 pores); and from *H. mustelinus* by having the head 71.9–81.1% HL (vs. 60.8–71.3 % HL), and 52-53 vertebrae (vs. 54–60 vertebrae). *Heptapterus* sp.n.B is distinguished from *H. mbya*, *H. qenqo*, *H. mustelinus* and *Heptapterus* sp.n.A by the presence of 8 to 19 lateral line pores (vs. more than 20 pores), 3–4 unbranched anal-fin rays (vs. 5 or more unbranched anal-fin rays), and 23–25 caudal-fin rays on the ventral lobe (vs. 26–31 caudal-fin rays on the ventral lobe). Two new species are endemic from the

Uruguay basin, *Heptapterus* sp.n.A restricted to the rio Pelotas and *Heptapterus* sp.n.B restricted to the upper portion of rio Ibicuí.

Key words: Uruguay River, endemic, Neotropical, taxonomic, catfish.

Resumo

O bagre de água doce neotropical *Heptapterus mustelinus* do sistema laguna dos Patos, Rio Uruguai e as bacias costeiras do Atlântico do sul Brasil e Uruguai são revisados. O grupo *Heptapterus mustelinus* é aqui reconhecido com base em análises morfológicas; representadas por *H. mbya*, *H. mustelinus*, *H. qenqo*, e duas novas espécies *Heptapterus* sp.n.A e *Heptapterus* sp.n.B. O grupo *Heptapterus mustelinus* pode distinguir-se de *H. bleekeri* e *H. tapanahoniensis* pela posição da origem da nadadeira adiposa, localizada anterior à origem da nadadeira anal (vs. origem da nadadeira adiposa, posterior à origem da nadadeira anal); de *H. panamensis* pela confluência das nadadeiras adiposa e caudal (vs. nadadeiras adiposa e caudal separadas); de *H. fissipinnis* e *H. panamensis*, por ter a nadadeira caudal truncada (vs. nadadeira caudal bifurcada); de *H. multiradiatus*, *H. stewarti* e *H. sympterygium* por ter de 15–23 raios na nadadeira anal (vs. 36, 30, 22–29, respectivamente); além disso, difere de *H. sympterygium* por ter as nadadeiras anal e caudal contínuas (vs. nadadeiras anal e caudal não contínuas). Duas novas espécies são descritas com base em dados moleculares e morfológicos. *Heptapterus* sp.n.A é diferenciado de *H. mbya* e *H. qenqo* por ter 18–21 raios na nadadeira anal (vs. 15–17 raios na nadadeira anal); de *Heptapterus* sp.n.B por ter 20–43 poros na linha lateral (vs. 8 a 19 poros); e de *H. mustelinus* pelo tamanho da cabeça 71.9–81.1% HL (vs. 60.8–71.3% HL) e por ter 52–53 vértebras (vs. 54–60 vértebras). *Heptapterus* sp.n.B distingue-se de *H. mbya*, *H. qenqo*, *H. mustelinus* e *Heptapterus* sp.n.A pela presença de 8–19 poros na linha lateral (vs. mais de 20 poros), 3–4 raios não ramificados na nadadeira anal (vs. 5–7 raios não ramificados na nadadeira anal), e 23–25 raios no lóbulo ventral na nadadeira caudal (vs. 26–31 raios no lóbulo ventral da nadadeira caudal). As duas novas espécies são endêmicas da bacia do Uruguai, *Heptapterus* sp.n.A restrita a parte alta do rio Pelotas e *Heptapterus* sp.n.B restrita a parte alta do rio Ibicuí.

Palavras chave: rio Uruguai, endêmico, Neotropical, taxonomia, bagre.

Introduction

Heptapteridae was recognized as a monophyletic group by Lundberg & McDade (1986) as an unnamed clade within Pimelodidae, posteriorly named as subfamily Rhamdiinae Bleeker (1862) by Lundberg *et al.* (1991a), and raised to Rhamdiidae by de Pinna (1993) in his unpublished Ph. D thesis. Silfvergrip (1996) pointed out the priority of the name Heptapterinae Gill (1861) over Rhamdiinae Bleeker (1862), Swarça *et al.* (2000) was the first to formally use Rhamdiidae as a family category based in de Pinna's thesis (1993); therefore, this group is treated as family Heptapteridae by Bockmann & Guazzelli in Reis *et al.* (2003). Currently 211 species are considered valid in Heptapteridae Eschmeyer & Fong (2017).

Heptapterus Bleeker (1858) is the type genus of Heptapteridae, and *Pimelodus mustelinus* Valenciennes (1835) is the type species of *Heptapterus*, as designated by Bleeker (1858) in the original description of the genus. Mees (1974) attributed 32 species to *Heptapterus* based on several characters. Due to the presence of primitive and derived features in Mees's diagnosis, *Heptapterus* remained undiagnosable (Buckup, 1988).

Heptapterus belongs to the monophyletic *Nemuroglanis* subclade, defined by the following synapomorphies proposed by Ferraris (1988) and Bockmann (1994): (1) laminar portion of complex *centrum* transverse process, posterior to branched segment, is triangular and extends nearly to the lateral tip of fifth vertebral transverse process; (2) first dorsal-fin basal pterygiophore is inserted behind Weberian complex, usually above vertebrae 7 to 10; (3) "dorsal-fin spine" is thin and flexible; (4) dorsal-fin lock (= first dorsal-fin spine or spinelet) absent; (5) pectoral-fin "spine" is thin and flexible for its distal half, rather than pungent; (6) mesocoracoid arch modified into a wide band; (7) two posterior proximal radials of pectoral fin are enlarged and flattened; (8) pectoral girdle delicate, with a short mesial contact line comprising only three weakly joined scapulo-coracoid dentations; (9) pointed process projected posteroventrally from the coracoid keel absent; (10) posterior chambers of swimbladder atrophied, conforming a bilobed, transversely aligned structure; (11) nasal bone long and weakly ossified; (12) ridges of neural arch of the fourth vertebra absent; (13) presence of a distinct deep medial notch which divides the posterior limb of the fourth transverse process into two divergent, approximately symmetrical, long arms; (14) tips of the parapophyses of

anterior free vertebrae distally expanded and ventrally concave; (15) hemal and neural spines of the caudal vertebrae oriented at about 35° to the vertebral column axis; and (16) hemal and neural spines of the last free precaudal vertebrae robust. Bockmann (1998) in his unpublished Ph. D thesis performed a phylogenetic analysis of Heptapteridae, providing a new classification for the family, especially at generic level, where *Heptapterus* would turn to be a monotypic genus, represented by *H. mustelinus* alone. Four characters that diagnose *Heptapterus* were provided by Bockmann (1998): 54–57 vertebrae; 18–20 anal-fin rays; more than 26 caudal-fin rays in ventral lobe and latero posterior region of body bearing black chromatophores along the myosepta, delineating the myomeres.

Heptapterus mustelinus originally described from Río de La Plata (Argentina) is widespread throughout Paraná River basin, Uruguay River basin and coastal streams from southern Brazil and Uruguay (Buckup, 1988; Bockmann & Guazzelli, 2003; Aguilera *et al.*, 2011). Two species more related to *Heptapterus mustelinus* were recently described from Argentina: *H. qenqo* (Aguilera *et al.*, 2011) endemic of endorheic Río Salí basin (Salta and Tucumán, Argentina); and *H. mbya* (Azpelicueta *et al.*, 2011) endemic of Azul and Moreno streams, headwaters of Garuhapé stream tributary of Paraná basin (Misiones, Argentina). The present study aims to review *Heptapterus mustelinus* from its entire distribution with morphological and molecular data. Two new species are recognized apart from *Heptapterus mustelinus* and an identification key is provided for recognition of the species occurring in the study area.

Material and Methods

Biological material

Specimens were analyzed from the Ichthyological collections of Universidade Federal do Rio Grande do Sul, Departamento de Zoologia (UFRGS); Museu de Ciências e Tecnologia, Pontifícia Universidade Católica do Rio Grande do Sul, Porto Alegre (MCP); Museu de Zoologia da Universidade de São Paulo, São Paulo (MZUSP); Museu Nacional, Universidade Federal do Rio de Janeiro, Rio de Janeiro (MNRJ); Laboratório de Ictiología de Ribeirão Preto, Departamento de Biología, Facultad de Filosofía, Ciencias e Letras, Universidad de São Paulo, Ribeirão Preto (LIRP); Colección de Zoología Vertebrados de la Facultad de Ciencias, Universidad de la Republica, Montevideo (ZVC) Museo Argentino de Ciencias Naturales “Bernardino Rivadavia”, Ciudad Autonoma de Buenos Aires (MACN) e Fundación Miguel Lillo,

San Miguel de Tucumán (CI-FML), Museum für Naturkunde, Leibniz-Institut für Evolutionsund Biodiversitätsforschung an der Humboldt-Universität, Berlin (ZMB). Institutional abbreviations followed Sabaj (2016).

In order to evaluate genetic variation within *H. mustelinus* a DNA was extracted from tissue samples of 27 specimens maintained in the fish collections of UFRGS and MCP. The following abbreviations are used to indicate the drainage of origin of these samples. Uruguay River drainage: rio Pelotas = PEL, upper rio Uruguai = URU, rio Ijuí = IJU, rio Ibicuí = IBI, rio Quaraí = QUA, rio Negro = NEG. Laguna dos Patos system: rio Taquari = TAQ, rio Jacuí = JAC, rio Camaquã = CAM, rio Jaguarão = JAG. Tramandaí river system: rio Maquiné = MAQ. Coastal streams: rio Mampituba = MAM.

Morphometric and meristic

Measurements were taken with digital caliper and are expressed to the nearest 0.1 mm. All measurements were point to point according to the landmarks illustrated in Fig. 1 and described in Table 1, on the left side of the specimen. Most of the terminology for measurements followed Lundberg & McDade (1986) and Bockmann & de Pinna (2004), except as indicated below. Additional measurements are added: head depth at interorbital (depth taken at level of orbital), head width at posterior nostril (taken at level of posterior nostril) and dorsal head length (taken from snout tip to posterior tip of supraoccipital process). Standard length (SL) is given in millimeters, and the other measurements are expressed in percentage of SL or head length (HL) for subunit of the head (Table 1). All morphometric variables were standardized against standard length and every variable standardized were used in the statistical analysis (VARSEDIG). VARSEDIG algorithm was used to identify the morphometric characters that significantly discriminate between two taxa and validate the morphological distinctness between them (Leigh & Bryant, 2015; Guisande *et al.*, 2016; Chuctaya *et al.*, in press), and the morphometric characters found to better discriminate the species are presented as linear regressions.

Quantitative variables were represented by Tukey box plots to provide a visual representation of the counts that differed among species. Such graphs better display the skewed or other nonparametric shapes of the meristic data than the mean and standard deviation. The graphs presented here display the sample median (= 50th percentile) and

the 25th and 75th percentiles represented as the lateral borders of the box plots. The 10th and 90th percentiles are represented by error bars.

Counts of fins rays, gill-rakers of first branchial arch, ribs, vertebrae (included the first five vertebrae in the Weberian apparatus and one from the hypural plate) were taken from cleared and stained (cs) specimens prepared according to Taylor & Van Dyke (1985) or x-ray images (xr) taken with Faxitron LX-60 digital system at LIRP. Osteology analyses were done following Bockmann (1998). Nomenclature of the laterosensory cephalic system followed Arratia & Huaquín (1995) and Schaefer & Aquino (2000). Geographic distribution map was prepared in the Quantum GIS version 2.18.10 software (Sherman *et al.*, 2012).

Molecular markers, DNA extraction, amplification and sequencing

The DNA was extracted from muscle tissues following a modified method of cetyltrimethyl ammonium bromide (CTAB) Doyle & Doyle (1987). The tissues were fragmented and placed in the tubes, 500 µl of CTAB and 15 µl of proteinase K were added, mix on the shaker and incubated at 60 °C for 2 hours; after that 500 µl of chloroform-isoamyl alcohol (CIA) was added and the tubes were vortex for 3 minutes until a homogeneous emulsion was obtained then centrifuged at 14000 rpm for 20 minutes; the aqueous phase was carefully removed over a new tube and 350 µl of ice-cold isopropanol (-20°C) was added and the tubes were refrigerated (-20°C) overnight. The next day the tubes were centrifuged at 14000 rpm for 20 minutes; then the supernatant liquid was removed without discarding the pellet, after that rinse with 500µl of ice cold (-20°C) alcohol of 70°, 80° and absolute; before the absolute alcohol was discarded the tubes were centrifuged at 14000 rpm for 3 minutes and after that the absolute alcohol was discarded; then dry the pellets that are in the tubes for 15 minutes or until the alcohol is evaporated to finally place 50 µl of Tris EDTA and refrigerated (-20°C) overnight.

Fragment amplifications and sequencing were made for two mitochondrial markers cytochrome oxidase subunit I (*COI*) and cytochrome b (*CytB*). Fragment amplification were performed in 20µL reactions containing 0.1µl Platinum Taq polymerase (Invitrogen, Sao Paulo, SP, Brazil), 0.6µl MgCl₂, 2µl buffer, 2µl deoxyribonucleotide triphosphate (dNTP), 2µl forward primer (2 mM), reverse primer (2 mM), 10.3µl dH₂O and 1µl extracted genomic DNA (gDNA). Genes were amplified

via standard polymerase chain reaction (PCR) using Eppendorf Thermocyclers programmed for PCR technique. *COI* gene were amplified with an initial denaturation stage of 1 min at 94°C followed by 35 cycles of 94°C for 30 s, annealing at 52°C for 40 s, and extension at 72°C for 1 min, followed by a final 10 min at 72°C extention. *CytB* gene was amplified with an initial denaturation stage of 2 min at 95°C followed 35 cycles of 95°C for 30 s, annealing at 48°C for 1 min, and extention at 72°C for 1 min 30 s, followed by a final 5 min at 72°C extention. For all genes, PCR product was run on a 2% agarose gel and purified using EXOSAP (Exonuclease I and Shrimp Alkaline Phosphatase GE Healthcare®, Piscataway, NJ, USA). After purification, the samples were sequenced in both directions by the termination method of each amplified chain Sanger *et al.* (1977) in the Brazilian company ACTGene (<http://ludwigbiotec.com.br/site/Services-de-Sequenamento>).

Edition, Alignment and phylogeny inference

The consensus was generated from chromatograms for forward and reverse sequences, the assembly of each consensus sequences was checked visually using MEGA6 (Tamura *et al.* 2013); the consensus sequences that did not have overlap or that had unusually ambiguities were reamplified and resequenced. All the consensus sequences were aligned using the MUSCLE algorithm Edgar (2004) as implemented in MEGA6 and after that alignments were manually edited.

The nucleotide (p) and haplotype diversity (hd) were calculated for Cytochrome oxidase subunit I (*COI*) gene in the software DNAsP v. 5 (Librado & Rozas, 2009) and Analysis of Molecular Variance (AMOVA) were done in the program ARLEQUIN 3.5 (Excoffier *et al.*, 2005). Genetic distances between a pair of sequences were calculated using the Kimura 2-parameter (K2P) model in MEGA6. Haplotype networks were constructed with the median- joining method (MJN) (Bandelt *et al.*, 1999) using the program network 5.0.0.1 (www.fluxus-engineering.com).

Alignments of protein coding gene sequences were evaluated based on their amino acid translation. Alignments of all loci were concatenated to create a single alignment consisting of 1412 bp and 27 individuals. In cases where a gene sequence was missing, matrix was completed with “?” (missing data). The final alignment data were deposited in Genbank. Genetic sequences for type specimens follow GenSeq nomenclature (Chakrabarty *et al.*, 2013).

Phylogenetic analysis of the concatenated alignment was conducted using both Maximum Likelihood (ML) and Bayesian Inference (BI) methods on the CIPRES supercomputing cluster Miller *et al.* (2010). *Acentronichthys leptos* and *Taunayia bifasciata*, was designated as the outgroup. Maximum likelihood analysis was conducted using RaxML (v8.0.0; Stamatakis, 2014) programmed with workflow bootstrap and consensus, based on a 1000 generation search of tree space. A Bayesian Inference Markov chain Monte Carlo search of tree space was conducted using MrBayes v3.2.6 Ronquist, Huelsenbeck (2003). MrBayes was programmed to run for 10 million generations using four chains (nchain = 4), two parallel runs; sampling every 1000 trees with the first 25 % of trees being discarded as burning. A determination of codon-specific models of molecular evolution for each gene under the Bayesian Information Criterion (BIC) was performed with PartitionFinder v1.1.1 Lanfear *et al.* (2012). A generalized model; with variable base frequencies, one transition rate and one transversion rate and gamma distribution rate variation among sites (HKY + Gamma) was determined to be the best model of molecular evolution for *COI* (1st and 2nd sites) and *CytB* (1st and 2nd sites); and with variable base frequencies, equal transversion rate, variable transversion rate and gamma distribution rate variation among sites (TrN + Gamma) was determined to be the best model of molecular evolution for *COI* (3rd site) and *CytB* (3rd site).

General Mixed Yule Coalescent program (GMYC) (Pons *et al.* 2006) was used for species delimitation based on Yule Process model available in the webserver GMYC Zhang *et al.* (2013), using a Ultrametric gene tree. Ultrametric gene tree (*COI*) were constructed with generalized model; variable base frequencies, one transition rate and one transversion rate a gamma distribution rate variation among sites (HKY + Gamma) for all sites with relaxed molecular clock using a lognormal time distribution and birth-death prior through BEAUTi and BEAST programs (Drummond *et al.*, 2012). BEAST was programmed to run for total of 40,000,000 generations, sampling every 1,000 trees. An effective sample size (ESS) for all metrics exceeded 200 was checked in the software Tracer v1.6 (Rambaut *et al.*, 2013). The remaining trees were used to build a majority consensus tree with 10% of trees discarded as burning using TreeAnnotator v1.7.5 program Rambaut & Drummond (2013).

Results

Heptapterus mustelinus group

Heptapterus mustelinus group are herein recognized based on morphological analyses represented by *H. myba*, *H. qenqo*, *H. mustelinus*, and two new species *Heptapterus* sp.n.A and *Heptapterus* sp.n.B.

Diagnosis. *Heptapterus mustelinus* group can be distinguishing from *H. bleekeri* and *H. tapanahoniensis* by the position of the adipose-fin origin, located anterior to anal-fin origin (vs. adipose-fin origin, posterior to anal-fin origin); from *H. panamensis* by the confluence of the adipose and caudal fins (vs. adipose and caudal fins separated); from *Heptapterus fissipinnis* and *H. panamensis* by having the caudal-fin truncate (vs. caudal-fin bifurcate); from *H. multiradiatus*, *H. stewarti* and *H. sympterygium* by having 15–23 anal-fin rays (vs. 36, 30, 22-29 respectively); additionally differs from *H. sympterygium* by having the anal-fin not continuous with the caudal-fin (vs. anal-fin continuous with the caudal-fin).

Key to species of *Heptapterus mustelinus* group

- 1A.** Lateral line with less than 19 pores; 23–25 caudal-fin rays on ventral lobe (Rio Ibicuí) *Heptapterus* sp.n.B
- 1B.** Lateral line with more than 20 pores; 26–31 caudal-fin rays on ventral lobe 2
- 2A.** Anal-fin with 15–17 total rays, 4 or 5 sensorial pores on supraorbital branch of the laterosensory system 3
- 2B.** Anal-fin with 18–23 total rays; 6 sensorial pores on supraorbital branch of the laterosensory system 4
- 3A.** Presence of rudimentary serrae on first pectoral-fin ray, adipose-fin length 40.9–47.4 % of SL; interdorsal length 9.5–13.2 % SL (Río Salí basin) *H. qenqo*
- 3B.** Absence of rudimentary serrae on first pectoral-fin ray; adipose-fin length 47.4–58.7 % of SL; interdorsal length 5.2–8.3 % SL (Azul and Moreno streams)
..... *H. myba*
- 4A.** Head narrow, width 60.8–71.3 % of HL; vertebrae 54–60 (Paraná and Uruguay River basin, coastal streams from southern Brazil and Uruguay) *H. mustelinus*

- 4B.** Head wide, width 71.9–81.1 % of HL; vertebrae 52–53 (Rio Pelotas).....
 *Heptapterus* sp.n.A

***Heptapterus mustelinus* (Valenciennes 1835)**

Fig. 2 A-C; Tab. 1

Pimelodus mustelinus Valenciennes, 1835: Pl. 2, figs. 1-4 (name available from plate in 1835). Cuvier & Valenciennes, 1840: 165 (original description; no type known, type locality Rio de la Plata).

Heptapterus mustelinus (Valenciennes, 1835). Buckup, 1988: 641-644, 647, 649-651 (comparison with *H. sympterygium*). Malabarba, 1989: 139 (listed to laguna dos Patos system). Burgess, 1989: 277 (listed in Pimelodidae). Gómez & Chebez, 1996: 59 (listed to Misiones, Argentina). Haro *et al.*, 1996: 6 (listed to Cordoba, Argentina). Sverlij *et al.*, 1998: 51 (listed to lower Uruguay River, Uruguay). Miquelarena *et al.*, 2002: 78 (listed). Bockmann & Guazzelli in Reis *et al.*, 2003: 413 (listed). López *et al.*, 2003: 61 (listed to Argentina). Menni, 2004: 83 (listed to Argentina). Ferraris, 2007: 184 (listed). Aguilera *et al.*, 2011: 240 (comparison with *H. qenqo*). Azpelicueta *et al.*, 2011: 325 (comparison with *H. mbya*). Litz & Koerber, 2014: 20 (listed to Uruguay). Sarmiento *et al.*, 2014: 191 (listed to Bolivia). Mirande & Koerber, 2015: 34 (listed to Argentina). Bertaco *et al.*, 2016: 417 (listed to Rio Grande do Sul, Brazil).

Heptapterus eigenmanni Steindachner 1907: 487 (type locality: Maldonado on Rio de la Plata, Uruguay). Buckup 1988: 649 (Lectotype designation; synonym of *Heptapterus mustelinus*).

Heptapterus ornatus Ahl, 1936: 110 (original description; type locality, “südliches Brasilien und die anschließenden La Plata-Staaten” [South Brazil and adjacent platinum countries]). Silfvergrip & Paepke, 1997: 165 (listed in catalog of type species in Zoological Museum Berlin). Paepke, 1995: 92 (type mentioned). Burgess, 1989: 277 (cited as Pimelodidae). Bockmann & Guazzelli in Reis *et al.* 2003: 413 (Checklist). Ferraris, 2007: 185 (listed as *Species inquirenda*, *Heptapterus*). Aguilera *et al.*, 2011: 243, 245 (comparison with *H. qenqo*). Azpelicueta *et al.*, 2011: 326 (comparison with *H. mbya*).

Diagnosis: *Heptapterus mustelinus* is distinguished from *H. mbya*, *H. qenqo* and *Heptapterus* sp.n.A by the head width (60.8–71.3 vs. 71.8–78.7, 72.0–83.9 and 71.9–81.1 % of HL respectively); additionally from *H. mbya* by the number of anal fin-rays (18–23 vs. 15–17 rays); from *H. qenqo* by having six supraorbital pores (vs. five); from *Heptapterus* sp.n.A by the number of vertebrae (54–60 vs. 52–53 vertebrae) and equal width of posterior and anterior cranial fontanel (vs. posterior cranial fontanel narrower than anterior); from *Heptapterus* sp.n.B by the number of lateral line pores (20–51 vs. 8–19 pores), unbranched anal-fin rays (5–7 vs. 3–4 rays) and caudal-fin rays on ventral lobe (26–31 vs. 23–25 rays).

Description. Morphometric data is presented in Tab. 1. Elongate body, in cross section almost cylindrical anteriorly until dorsal fin and compressed gradually until caudal peduncle. Dorsal body profile slightly convex, curving in arch from orbital to base of dorsal fin. Dorsal profile nearly straight from dorsal-fin base to adipose-fin origin and gently convex from adipose-fin origin to base of caudal fin. Ventral profile of head slightly convex from snout tip to opercular opening, convex from that point to pelvic girdle and nearly straight from pelvic girdle to base of caudal fin. Forty-nine chevron shape myotomes visible through skin, progressively narrowing and more angled posteriorly. Deposits of fatty material in globose bodies, commonly seen in heptapterids, perceptible through skin, ventral surface of body with small papillae. Anus and urogenital pore very close to each other. Head small (4.5–6.0 times its SL), width (1.4–1.6 times its HL), depth (1.9–2.7 times its HL) and trapezoid in dorsal view (Fig. 1B). Anterior nostril close to upper lip. Posterior nostril more close to eye margin than anterior nostril. Distance between posterior nostrils slightly greater than between anterior nostrils. Four nostrils arranged as in vertices of a trapezium. Mouth wide, subterminal, with snout projecting gently beyond jaw. Jaw barbels slender and tapering progressively towards their distal extremities. Maxillary barbel longest, inserted above upper lip and lateral to anterior nostril; tip maxillary barbel surpassing the pectoral-fin insertion. Mental-barbel base inserted midway between anterior border of lower jaw and gular fold. Outer mental barbel longer than inner barbel, and inserted nearly behind fourth pore of preoperculomandibular laterosensory canal (pm4), tip of outer mental barbel passing outer border of branchiostegal membrane. Inner mental barbel inserted slightly in advance of vertical through origin of outer mental barbel, approximately behind second pore of preoperculomandibular laterosensory canal (pm2), tip of inner

mental barbel reaching the inner border of branchiostegal membrane. Small eyes, elliptical horizontally. Skin over eye, with lens slightly visible. Eye gently dorsal positioned, anteriorly at midpoint between tip of snout and corner of opercular membrane. Pupil rounded.

Dorsal fin distally rounded in profile. First dorsal-fin ray unbranched and soft, small and distal tip triangular, followed by six branched rays; origin of dorsal fin approximately on vertical or anteriormost portion of pelvic fin base. Pectoral fin convex posteriorly, with $i+7(136)$ rays; first fin ray unbranched; slightly convex (0.5–0.9 times entire pectoral length), most of proximal portion slightly rigid and distal portion soft; second pectoral-fin ray (first branched) slightly longer than third ray (second branched). Pelvic fin with distal margin rounded, with $i+5(136)$ rays; first pelvic-fin ray unbranched, completely flexible and slightly shorter than second and third rays (first and second branched rays, respectively); tip of pelvic fin surpassing anus and urogenital papillae; pelvic-fin origin well ahead of midpoint of body (excluding caudal fin), and on vertical through base of first branched dorsal-fin ray. Anal-fin margin straight or slightly convex in lateral profile, with 18–23 rays ($v+13(7)$, $v+14(7)$, $v+16(3)$, $v+17(1)$, $v+18(1)$, $vi+12(3)$, $vi+13(6)$, $vii+12(5)$, $vii+13(1)$, $vii+14(1)$); anal-fin base small (0.2–0.3 times its SL), base covered basally with thick muscular tissue; origin of anal-fin base slightly posterior of adipose-fin origin, posterior limit of anal-fin base posterior to middle adipose-fin base length. Adipose fin long (0.4–0.5 times its SL), gently convex in lateral profile, base with fleshy tissues; distance from last dorsal-fin ray to adipose-fin origin less than length of dorsal-fin base; origin of adipose fin at midpoint of body (excluding caudal fin) and posterior adipose-fin continuing to procurent rays of dorsal caudal-fin lobe. Caudal fin rounded; dorsal lobe longer than ventral lobe, six or seven branched rays in dorsal lobe and seven or 8 branched rays in ventral lobe; total caudal fin-rays 41–50, with 15–19 rays in dorsal lobe and 26–31 rays in ventral lobe.

Sensory canals of head with simple tubes ending in single pores. Supraorbital canal usually with six pores: s_1 , s_{2+i2} , s_3 , s_6 (epiphyseal branches fused to each other, with single pore), s_7 and s_8 . Infraorbital canal with five pores: i_1 , i_3 , i_4 , i_5 and i_6 . Preoperculomandibular canal with 11 pores: pm_1 , pm_2 , pm_3 , pm_4 , pm_5 , pm_6 , pm_7 , pm_8 , pm_9 , pm_{10} and pm_{11} . Postotic canal with 3 pores: po_1 , po_2 and po_3 . Lateral line incomplete; straight and continuous without interruption until vertical through posterior dorsal fin base to midway of caudal peduncle, with 20 to 51 pores.

Total vertebrae 54(3), 55(8), 56(11), 57(13) or 60(2); 16(2), 17(20) or 18(5) pre-caudal vertebrae; and 37(3), 38(7), 39(8), 40(6) or 43(2) caudal vertebrae. Ribs 7(4), 8(15) and 9(8). Insertion of dorsal fin posterior to 12(27) vertebrae and insertion of anal fin anterior to 27–30 vertebrae.

Color in alcohol: Dorsal and lateral of body brownish and ventral surface cream. Upper portion of head and checks covered by dark brown pigment becoming gradually less concentrate ventrally; dark brown trapezoid spot dorsally on head, between eyes and supraoccipital; dark longitudinal stripe on post orbital, between posterior orbital to inner border of branchiostegal membrane. Maxillary barbel dark brown dorsally and ventrally, with tip unpigmented. External and internal mental barbels dark brown dorsally, ventrally and tips unpigmented. Trunk coloration varying from dark brown to light brown. Upper portion of trunk with four dark brown transverse bars; first one narrow behind head, extended from one side of pectoral-fin insertion to other side; second one in front of dorsal-fin origin, third one reaching to dorsal fin base and last one in front of adipose-fin origin. Base of caudal fin with dark brown spot semicircle-shaped, caudal fin rays brown and interradial caudal-fin membrane devoid of chromatophores. Dorsal, anal, pectoral and pelvic-fins rays with high concentration of gray or brown chromatophores and interradial membranes translucent; base of dorsal and pectoral fins darker brown than distal. Adipose fin brown, base with intense concentration of dark brown chromatophores. Black thin stripe along lateral line, straight from pectoral fin to middle caudal peduncle.

Sexual dimorphism: Urogenital pore tubular in males and trapezoidal in females. No additional sexual external dimorphic characters were found.

Geographic distribution: *Heptapterus mustelinus* is distributed along the La Plata, Uruguay and Paraná River in Argentina, Brazil and Uruguay; and Laguna dos Patos system, Tramandaí system and coastal streams of southern of Brazil and Uruguay. (Fig. 7).

Material examined

Rio de la Plata basin: Argentina: Buenos Aires: MACN 6744, 3, 27.64–37.9 mm SL, route to Cañuelas. MACN 6913, 5, 59.1–109.4 mm SL, río Reconquista, Cascallares. MACN 8279, 1, 262.9 mm SL, río Reconquista, Escobar. MACN 10857, 2, 77.2–142.3

mm SL, dam Roggero. MACN 10858, 1, 200.3 mm SL, arroyo El Durazno tributary to río Matanza-Riachuelo, Plomer. Uruguay: ZVC 968, 2, 103.7–115.8 mm SL, arroyo Mataojo, Aguas Blancas, Lavalleja. ZVC 5759, 1, 153.3 mm SL, Laguna del Sauce, Maldonado. ZVC 13550, 1, 56.9 mm SL, arroyo Vizcaíno, Canelones. Argentina: Buenos Aires: MACN 359, 1, 195.4 mm SL, Olivos ($34^{\circ}30'30.77''S$ $58^{\circ}28'26.02''W$). MACN 2050, 1, 123.1 mm SL, Buenos Aires. MACN 3370, 3, 114.0–137.7 mm SL, Vicente López ($34^{\circ}31'19.66''S$ $58^{\circ}28'05.14''W$). MACN 4649, 2, 85.8–155.1 mm SL, Vicente López. MACN 5251, 1, 139.8 mm SL, rio Santo Antonio, Tigre. MACN 6187, 9, 135.1–228.8 mm SL, (O.S.N.). MACN 11573, 1, 155.5 mm SL. **Rio Paraná basin:** Argentina: MACN 4459, 1, 166.0 mm SL, río Paraná. MACN 11663, 1, 110.2 mm SL, Rosario, Santa Fe. Paraguay: MACN 6480, 6, 77.2–144.1 mm SL, Capitán Viega, Alto Paraná. **Rio Uruguay basin:** Lower Uruguay basin: Argentina: Misiones: MCP 13326, 7, 39.0–48.8 mm SL, arroio Itacaruare, Itacaruare. MCP 13468, 1, 23.8 mm SL, arroio Itacaruare, Itacaruare. Brazil: UFRGS 20298, 2, 59.7–106.2 mm SL, arroio Mutui. Uruguay: UFRGS 10972, 1, 82.4 mm SL, Salto. Uruguay: Salto: UFRGS 7736, 4, 80.3–101.0 mm SL, rio Uruguay, Belén ($30^{\circ}47'7.00''S$ $57^{\circ}47'5.00''W$). UFRGS 8570, 18 (2 c&s), 42.5–118.1 mm SL, arroio Tala ($31^{\circ}23'9.00''S$ $57^{\circ}33'46.00''W$). Artigas: UFRGS 8081, 6 (1c&s), 54.6–75.5 mm SL, arroyo Mandiyú ($30^{\circ}31'55.00''S$ $57^{\circ}39'57.00''W$). UFRGS 8090, 7, 64.1–91.61, arroyo Sarandi, tributary to arroyo Yacuy ($30^{\circ}43'59.00''S$ $57^{\circ}40'43.00''W$). Rio Negro drainage: Uruguay: Durazno: UFRGS 7446, 2, 40.7–57.2 mm SL, arroyo Maestre de Campo, tributary to rio Yi, Durazno ($33^{\circ}24'55.00''S$ $56^{\circ}12'6.00W$). ZVC 413, 2, 26.8–34.2 mm SL, arroyo Cordobés. ZVC 3309, 13, 66.5–158.7 mm SL, arroyo Las Higueras, Carpinteria. ZVC 3319, 4, 59.4–65.8 mm SL, Cordobés, Laguna Lateral. ZVC 5363, 3, 37.6–67.4 mm SL, arroyo Cordobés. Flores: ZVC 11465, 3, 114.6–128.4 mm SL, arroyo Maciel, Paso de la Cadena. Rivera: UFRGS 11930, 2, 61.1–63.7 mm SL, arroio Yaguarí. ZVC 2812, 1, 62.2 mm SL, puddle nex to arroyo Cuñapirú. Tacuarembó: UFRGS 7409, 2, 37.9–50.9 mm SL, arroyo Batovi, tributary to rio Tacuarembó, Tacuarembó ($31^{\circ}54'30.00''S$ $56^{\circ}1'4.00''W$). UFRGS 12434, 1, 69.5 mm SL, rio Tacuarembó. ZVC 135, 13, 34.9–74.6 mm SL, arroyo Laureles, Rincón da Vasoura. ZVC 417, 2, 42.3–51.9 mm SL, arroyo Laureles, Ricón da Vasoura. ZVC 3908, 1, 83.0 mm SL, arroyo Jabonería. ZVC 11758, 2, 122.5–135.4 mm SL, arroyo Carpintería, Yaguarí.

ZVC 13208, 1, 32.0 mm SL, creek in San Gregorio de Polanco. Brazil: Rio Grande do Sul: Bagé: UFRGS 8347, 2, 68.3–69.0 mm SL, arroio Piraí, ($31^{\circ}13'12.00''S$ $54^{\circ}16'30.00''W$). UFRGS 21202, 65 (1c&s), 26.2–150.7 mm SL, creek tributary to arroio Quebrado, ($31^{\circ}17'56.85''S$ $53^{\circ}56'9.55''W$). UFRGS 22129, 13, 47.8–118.1 mm SL, arroio Igrejinha. MCP 35148, 5, 46.5–88.1 mm SL, arroio Santa Tecla. Rio Arapey Grande drainage: Uruguay: Salto: ZVC 13081, 2, 64.3–75.6 mm SL, arroyo Mataojo, Pueblo Fernandez. ZVC 13169, 7, 55.4–98.71 mm SL, Colonia Lavalleja, Paso Elías. Rio Paysandú drainage: Uruguay: Paysandú: ZVC 4160, 3, 40.5–52.0 mm SL, río Queguay. ZVC 13437, 5, 57.0–117.5 mm SL, arroyo Bacacuá Grande. ZVC 7482, 2, 45.0–101.5 mm SL, río Quegay Chico. ZVC 11602, 4, 57.8–134.4 mm SL, río Queguay, Paso Andrés Perez. ZVC 13396, 42, 33.2–130.1 mm SL, río Queguay chico, Paso del Parque. ZVC 13312, 7, 69.2–95.9 mm SL, arroyo Corrales, Paso Castillo. Rio Quaraí drainage: Uruguay: Artigas: UFRGS 7765, 9 (1 c&s), 58.6–90.6 mm SL, 69.4 mm SL, arroyo Cuaró Grande ($30^{\circ}47'3.00''S$ $56^{\circ}46'54.00''W$). UFRGS 7817, 4 (1 c&s), 35.8–71.1 mm SL, 67.3 mm SL, arroyo Tres Cruces Grandes ($30^{\circ}35'31.00''S$ $56^{\circ}37'34.00''W$). Rio Ibicuí drainage: Brazil: Rio Grande do Sul: UFRGS 6788, 4 (2 c&s), 44.9–96.6 mm SL, creek tributary to arroio Gueromana, Rosário do Sul ($30^{\circ}0'60.00''S$ $55^{\circ}23'18.00''W$). UFRGS 13980, 7, 54.8–123.5 mm SL, arroio Pau Fincado, São Gabriel ($29^{\circ}53'30.00''S$ $54^{\circ}19'58.00''W$). UFRGS 21200, 47 (1 c&s), 29.6–140.3 mm SL, Quebra Dentes, Jari ($29^{\circ}24'0.98''S$ $54^{\circ}18'5.71''W$). UFRGS 21519, 38 (2c&s), 22.6–138.3 mm SL, Lajeado Cunha, Manoel Viana ($29^{\circ}31'27.80''S$ $55^{\circ}32'41.90''W$). UFRGS 7693, 3, 15.8–21.53 mm SL, creek tributary to rio Ibicuí, Rosário do Sul ($30^{\circ}12'42.00''S$ $55^{\circ}3'17.00''W$). UFRGS 8369, 18, 21.4–124.8 mm SL, arroio Santa Maria Chico, tributary to rio Santa Maria, Bagé. UFRGS 11763, 2, 50.1–93.6 mm SL, arroio Taquarambó, Dom Pedrito. UFRGS 11765, 1, 82.3 mm SL, arroio de Taquarembó, Dom Pedrito. UFRGS 13964, 1, 56.7 mm SL, Sanga do Areal, São Gabriel. UFRGS 13982, 1, 91.2 mm SL, creek tributary rio Ibicuzinho, São Gabriel. UFRGS 14975, 1, 47.9 mm SL, creek tributary, Santa Maria. UFRGS 22375, 1, 36.1 mm SL, sanga das Tunas, Quevedos. MCP 27492, 3, 61.1–99.5 mm SL, arroio Lagoão, Santiago. MCP 11180, 2, 32.8–40.8 mm SL, rio Ibirapuitã, Rosário do Sul. MCP 11249, 374, 20.7–160.4 mm SL, rio Ibirapuitã, Rosário do Sul. MCP 11347, 1, 57.4 mm SL, creek tributary, Alegrete. MCP 14137, 1, 61.4–74.6 mm SL, creek

tributary, Dom Pedrito. MCP 14216, 1, 46.7 mm SL, creek tributary, Dom Pedrito. MCP 15208, 3, 42.9-87.9 mm SL, creek tributary, Uruguaiana. MCP 17556, 2, 52.3-72.2 mm SL, Areal do Sodré, Cacequi. MCP 20307, 6, 46.5-84.7 mm SL, arroio Imbaá, Uruguaiana. MCP 21440, 1, 122.2 mm SL, barragem Sanchuri, Uruguaiana. MCP 23091, 3, 21.5-39.6 mm SL, arroio Sanga Funda, São Francisco de Assis. MCP 23094, 1, 38.4 mm SL, rio Inhacunda, São Francisco de Assis. MCP 25191, 1, 61.5 mm SL, rio Inhacunda, São Francisco de Assis. MCP 25214, 2, 74.7-94.3 mm SL, arroio Taquari, São Francisco de Assis. MCP 27484, 2, 57.18-65.45 mm SL, rio Itu, Santiago. MCP 27501, 1, 52.9 mm SL, arroio Restinga, São Francisco de Assis. MCP 27553, 1, 39.8 mm SL, arroio do Funcho, Jaguari. MCP 27557, 1, 39.2 mm SL, creek tributary of rio Santana, Tupanciretã. MCP 27560, 2, 26.3-136.2 mm SL, arroio do Tigre, Jaguari. MCP 27570, 5, 29.94-63.34 mm SL, creek tributary of rio Tunas, Jaguari. MCP 27586, 2, 78.7-83.8 mm SL, arroio Camabará, Jaguari. MCP 27600, 1, 34.58 mm SL, creek tributary, Jaguari. MCP 27613, 6, 45.36-63.84 mm SL, arroio Capivari, Jaguari. MCP 27622, 1, 60.2, mm SL, rio Santana, Tupanciretã. MCP 27638, 1, 79.0 mm SL, arroio Caracol, Jaguari. MCP 29210, 2, 51.8-106.5 mm SL, rio Ibicuí-Mirim, Santa Maria. MCP 43909, 7, 30.6-43.6 mm SL, arroio Jaguari tributary of rio Santa Maria, São Gabriel. MCP 43921, 9, 28.2-123.9 mm SL, arroio Jaguari tributary of rio Santa Maria, Lavras do Sul. MCP 46739, 3, 41.0-70.6 mm SL, rio Jaguari, Dom Pedrito. MCP 47729, 6, 52.7-74.3 mm SL, creek tributary of rio Ibirapuitã, Alegrete. Rio Piratinim drainage: Rio Grande do Sul: MCP 12709, 2, 65.8---85.4 mm SL, arroio Passo do Rosário, Santo Antônio das Missões. MCP 12723, 5, 56.3-62.7 mm SL, arroio Passo do Alto, São Nicolau. Rio Ijuí drainage: Brazil: Rio Grande do Sul: UFRGS 21107, 21 (4c&s), 40.6-151.8 mm SL, riacho Lajeado Grande, Dezesseis de Novembro (28°10'7.68"S 55° 3'58.79"W). UFRGS 13224, 6, 37.5-61.9 mm SL, UHE São José, Cerro Largo (28°10'32.00"S 54°49'11.00"W). UFRGS 10425, 2, 62.7-84.2 mm SL, creek tributary to rio Ijuizinho, Entre Ijuís (28°25'0.00"S 54°17'56.00"W). UFRGS 7063, 4, 43.0-58.2 mm SL, creek tributary to rio Ijuí, São Nicolau (28°10'30.00"S 55° 4'1.00"W). UFRGS 4167, 1, 45.7 mm SL, riacho do Cruzamento, Ijuí. UFRGS 21955, 5, 57.7-145.8 mm SL, arroio Nock, Ijuí. UFRGS 11320, 3, 77.2-108.2 mm SL, UHE São José, Cerro Largo. MCP 11695 1, 161.4 mm SL, rio Cambará, Pejuçara. MCP 11868, 1, 89.9 mm SL, rio Potiribu, Ijuí. MCP 16766, 1, 21.9 mm SL, arroio Lageado

do Moinho tributary of rio Ijuizinho, Entre-Ijuís. MCP 16787, 4, 53.5–70.6 mm SL, arroio tributary of rio Ijuizinho, Jóia. MCP 34868, 2, 36.4–41.4 mm SL, arroio Forte, Rolador. MCP 34892, 1, 71.5 mm SL, arroio Pedra, 16 de Novembro. MCP 34901, 1, 69.4 mm SL, arroio Cinamomo, Roque Gonzales. MCP 34952, 4, 33.4–40.9 mm SL, arroio Alexandrino, Salvador das Missões. MCP 34967, 2, 58.1–61.9 mm SL, arroio Portão, Roque Gonzales. MCP 34984, 1, 61.4 mm SL, arroio Encantado, Cerro Largo. MCP 35313, 8, 35.3–73.0, mm SL, creek tributary, 16 de Novembro. MCP 35326, 2, 65.9–95.6 mm SL, arroio Cinamomo, Roque Gonzales. MCP 35331, 3, 37.7–52.4 mm SL, arroio Albino, São Pedro do Butiá. MCP 35360, 4, 45.3–57.9 mm SL, arroio Limoeiro, 16 de Novembro. MCP 35362, 3, 45.3–77.1, arroio Portão, Roque Gonzales. MCP 35366, 10, 36.0–66.9 mm SL, arroio Brum, Cerro Largo. MCP 35368, 1, 48.5 mm SL, arroio Forte, Rolador. MCP 35375, 3, 46.7–78.8 mm SL, arroio Pobre, Salvador das Missões. MCP 35401, 4, 44.7–70.0 mm SL, arroio Encantado, Cerro Largo. MCP 35423, 6, 51.4–65.3 mm SL, arroio Alexandrino, Salvador das Missões. MCP 37014, 6, 59.0–86.3 mm SL, arroio Pobre, Salvador das Missões. MCP 37018, 7, 49.3–94.5 mm SL, arroio Encantado, Cerro Largo. MCP 37031, 10, 51.6–82.0 mm SL, arroio Alexandrino, Salvador das Missões. MCP 37046, 4, 48.8–84.8 mm SL, arroio Forte, Rolador. MCP 37049, 1, 63.0 mm SL, creek tributary, 16 de Novembro. MCP 37211, 1, 29.8 mm SL, arroio Portão, Roque Gonzales. MCP 37255, 4, 33.9–63.1 mm SL, arroio Alexandrino, Salvador das Missões. MCP 37259, 1, 66.7 mm SL, arroio Forte, Rolador. MCP 37268, 8, 33.2–74.5 mm SL, creek tributary, 16 de Novembro. Rio Turvo drainage: Brazil: Rio Grande do Sul: UFRGS 5964, 3, 52.7–118.6 mm SL, Lageado do Pessegueiro, Santa Rosa ($27^{\circ}52'46.08"S$ $54^{\circ}30'9.19"W$). UFRGS 4157, 1, 75.8 mm SL, creek tributary to rio Turvo, Tenente Portela. UFRGS 15760, 1, 82.0 mm SL, creek tributary, Três Passos. MCP 5718, 3, 20.3–74.7 mm SL, rio Tuparendi, Tuparendi. MCP 48561, 1, 52.6 mm SL, rio Bonifácio, Derrubadas. MCP 48570, 1, 56.6 mm SL, arroio Calixto, Derrubadas. Upper rio Uruguay drainage: Brazil: Rio Grande do Sul: UFRGS 10722, 1, 42.5 mm SL, rio do Lobo, Trindade do Sul. UFRGS 10891, 3, 68.6–114.4 mm SL, rio da Várzea, Frederico Westphalen. UFRGS 10885, 1, 96.5 mm SL, rio Fortaleza, Taquaruçú ($27^{\circ}25'51.00"S$ $53^{\circ}32'50.00"W$). UFRGS 20687, 10 (1 c&s), 70.1–95.0 mm SL, arroio Lajeado do Tigre, Barra do Guarita ($27^{\circ}11'50.00"S$ $53^{\circ}42'29.00"W$). Santa Catarina: UFRGS 4343, 1, 76.1 mm SL, arroio Santa Fé,

Itapiranga ($27^{\circ} 9'60.00''S$ $53^{\circ}43'0.00''W$). UFRGS 10908, 1, 104.5 mm SL, rio Macuco, Mondaí ($27^{\circ}11'50.00''S$ $53^{\circ}42'29.00''W$). UFRGS 4182, 1, 81.1 mm SL, rio Passarinhos, Palmitos. UFRGS 22679, 1, 47.8 mm SL, rio do Peixe, Ouro. UFRGS 22603, 3, 38.6–89.9 mm SL, Rio Forquilha, Paim Filho. UFRGS 22604, 3, 57.7–102.0 mm SL, Rio Forquilha, Maximiliano de Almeida. MCP 10872, 2, 27.9–92.8 mm SL, Sanga das Águas Frias, Iraí. MCP 19270, 5, 26.7–124.9 mm SL, arroio Lageado União, Palmitinho. MCP 20881, 1, 85.8 mm SL, arroio Mondaizinho, Mondaí. MCP, 31769, 4, 24.0–32.0 mm SL, rio Passo Fundo, Passo Fundo. MCP 31772, 3, 57.0–68.3 mm SL, rio Passo Fundo, Passo Fundo. MCP 40032, 4, 48.5–86.2 mm SL, Mondaí. MCP 41527, 4, 68.8–91.7 mm SL, creek tributary of rio Ariranhas, Seara. MCP 46714, 1, 65.6 mm SL, arroio Sepultura, Campinas do Sul. MCP 46723, 2, 63.2–81.8 mm SL, creek tributary of Lageado Tombe, São Valentim. MCP 46770, 1, 56.5 mm SL, arroio Bugio, Coxilha. MCP 46802, 3, 22.5–79.4 mm SL, creek tributary of arroio Inhupacá, Sertao. Rio Pelotas drainage: Brazil: Santa Catarina: UFRGS 6984, 4, 40.1–52.9 mm SL, rio Águas Pretas, Ponte Alta. Rio Grande do Sul: UFRGS 10119, 1, 60.3 mm SL, rio Marmeiro, Barracão ($27^{\circ}38'10.00''S$ $51^{\circ}29'41.00''W$). UFRGS 4927, 1, 99.7 mm SL, rio Manoel Leão, Bom Jesus. UFRGS 14488, 1, 40.4 mm SL, arroio Lageado dos Vivos, Capão Bonito do Sul. UFRGS 6978, 5, 39.9–79.4 mm SL, rio da Areia, Otacílio Costa. UFRGS 10510, 2, 84.2–104.3 mm SL, rio Marmeiro, Barracão. MCP 13471, 1, 106.0 mm SL, rio Canoas, Abdon Batista. Rio Grande do Sul: MCP 9000, 1, 37.57 mm SL, Sananduva. MCP 14400, 2, 69.4–104.8 mm SL, creek tributary of rio Dos Touros, Bom Jesus. MCP 14563, 1, 43.1 mm SL, rio Ligeiro, São João da Urtiga. MCP 41500, 3, 38.7–58.3 mm SL, rio Forquilha, Paim Filho. **Coastal streams of Atlantic:** Rio Urussanga drainage: Santa Catarina: UFRGS 9062, 5, 50.1–66.1 mm SL, creek tributary, Urussanga. UFRGS 21391, 23, 25.4–122.8 mm SL, rio Cocal, Urussanga. Rio Araçatuba drainage: Santa Catarina: MCP 28730, 1, 30.3 mm SL, creek tributary, Garopaba. Rio Araranguá drainage: Santa Catarina: UFRGS 15388, 5 (2 c&s), 38.6–100.0 mm SL, rio Mãe Luzia, Treviso ($28^{\circ}28'1.00''S$ $49^{\circ}28'19.00''W$). UFRGS 6341, 3 (1 c&s), 47.1–54.7 mm SL, rio Mãe Luzia, Treviso ($28^{\circ}27'58.00''S$ $49^{\circ}28'18.00''W$). UFRGS 584, 1, 193.1 mm SL, rio Jordão, Siderópolis. UFRGS 585, 1, 120.9 mm SL, rio Jordão, Siderópolis. UFRGS 587, 1, 112.8 mm SL, rio Jordão, Siderópolis. UFRGS 588, 1, 100.8 mm SL, rio Jordão, Siderópolis. UFRGS 591, 1, 86.1 mm SL, rio Jordão, Siderópolis. UFRGS 12547, 2, 37.2–51.6 mm SL, rio Jordão Alto,

Nova Veneza. UFRGS 12563, 1, 68.5 mm SL, rio Manin, Treviso. UFRGS 21183, 1, 64.3 mm SL, rio Jordão, Jordão. MCP 7036, 55, 25.5–151.7 mm SL, rio Jordão, Nova Veneza. MCP 7037, 1, 61.9 mm SL, rio Itoupava, Araranguá. MCP 23572, 1, 36.88 mm SL, creek tributary of rio Morto, Meleiro. MCP 50026, 1, 68.0 mm SL, rio Mãe Luzia, Treviso. Rio Mampituba drainage: Rio Grande do Sul: UFRGS 15996, 25 (3 c&s), 37.9–83.5 mm SL, Vila São João ($29^{\circ}13'14.00"S$ $49^{\circ}52'49.00"W$). UFRGS 15975, 16 (4 c&s), 45.2–64.8 mm SL, Vila São João ($29^{\circ}14'56.80"S$ $49^{\circ}50'55.50"W$). UFRGS 10828, 1, 51.8 mm SL, creek tributary, Praia Grande. UFRGS 15891, 2, 59.8–70.1 mm SL, rio dos Mengues, Morrinhos do Sul. UFRGS 15935, 1, 70.3 mm SL, rio Morro Azul, Morro Azul. UFRGS 15938, 1, 70.5, rio Morro Azul, Morro Azul. UFRGS 16001, 17, 37.5–75.3 mm SL, Vila Lothhammer, Torres. UFRGS 16011, 7, 35.0–74.2 mm SL, Vila Lothhammer, Torres. UFRGS 16015, 11, 42.7–68.5 mm SL, Vila Lothhammer, Torres. UFRGS 16021, 3, 48.9–87.2 mm SL, Vila Lothhammer, Torres. UFRGS 16033, 5, 25.4–85.0 mm SL, Vila Lothhammer, Vila São João. UFRGS 16055, 1, 66.1 mm SL, Vila Lothhammer, Vila São João. UFRGS 16090, 1, 34.2 mm SL, Praia Grande. UFRGS 15682, 2, 43.4–51.3 mm SL, arroio Perdida, Morrinhos do Sul. MCP 23698, 24, 39.3–108.7 mm SL, rio Mangue, Morrinhos do Sul. MCP 23724, 24, 35.6–74.6 mm SL, rio Negro, Morrinhos do Sul. MCP 23727, 7, 34.3–94.6 mm SL, rio Panela tributary of rio da Praça, Mampituba. Santa Catarina: MCP 7034, 42, 20.2–90.9 mm SL, rio Faxinalzinho, Praia Grande. MCP 14684, 1, 102.7 mm SL, rio Canoas, Praia Grande. MCP 23546, 8, 36.2–105.4 mm SL, arroio Facão, Praia Grande. MCP 23549, 1, 59.8 mm SL, arroio tributary of rio Sertão, Praia Grande. MCP 23626, 8, 30.1–112.0 mm SL, arroio Maia Coco, Praia Grande. UFRGS 11081, 6 (3 c&s), 62.9–91.1 mm SL, Praia Grande ($29^{\circ}11'57.00"S$ $49^{\circ}57'5.00"W$). **Tramandaí system:** Rio Maquiné drainage: Rio Grande do Sul: MCP 10768, 2, 50.1–51.6 mm SL, arroio Agua Parada, Maquiné ($29^{\circ}40'30.00"S$ $50^{\circ}11'57.00"W$). UFRGS 4989, 1, 77.5 mm SL, arroio Água Parada, Maquiné. Rio Três Forquilhas drainage: Rio Grande do Sul: MCP 23675, 1, 92.1 mm SL, arroio do Padre, Itati ($29^{\circ}29'11.00"S$ $50^{\circ}7'12.00"W$). MCP 23682, 1, 104.1 mm SL, arroio do Padre, Itati ($29^{\circ}29'29.00"S$ $50^{\circ}8'36.00"W$). MCP 29695, 1, 38.2 mm SL, creek tributary to arroio do Padre, Itati ($29^{\circ}29'51.00"S$ $50^{\circ}9'51.00"W$). **Laguna dos Patos system:** Rio Taquari drainage: UFRGS 16819, 11 (2 c&s), 45.9–109.83 mm SL, creek tributary to rio Taquari, Arroio do Meio ($29^{\circ}17'26.00"S$ $51^{\circ}55'5.00"W$). UFRGS 6958, 20 (3 c&s), 48.1–130.7 mm SL, rio

Carreiro, (28°53'41.09"S 51°48'30.72"W). UFRGS 16759, 19 (2c&s), 36.7–88.9 mm SL, creek tributary to rio Guaporé, União da Serra (28°47'49.00"S 52° 0'12.00"W). UFRGS 17672, 4, 78.6–154.6 mm SL, creek tributary to rio Guaporé, Vila Maria (28°32'3.00"S 52° 5'28.00"W). UFRGS 13893, 6, 48.4–93.7 mm SL, arroio Caçador, Serafina Corrêa. UFRGS 14230, 1, 58.7 mm SL, arroio Travesseiro, Travesseiro. UFRGS 14296, 4, 79.7–105.7 mm SL, arroio Forquetinha, Forquetinha. UFRGS 14305, 2, 46.1–108.2 mm SL, arroio Travesseiro, Travesseiro. UFRGS 16763, 14, 39.3–145.9 mm SL, creek tributary to rio Guaporé, Serafina Corrêa. UFRGS 16774, 14, 35.1–92.9 mm SL, arroio Faxinal tributary to rio São Marcos, Caxias do Sul. UFRGS 16783, 6, 46.6–130.5 mm SL, rio Lajeado Engenho Velho tributary to rio Guaporé, Nova Alvorada. UFRGS 16900, 2, 89.2–100.7 mm SL, rio Forquetinha, Canudos do Vale. UFRGS 17890, 8, 32.1–103.9 mm SL, rio da Prata, André da Rocha. UFRGS 14772, 2, 64.7–80.8 mm SL, arroio Não Sabia tributary to rio Carreiro, Guaporé. UFRGS 6417, 1, 74.0 mm SL, creek tributary to rio Carreiro, Dois Lajeados. UFRGS 22594, 2, 44.3–54.6 mm SL, Rio das Antas, Cotiporã. UFRGS 20389, 11, 52.7–90.7 mm SL, arroio Forqueta, Forquetinha. MCP 17497, 9, 63.1–119.0 mm SL, creek tributary to arroio Castelhano, Venâncio Aires. MCP 17671, 3, 91.3–113.3 mm SL, Arroio Canoas, Barão. MCP 25616, 3, 30.7–69.3 mm SL, arroio Jaboticaba, Vila Flores. MCP 48420, 1, 77.3 mm SL, arroio Jararaca, Nova Treviso. MCP 48481, 1, 29.0 mm SL, rio Carreiro, Serafina Corrêa. MCP 49496, 2, 51.8–69.8 mm SL, creek tributary, Turvo. MCP 49473, 1, 43.7 mm SL, arroio Anastasio, Nova Bassano. MCP 49484, 2, 29.7–29.5 mm SL, creek tributary, Vila Flores. MCP 49476, 1, 551.6 mm SL, creek tributary, Turvo. MCP 35046, 1, 69.1 mm SL, rio Turvo, Turvo. MCP 35048, 2, 49.4–85.4 mm SL, rio da Prata, Guabiju. MCP 40947, 2, 58.8–82.0 mm SL, Arroio Herval, Nova Prata. MCP 40932, 6, 46.9–86.3 mm SL, rio da Prata, Nova Prata. MCP 40934, 3, 75.8–109.7 mm SL, rio Carreiro, Serafina Corrêa. MCP 21110, 4, 21.2–80.4 mm SL, arroio Herval, Guabiju. MCP 22200, 4, 20.9–119.3 mm SL, rio da Prata, Guabiju. MCP 22256, 5, 39.3–87.9 mm SL, arroio Atanasio, Nova Bassano. MCP 22268, 2, 40.0–43.0 mm SL, creek tributary of rio Guaporé, Dois Lajeados. Rio Jacuí drainage: UFRGS 8785, 13 (2 c&s), 34.8–124.6 mm SL, creek in Fazenda Sanga Funda, Pantano Grande (30°17'38.00"S 52°20'59.00"W). UFRGS 17415, 12, 40.8–84.1 mm SL, creek tributary to arroio Calombos, Eldorado do Sul (30° 6'44.30"S

51°40'44.20"W). UFRGS 21199, 87 (2 c&s), 27.6–133.8 mm SL, creek tributary to arroio Caiboate-Mirim, São Gabriel (30° 7'30.47"S 54°19'34.37"W). UFRGS 18172, 3, 62.0–87.2 mm SL, creek in Estação Agronômica da UFRGS (30° 6'49.10"S 51°41'0.01"W). UFRGS 2548, 1, 32.4 mm SL, arroio Passo dos Buracos, Santa Maria. UFRGS 8184, 20, 38.6–149.9 mm SL, creek tributary to arroio Capivari, Encruzilhada do Sul. UFRGS 8698, 17, 33.5–90.0 mm SL, creek in Fazenda Panorama, Santa Margarida do Sul. UFRGS 19967, 5, 41.0–53.4 mm SL, rio dos Caixões, Espumoso. UFRGS 14983, 1, 35.0 mm SL, arroio Passo dos Buracos, Júlio de Castilhos. UFRGS 8713, 3, 44.1–81.4 mm SL, tributary, Butiá. UFRGS 20359, 14, 48.4–90.1 mm SL, arroio Giuliani, Faxinal do Soturno. UFRGS 8721, 28, 535–106.0 mm SL, creek tributary, Rio Pardo. MCP 16291, 1, 120.0 mm SL, Arroio Pessegueiro, Caçapava do Sul. MCP 17330, 5, 28.9–71.2 mm SL, Arroio Martins, Butiá. MCP 18628, 2, rio Pardo, Candelária. MCP 9284, 1, 62.4 mm SL, arroio Paraíso, Cachoeira do Sul. MCP 18250, 2, 62.2–78.8 mm SL, creek tributary to rio Soturno, Faxinal do Soturno. MCP 17247, 7, 31.0–61.7 mm SL, rio São Sepé, São Sepé. MCP 9485, 1, 107.5 mm SL, rio Pardinho, Santa Cruz do Sul. MCP 21579, 1, 51.3 mm SL, rio Pequeno, Sinimbu. MCP 21222, 2, 75.6–120.7 mm SL, creek tributary, Agudo. MCP 21294, 1, 73.2 mm SL, Agudo. MCP 21307, 1, 75.5 mm SL, arroio Corupá, Agudo. MCP 34807, 19, 42.9–125.3 mm SL, arroio Quitéria tributary to arroio dos Ratos, São Jerônimo. MCP 34806, 5, 45.4–132.8 mm SL, creek tributary to arroio dos Ratos, São Jerônimo. MCP 39214, 7, 68.0–130.2 mm SL, creek tributary, Encruzilhada do Sul. MCP 34534, 2, 156.0–152.9 mm SL, creek tributary to arroio Grande, Mariana Pimentel. MCP 21243, 2, 99.5–112.9 mm SL, arroio Linha das Flores, Agudo. MCP 27764, 2, 119.4–119.0 mm SL, arroio Corupá, Agudo. MCP 22719, 2, 58.5–86.1 mm SL, creek tributary of rio Soturno, Faxinal do Soturno. MCP 25725, 2, 67.9–82.0 mm SL, arroio Corupá, Agudo. MCP 26984, 3, 72.6–93.8 mm SL, arroio Corupá, Agudo. Lago Guaíba drainage: UFRGS 15137, 1, 47.6 mm SL, creek tributary, Porto Alegre. UFRGS 15138, 3, 82.5–144.9 mm SL, creek tributary, Porto Alegre. UFRGS 592, 1, 145.6 mm SL, arroio pequeno Dilúvio, Viamão. MCP 18804, 2, 48.3–48.9 mm SL, banhado na fazenda São Maximiano, Guaíba. Laguna dos Patos drainage: UFRGS 7644, 9, 36.3–58.0 mm SL, creek tributary to arroio Grande, Herval UFRGS 12573, 1, 190.8 mm SL, Arroio do Pinto, São Lourenço do Sul. MCP 23774, 3, 59.7–152.1 mm SL, creek tributary to do

arroio Grande, São Lourenço do Sul. MCP 23777, 6, 36.0–65.2 mm SL, creek tributary of arroio Viúva Teresa, São Lourenço do Sul. MCP 23778, 20, 39.0–163.5 mm SL, creek tributary to arroio São Lourenço, São Lourenço do Sul. Rio Caí drainage: UFRGS 19736, 14, 45.7–122.8 mm SL, rio Piaí, Caxias do Sul. MCP 11480, 1, 128.5 mm SL, Arroio do Ouro, Feliz. MCP 11194, 4, 53.4–64.5 mm SL, rio Cadeia, Nova Petrópolis. MCP 11140, 13, 44.3–51.3 mm SL, creek tributary to rio Santa Cruz, São Francisco de Paula. MCP 20031, 1, 202.1 mm SL, arroio Feitoria, Ivoiti. MCP 11361, 1, 41.8 mm SL, São Sebastião do Caí. MCP 23006, 6, 44.2–57.6 mm SL, arroio Bom Jardim, Triunfo. MCP. Rio Gravataí drainage: UFRGS 22346, 1, 114.1 mm SL, creek tributary, Viamão. MCP 23878, 3, 32.64–68.3 mm SL, arroio Itajaçu, Glorinha. Rio Rolante drainage: UFRGS 2475, 1, 20.3 mm SL, arroio Dom Pedro, São Francisco de Paula. MCP, 10037, 8, 33.0–51.9 mm SL, arroio Moreira, Três Coroas. MCP 21729, 1, 40.7 mm SL, creek tributary, Dois Irmãos. Rio Piratini drainage: UFRGS 7646, 9 (1 c&s), 42.11–61.71 mm SL, arroio Paraguay, Pinheiro Machado ($31^{\circ}35'59.00"S$ $53^{\circ}24'15.00"W$). UFRGS 7648, 15 (2 c&s), 27.9–101.2 mm SL, flooded on the border BR-116, Pedro Osorio ($31^{\circ}54'50.00"S$ $52^{\circ}41'11.00"W$). UFRGS 4174, 1, 52.2 mm SL, arroio Ximbacú, São Luis Gonzaga. UFRGS 7645, 6, 35.8–75.6 mm SL, creek tributary to arroio Basílio, Herval. UFRGS 10167, 1, 66.2 mm SL, creek tributary to arroio Basílio. UFRGS 13667, 3, 46.1–80.4 mm SL, creek tributary to arroio Banhado Grande. UFRGS 13976, 1, 92.1 mm SL, arroio Basílio, Pelotas. UFRGS 13989, 1, 65.1 mm SL, creek tributary to arroio Mata Olho, Pelotas. UFRGS 13990, 1, 71.9 mm SL, creek tributary to arroio Caraça, tributary to arroio Basílio, Pelotas. UFRGS 13993, 6, 41.0–73.6 mm SL, creek tributary to arroio Basílio, Pelotas. UFRGS 13999, 1, 71.9 mm SL, creek tributary to rio Piratinizinho, Pelotas. UFRGS 14000, 1, 52.9 mm SL, arroio do Mudo, Pelotas. MCP 25141, 5, 57.7–1212.1 mm SL, arroio Arambaré, Pedro Osório. MCP 25066, 1, 48.1 mm SL, Arroio Reduzindo, Pedro Osório. MCP 25078, 19, 44.3–82.8 mm SL, arroio Santa Fé, Piratini. MCP 25166, 9, 54.2–123.3 mm SL, creek tributary, Pedro Osório. MCP 25065, 1, 40.7 mm SL, creek tributary, Piratini. MCP 25145, 6, 40.1–73.0 mm SL, arroio Paraguaia, Pinheiro Machado. MCP 38367, 33, 31.2–104.7 mm SL, creek tributary to arroio Arambaré, Pedro Osório. MCP 38376, 9, 50.4–179.4 mm SL, arroio Arambaré, Pedro Osório. MCP 34733, 9, 42.8–116.9 mm SL, arroio Arambaré, Herval. MCP 34751, 8, 45.0–134.3 mm SL, arroio dos Pires,

Pinheiro Machado. MCP 20547, 9, 30.9–145.0 mm SL, creek tributary, Pedro Osório. MCP 25173, 4, 59.7–152.1 mm SL, arroio Mata Olho, Pedro Osório. MCP 21430, 2, 73.0–116.7 mm SL, creek tributary of arroio Arambaré, Erval. MCP 21431, 4, 44.8–70.3 mm SL, arroio Reduzinho, Pedro Osório. MCP 25043, 3, 39.8–51.9 mm SL, arroio Piratinizinho, Piratini. MCP 25150, 3, 45.7–64.4 mm SL, rio Piratini, Piratini. MCP 25165, 14, 45.8–107.1 mm SL, arroio dos Pires, Pinheiro Machado. Rio Camaquã drainage: drainage: UFRGS 8384, 10 (1 c&s), 26.4–88.3 mm SL, rio Santa Maria, Bagé ($31^{\circ} 0'0.00''S$ $54^{\circ} 0'0.00''W$). UFRGS 13604, 2, 73.0–73.8 mm SL, creek in Fazenda Ferraria, Amaral Ferrador ($30^{\circ}50'46.26''S$ $52^{\circ}23'16.50''W$). UFRGS 13708, 11 (2 c&s), 40.4–61.2 mm SL, creek tributary to arroio Boici, Pinheiro Machado ($31^{\circ}29'37.00''S$ $53^{\circ}29'57.00''W$). UFRGS 8467, 1, 64.0 mm SL, creek tributary, Canguçu. UFRGS 8468, 1, 39.4 mm SL, creek tributary, Encruzilhada do Sul. UFRGS 10839, 16, 35.3–89.0 mm SL, creek tributary to arroio da Caneleira, Encruzilhada do Sul, UFRGS 13664, 8, 35.8–51.4 mm SL, creek tributary, Pinheiro Machado, UFRGS 21201, 44, 41.4–138.2 mm SL, Arroio Olaria, Santana da Boa Vista UFRGS 22110, 13, 35.8–56.9 mm SL, arroio das Neves, Santana da Boa Vista. MCP 25767, 5, 55.3–141.0 mm SL, creek tributary to arroio das Neves, Santana da Boa Vista. MCP 23776, 6, 27.3–56.5 mm SL, arroio Faxinal tributary to arroio Velhaco, Sentinela do Sul. MCP 25798, 7, 32.3–49.6 mm SL, arroio do Tigre, Bagé. MCP 25919, 6, 34.3–109.8 mm SL, creek tributary to arroio Camaquã Chico, Lavras do Sul. MCP 25923, 9, 28.6–122.0 mm SL, arroio da Mantiqueira, Lavras do Sul. MCP 25854, 9, 37.0–89.7 mm SL, arroio Camaquã Chico, Bagé. MCP 25943, 8, 34.9–80.0 mm SL, arroio Hilário, Lavras do Sul. MCP 25795, 2, 41.0–53.5 mm SL, arroio do Banhado, Caçapava do Sul. MCP 40838, 29, 26.8–70.4 mm SL, arroio Mantiqueira, Lavras do Sul. MCP 40804, 5, 50.5–74.6 mm SL, creek tributary to arroio das Lavras, Lavras do Sul. MCP 40756, 1, 47.2 mm SL, creek tributary to arroio das Lavras, Lavras do Sul.. MCP 25773, 1, 42.5 mm SL, creek tributary of arroio Pessegueiro, Caçapava do Sul. MCP 25903, 6, 27.5–103.7, rio Camaquã Chico, Lavras do Sul. Rio Jaguarão drainage: UFRGS 7649, 14 (1 c&s), 31.8–81.3 mm SL, arroio Bote, Herval ($32^{\circ} 7'58.50''S$ $53^{\circ}36'34.60''W$). UFRGS 3898, 5, 34.6–79.5 mm SL, arroio Candiota, Bagé ($31^{\circ}37'0.00''S$ $53^{\circ}41'0.00''W$). UFRGS 10612, 7 (1 c&s), 28.4–61.8 mm SL, creek tributary to rio Jaguarão, Candiota ($31^{\circ}26'55.00''S$ $53^{\circ}46'22.00''W$). UFRGS 15690, 2, 47.6–73.3 mm SL, creek tributary

to rio Jaguarão, Candiota ($31^{\circ}30'42.00"S$ $53^{\circ}49'32.00"W$). UFRGS 3901, 6, 39.1–89.4 mm SL, arroio Candiota, Bagé. UFRGS 3907, 9, 19.9–72.4 mm SL, arroio Candiota, Bagé. UFRGS 3911, 1, 22.0 mm SL, arroio Candiota Bagé. UFRGS 7647, 11, 40.3–65.3 mm SL, creek tributary to Jaguarão Chico UFRGS 8386, 5, 22.4–36.9 mm SL, arroio Minuano, Aceguá. UFRGS 11802, 4, 39.3–45.5 mm SL, rio Jaguarão Chico, Hulha Negra. UFRGS 6603, 38.5 mm SL, arroio Quebra Jugo, Candiota. UFRGS 10662, 19, 174.8 mm SL, Candiota. MCP 27181, 1, 25.6 mm SL, arroio Candiota, Candiota. MCP 27185, 4, 25.7–34.9 mm SL, arroio Quebra Jugo, Candiota. MCP 27188, 2, 22.4–107.0 mm SL, arroio Candiota, Candiota. MCP 26157, 11, 25.3–72.8 mm SL, arroio Candiota, Candiota.

Genseq-4 COI. UFRGS 17557; GenBank accession number XX##### and GenBank accession number XX#####. UFRGS 17890; GenBank accession number XX#####. UFRGS 21199; GenBank accession number XX#####, GenBank accession number XX##### and GenBank accession number XX#####. UFRGS 21201; GenBank accession number XX##### and GenBank accession number XX#####. UFRGS 18089; GenBank accession number XX##### and GenBank accession number XX#####. UFRGS 11930; GenBank accession number XX##### and GenBank accession number XX#####. 21202; GenBank accession number XX#####. UFRGS 11933; GenBank accession number XX##### and GenBank accession number XX#####. UFRGS 21200; GenBank accession number XX#####. UFRGS 21955; GenBank accession number XX#####. UFRGS 20687; GenBank accession number XX##### and GenBank accession number XX#####.

Genseq-4 CytB. UFRGS 21519; GenBank accession number XX#####, UFRGS 11933; GenBank accession number XX#####, UFRGS 11930; GenBank accession number XX#####, UFRGS 17890; GenBank accession number XX#####, UFRGS 17557; GenBank accession number XX#####.

***Heptapterus* sp.n.A, new species**

(Figs. 4 A–C; Tab. 2)

Holotype. UFRGS 22840, 106.9 mm SL, Brazil, Rio Grande do Sul, Vacaria, creek Passo do Portão tributary of rio Pelotas, upper rio Uruguay basin, 28°11'4"S 51°00'02", 11 Nov 2014, T. Guimarães, C. Hartmann, B. Menezes, M. Ângelo & F. Luiz Henrique.

Paratypes: All from Brazil. Upper rio Uruguai drainage: Rio Grande do Sul: MNRJ 50716, 2, 46.4–67.85 mm SL; MUSM 60281, 2, 59.4–74.7 mm SL; UFRGS, 22061, 17, (2 c&s) 46.1–138.0 mm SL, collected with the holotype. LIRP XXXX, 5, 56.5–128.6 mm SL; MNRJ 50717, 2, 61.5–106.3 mm SL; UFRGS 21105, 57 (5 c&s), 35.8–122.8 mm SL, Vacaria, stream Passo dos Cabos tributary of rio Pelotas, 28°11'47"S 50°58'20"W, 11 Nov 2014, T. Guimarães, C. Hartmann, B. Menezes, M. Ângelo & F. Luiz Henrique. MUSM 60282, 2, 55.5–123.7 mm SL; UFRGS 22062, 15 (6, 9) (2 c&s), 36.5–126.8 mm SL, Vacaria, creek tributary of rio Leão tributary of rio Pelotas, 28°10'10"S 50°57'57"W, 10 Nov 2014, T. Guimarães, C. Hartmann, B. Menezes, M. Ângelo & F. Luiz Henrique. Santa Catarina: UFRGS 22060, 5, 44.7–131.3 mm SL, Painel, rio Pelotinhos tributary of rio Pelotas, 27°59'09"S 50°11'10"W, 8 Nov 2014, T. Guimarães, C. Hartmann, B. Menezes, M. Ângelo & F. Luiz Henrique.

Genseq-2 COI. UFRGS 21105; GenBank accession number XX#####.

Diagnosis: *Heptapterus* sp.n.A is distinguished from *H. mbya* and *H. qenqo* by the number of anal-fin rays (18–21 vs. 15–17 rays), additionally from *H. mbya* by the orbital diameter (9.9–13.3 vs. 13.8–17–9 % of HL) and short adipose fin (40.9–46.0 vs. 47.4–58.7 % of SL); from *H. qenqo* by the caudal peduncle length (15–19.7 vs. 19.8–25.4 % of SL); from *Heptapterus* sp.n.B by the number of lateral line pores (20–43 vs. 8–19 pores), unbranched anal-fin rays (5 vs. 3–4 rays) and body width (12.8–15.2 vs. 10.6–12.6 % of SL); from *H. mustelinus* by the head width (71.9–81.1 vs. 60.8–71.3 % of HL), number of vertebrae (52–53 vs. 54–60 vertebrae) and posterior cranial fontanel narrower than anterior (vs. posterior and anterior fontanel of equal width).

Description. Morphometric data presented in Tab. 2. Body elongate, in cross section almost cylindrical anteriorly until dorsal fin and compressed gradually until caudal

peduncle. Dorsal body profile convex, curving in arch from supraoccipital to base of dorsal fin; dorsal profile nearly straight from dorsal fin base to adipose-fin origin and gently convex from adipose fin origin to base of caudal fin. Ventral profile of head slightly convex from snout tip to opercular opening; body convex from opercular opening to pelvic girdle and nearly straight from pelvic origin to base of caudal fin. Forty-five chevron shaped myotomes visible through skin, progressively narrower and more angled posteriorly. Dense deposits of fatty material in globose bodies (papillae), commonly seen in heptapterids, dorsal surface more perceptible than ventral, skin with large papillae. Anus and urogenital pore very close to each other. Head small (0.2 times its SL), wide (0.7–0.8 times its HL), depressed (0.4–0.5 times its HL) and trapezoid in dorsal view (Fig. 4 B). Anterior nostril close to upper lip. Posterior nostril more close to margin of eye than anterior nostril. Distance between posterior nostrils same as between anterior nostrils. Four nostrils arranged as in vertices of rectangle. Posterior and anterior nostrils lacking barbels. Mouth wide, subterminal, with snout projecting slightly beyond jaw. Barbels jaw short, slender and tapering progressively towards their distal extremities. Maxillary barbels longest, inserts above upper lip and lateral to anterior nostrils; tip maxillary barbels surpassing the pectoral-fins insertion. Mental-barbels base inserted midway between anterior border of lower jaw and gular fold. Outer mental barbels longer than inner barbels, and inserted nearly behind fourth pore of preoperculomandibular laterosensory canal (pm4), tip reaching outer border of branchiostegal membrane. Inner mental barbels inserted slightly in advance of vertical through origin of outer mental barbel, approximately behind third pore of preoperculomandibular laterosensory canal (pm3), tip of inner mental barbel passing inner border of branchiostegal membrane. Small eyes, elliptical horizontally. Skin over eye, with lens slightly visible. Eye gently dorsal positioned, anteriorly at midpoint between tip of snout and corner of opercular membrane. Pupil rounded.

Dorsal fin distally rounded in profile; first dorsal-fin ray unbranched, soft, slightly small (0.7–0.9 times maximum length) and triangular; followed by 6 branched rays; origin of dorsal fin approximately on vertical or gently anterior portion of pelvic-fin origin. Pectoral fin with distal margin rounded, with i,7(30) rays; first fin ray slightly convex, most proximal portion of first ray slightly rigid and distal portion soft, slightly small (0.6–0.8 its maximum length); second pectoral-fin ray (first branched) gently shorter than third ray (second branched). Pelvic fin with distal margin rounded, with i+5

(30) rays; first pelvic fin ray unbranched, completely flexible and slightly smaller than second and third rays (first and second branched rays, respectively); tip of pelvic fin surpassing anus and urogenital papillae; pelvic-fin origin ahead of midpoint of body (excluding caudal fin) and behind vertical through base of first branched dorsal-fin ray. Anal-fin margin straight or slightly convex in lateral profile; with 19–20 rays (v+14(1), v+15(3)); anal-fin base small (0.18–0.25 times its SL), base covered basally with muscular tissue; origin of anal-fin posterior of adipose-fin origin, posterior limit of anal-fin base posterior to middle adipose-fin base length. Adipose fin long (0.41–0.46 times its SL), convex in lateral profile, base with darker fleshy tissues; distance from last dorsal-fin ray to adipose-fin origin less than length of dorsal-fin base; origin of adipose fin posterior of midpoint of body (excluding caudal fin) and posterior adipose-fin continuing to procurent rays of dorsal caudal-fin lobe. Caudal fin rounded; dorsal lobe slightly longer than ventral lobe, six or seven branched rays in dorsal lobe and eight branched rays in ventral lobe. Total caudal fin-rays 46(1), 47(2) or 48(1); with 18(3) or 19(1) rays in dorsal lobe; and 28(2), 29(1) or 30(1) rays in ventral lobe.

Sensory canals of head with simple tubes ending in single pores. Supraorbital canal with six pores: s1, s2+i2, s3, s6 (epiphyseal branches fused to each other, with a single pore), s7 and s8. Infraorbital canal with five pores: i1, i3, i4, i5 and i6. Preoperculomandibular canal with 11 pores: pm1, pm2, pm3, pm4, pm5, pm6, pm7, pm8, pm9, pm10 and pm11. Postotic canal with 3 pores: po1, po2 and po3. Lateral line incomplete; straight and continuous without interruption until posterior dorsal fin base to vertical through base of last unbranched anal-fin ray, with 20 to 43 pores. Total vertebrae, 52(2) or 53(3); 17(5) pre-caudal vertebrae and 35(2) or 36(3) caudal vertebrae. Ribs, 7(4) or 8(1) pairs. Insertion of dorsal fin behind to 12(5) vertebrae and anal fin anterior to 26 vertebrae.

Color in alcohol: Dorsal and sideways of body dim gray and ventral surface cream. Upper portion of head and checks covered by dim gray pigment becoming gradually less intensive ventrally, ventral surface of head cream; dark brown trapezoid spot dorsally on head between eyes and supraoccipital; dark brown longitudinal stripe on post orbital, between posterior orbital to border inner of branchiostegal membrane. Maxillary barbel dark brown dorsally and ventrally, with tip unpigmented. External mental barbel dark brown dorsally, tip and ventral surface unpigmented. Internal mental

barbel dark brown, tip and dorsal surface unpigmented. Trunk coloration varying from dim gray to brown; upper portion of trunk with four unclear dark brown transverse bars; first one narrow behind head, extended from one side of pectoral fin insertion to other side; second one in front of dorsal fin origin, third one reaching to dorsal fin base and last one in front of adipose-fin origin. Base of caudal-fin with diffuse dark brown spot semicircle-shape, caudal fin rays dim gray and interradial caudal-fin membrane brown. Dorsal, anal, pectoral and pelvic fins rays with high concentration of gray chromatophores and interradial membranes brown; fins base darker than distal. Adipose fin gray, base with intense concentration of dark chromatophores. Black thin stripe along lateral line, gently convex above pectoral-fin and from that point to middle caudal peduncle straight.

Sexual dimorphism: No external sexual dimorphism observed, males and females identified through dissection only.

Geographic distribution: *Heptapterus* sp.n.A is distributed in tributaries of rio Pelotas, tributary of upper Uruguay basin in Rio Grande do Sul and Santa Catarina, Brazil. (Fig. 7).

Heptapterus sp.n.B, new species

Figures 6 A–C; Table 3.

Holotype: UFRGS 22500, 64.0 mm SL, Brazil, Rio Grande do Sul, Quevedos, Sanga das Tunas, tributary of rio Ibicuí, rio Uruguai drainage, 29°21'1"S 54°12' 38"W, 12 Mar 2014, Dala Corte R. B., Hartmann C., Lampert V. & Santos M.

Paratypes: All from Brazil: rio Ibicuí drainage: Rio Grande do Sul: LIRP 14134, 20, 43.6–63.7 mm SL; MNRJ 50718, 2, 50.4–61.1 mm SL; MUSM 60283, 5, XX–XX mm SL; UFRGS 19799, 69, (2 c&s), 30.1–73.8 mm SL, collected with holotype. MCP 27557, 1, 39.2 mm SL, Tupanciretã, creek tributary of rio Santana, rio Jaguari, near Jari, 29°13'56"S 54°21'23"W, 11 May 2001 Lucena C., Silva J., Pereira E. & Bertaco V. MCP 27622, 1, 60.2 mm SL, Tupanciretã, rio Santana, near Jari, tributary of rio Ibicuí, 29°14'33"S 54°16'47"W, 11 May 2001 Lucena C., Silva J., Pereira E. & Bertaco V. MUSM 60284, 2, 56.2–76.8 mm SL; UFRGS 19796, 26 (2 c&s), 38.6–72.3 mm SL, Quevedos, Sanga das Tunas, 29°21'1"S 54°12'38"W, 12 Mar 2014, Dala Corte R. B., Hartmann C., Lampert V. & Santos, M. MNRJ 50719, 2, 42.5–75.0 mm SL; UFRGS

19797, 12, 29.2–73.6 mm SL, Jari, tributary of arroio Sampaio, 29°17'38"S 54°2'3"W, 11 Mar 2014, W Dala Corte R. B., Hartmann C., Lampert V. & Santos, M. UFRGS
19798, 2, 31.5–46.3 mm SL, Quevedos, Lajeado Monjolo, 29°19'4"S 54°7'19"W, 11 Mar 2014, Dala Corte R. B., Hartmann C., Lampert V. & Santos, M. UFRGS 22546, 6, 24.7–51.3 mm SL, Jari, Lajeado, Quebra Dentes, 29°24'1"S 54°18'5.7"W, 10 Mar 2014, Hartmann C., Dala Corte R. B., Lampert V. & Santos, M.

Genseq-2 COI. UFRGS 19796, GenBank accession number XXXXXXXXX. UFRGS
19797, GenBank accession number XXXXXXXXX.

Genseq-2 CytB. UFRGS 19796, GenBank accession number XXXXXXXXX. UFRGS
19797, GenBank accession number XXXXXXXXX.

Diagnosis: *Heptapterus* sp.n.B is distinguished from *H. mbya* and *H. qenqo* by having six supraorbital pores (vs. four and five, respectively); additionally *Heptapterus* sp.n.B is further distinguished from *H. mbya* by the orbital diameter (8.4–12.8 vs. 13.8–17.9 % of HL); from *H. qenqo* by the depth head at supra-occipital (32.2–41.8 vs. 42.0–54.4 % of SL); from *H. mustelinus* and *Heptapterus* sp.n.A by the number of lateral line pores (8–19 vs. 20–51 and 20–43 pores respectively), unbranched anal-fin rays (3–4 vs. 5–7 and 5 rays respectively), caudal-fin rays on the ventral lobe (23–25 vs. 26–31 and 28–30 rays respectively); additionally from *H. mustelinus* by the number of vertebrae (51–53 vs. 54–60 vertebrae); from *Heptapterus* sp.n.A by the body width (10.6–12.6 vs. 12.8–15.2 % of SL) and posterior cranial fontanel equal than anterior (vs. posterior fontanel narrower than anterior).

Description: Morphometric data presented in Table 3. Body elongate, nearly cylindrical in cross section until dorsal fin and compressed on caudal peduncle. Head depressed, dorsal profile straight from snout tip to supra-occipital. Dorsal profile slightly convex from supra-occipital to dorsal-fin base, nearly straight from dorsal-fin base to adipose-fin origin and gently convex from that point to caudal fin. Ventral profile of head slightly convex from snout tip to opercular opening, nearly convex from that point to pelvic girdle, straight from pelvic-fin insertion to anal-fin insertion and nearly convex from that point to base of caudal fin. Deposits of fatty material in globose bodies, commonly seen in heptapterids, perceptible through skin. Skin of top head, opercle and lateral of body anterior to dorsal fin with papillae. Skin of ventral surface of body

without papillae. Anus and urogenital pore close to each other. Head small, depressed and trapezoid in dorsal view (Fig. 6 B). Anterior nares tubular close to upper lip. Posterior nares more close to anterior margin of eye than to anterior nares. Distance between posterior nares greater than between anterior nares. Four nares arranged as in vertices of trapezoid. Posterior and anterior nares lacking barbels. Mouth wide, subterminal, with snout projecting gently beyond lower jaw. Mental barbels short, slender and tapering progressively towards distal extremity. Maxillary barbel longest, inserted above upper lip and lateral or slightly posterior to anterior nares; tip of maxillary barbel surpassing pectoral-fin insertion in large specimens. Mental-barbel base inserted midway between anterior border of lower jaw and gular fold. Outer mental barbel longer than inner barbel, and inserted nearly behind fourth pore of preoperculomandibular laterosensory canal (pm4); tip of outer mental barbel passing the outer border of branchiostegal membrane. Inner mental barbel inserted slightly in advance of vertical through origin of outer mental barbel, approximately behind second pore of preoperculomandibular laterosensory canal (pm2); tip of inner mental barbel reaching the inner border of branchiostegal membrane. Eyes small, elliptical horizontally. Skin over eye thin, with lens slightly visible. Eye dorsally positioned, anterior to midpoint between tip of snout and corner of opercular membrane. Pupil rounded.

Dorsal fin distally rounded in profile. First dorsal-fin ray (soft) small and distal tip triangular, followed by 6 branched rays; origin of dorsal fin approximately on vertical or gently anterior to pelvic-fin origin. Pectoral fin with distal margin rounded, with one unbranched and 7(30) branched rays. First fin ray slightly convex; short (6.2–7.8 of its entire pectoral length) and most of proximal portion inflexible and distal portion soft. Second pectoral-fin ray (first branched) approximately as long as third ray (second branched). Pelvic fin convex posteriorly, with i+5(30) rays. Unbranched pelvic-fin ray completely flexible, segmented and slightly shorter than second and third rays (first and second branched rays, respectively). Tip of pelvic fin surpassing anus and urogenital papillae. Pelvic-fin insertion well ahead of midpoint of body (excluding caudal fin) and on vertical through base of first unbranched dorsal-fin ray. Anal-fin margin straight or slightly convex in lateral profile; with iii+14(1), iv+13(1), iv+14(2) rays. Anal-fin base small, covered basally with thick muscular tissue. Anal-fin origin clearly posterior of adipose-fin origin; posterior limit of anal-fin base posterior to

middle adipose-fin base length. Adipose fin long reaching up to nearly half of standard length, gently convex in lateral profile, base with fleshy tissues more dark. Distance from dorsal-fin to adipose-fin more than length of dorsal-fin base, origin of adipose fin gently posterior of midpoint of body (excluding caudal fin) and posterior adipose-fin continuing to procurent rays of caudal-fin. Dorsal lobe of caudal fin rounded and longer than ventral lobe; six and five branched rays in dorsal and ventral lobes, respectively (4 c&s specimens). Total caudal-fin rays 42(3) and 43(1); with 23(1), 24(1) and 25(2) fin rays on the ventral lobe; 11(2), 12(1), and 13(1) branched rays on principal caudal-fin.

Sensory canals of head with simple tubes ending in single pores. Supraorbital canal usually with six pores: s1, s2+i2, s3, s6 (epiphyseal branches not fused to each other, each one with its pore), s7 and s8. Infraorbital canal with five pores: i1, i3, i4, i5 and i6. Preoperculomandibular canal with 11 pores: pm1, pm2, pm3, pm4, pm5, pm6, pm7, pm8, pm9, pm10 and pm11. Postotic canal with 3 pores: po1, po2 and po3. Lateral line incomplete, straight and continuous until region below dorsal fin origin and adipose fin origin, with 8 to 19 pores. Total vertebrae 51(1), 52(2) and 53 (1); 15(2) or 16(2) precaudal vertebrae and 35(1), 36(1), 37(1) or 38(1) caudal vertebrae. Seven (4) pairs of ribs. Insertion of dorsal fin behind to 11(4) vertebrae and anal fin anterior to 26 vertebrae.

Color in alcohol: Body brownish dorsally to cream ventrally. Upper portion of head and cheeks covered by dark brown pigment becoming less concentrated with scattered melanophores ventrally. Dark brown trapezoid spot dorsally on head between eyes and supraoccipital. Maxillary barbel dark brown dorsally and light brown ventrally, with tip unpigmented. External mental barbel light brown dorsally at base, unpigmented ventrally. Internal mental barbel unpigmented. Overall trunk coloration varying from dark brown, light brown and cream. Trunk with narrow dark brown bar above pectoral fins, contacting each other dorsally. Upper portion of trunk with four dark brown transverse bars; one behind head, extended from just above pectoral-fins insertion and contacting each other dorsally; second nearly rectangular and elongated anteriorly before dorsal fin insertion; third small and narrow along the base of last dorsal-fin rays, and fourth not clearly delineated in front of adipose-fin origin. Area between dorsal and adipose fins light brown. Thirty-eight chevrons shaped lines marking the myosepta, progressively narrower and more angled posteriorly. Base of caudal-fin with semicircle-

shape dark spot, caudal-fin rays densely brown-pigmented and interradial caudal-fin devoid of chromatophores. Dorsal, anal, pectoral and pelvic fins rays with high concentration of gray or brown chromatophores and interradial membranes translucent. Base of adipose fin with intense concentration of brown chromatophores and distal region translucent. Black thin stripe along lateral line, slightly convex above pectoral-fin and from that point to middle caudal peduncle straight.

Sexual dimorphism and notes: Urogenital pore tubular in males and trapezoidal in females. The stomach content is mainly composed of Ephemeroptera and larvae of Coleoptera, all of them autochthonous (aquatic), which allows characterize it as insectivorous.

Geographic distribution: Tributaries of rio Ibicuí, río Uruguay drainage, Rio Grande do Sul, Brazil (Fig. 3).

Molecular results

Comparisons of Kimura 2 parameters (K2P) genetic distance among *Heptapterus* sp.n.B and *H. mustelinus* populations, *Heptapterus* sp.n.A and *H. mustelinus* populations further supported the recognition of these two different species. The values of pairwise K2P distance range were 0.3% to 1.4% between *H. mustelinus* populations; 4.7% to 5.1% between *H. mustelinus* and *Heptapterus* sp.n.B; 2.6% to 3.1% between *H. mustelinus* and *Heptapterus* sp.n.A.

Fourteen distinct haplotypes of *COI* were found for *Heptapterus mustelinus*. Eleven haplotypes were exclusive of the twelve *H. mustelinus* populations distributed in the rio Uruguai (H1 - Alto Uruguai; H2 - rio Ijuí; H3 - rio Ibicuí; and H4 - rio Quaraí), rio Negro and rio Maquiné (H5), and Laguna dos Patos drainages (H6 - rio Taquari; H7 - rio Jacuí; H8 – rio Camaquã; and H9 - rio Jaguarão) and rio Mampituba (H10 and H11); one haplotype was exclusive of *Heptapterus* sp.n.A (H-12) and two haplotypes were exclusive of *Heptapterus* sp.n.B (H-13 and H14). There are at least 13 mutations between *H. mustelinus* and *Heptapterus* sp.n.A haplotypes; and 27 mutations between *H. mustelinus* and *Heptapterus* sp.n.B haplotypes (Fig. 13).

Molecular phylogenetic analysis of the concatenated alignment showed *Heptapterus* sp.n.A, *Heptapterus* sp.n.B and *H. mustelinus* as monophyletic groups with strong statistical support for each molecular analysis. Maximum Likelihood (ML)

analyses showed all nodes with strong support (ML: 100), with *Heptapterus mustelinus* as monophyletic and compound by three different lineage (Ibicuí, Ijuí and Mampituba). Although the composition of three different lineages inside of *H. mustelinus* clade, under high statistical support, these does not have morphological differences and it is justification to keep them as *H. mustelinus* and not as new species. Strong statistical support (ML: 100) were also recovered for the new species (Fig. 14). Bayesian Inference (BI) analyses found strong support for *Heptapterus* sp.n.A and *Heptapterus* sp.n.B (BI: 1) as independent linages; and found strong support for *H. mustelinus* clades monophyletic (BI: 0.88) (Fig. 15).

Species delimitation analyses using the General Mixed Yule-Coalescent (GMYC) estimated under a Birth-Death model prior of branching rates showed a threshold time of $-2,3 \times 10^{-3}$, which indicates the time before all nodes reflect diversification (left red bar) and after which all nodes reflects the coalescent events (right red bar) (Fig. 16). The maximum likelihood for the null model was 183.397, and the maximum likelihood for the GMYC model was 183.801. Single threshold models from GYMC also supported the presence of seven operational taxonomy units (OTUs) (Fig. 16); three of them are morphologically distinct. The results obtained in *Heptapterus mustelinus* group showed that the species limits appears in a fixed order; in some cases, the morphological limits appeared before the genetic limits as observed *Heptapterus* sp.n.A and *Heptapterus* sp.n.B, and in other cases genetic limits appeared before morphological limits as observed in *Heptapterus mustelinus* population from Ibicuí, Ijuí and Mampituba. The results for *Heptapterus mustelinus* populations shows that it is a species complex using these techniques if we explore them with other techniques and methodologies we can clarify the underestimated diversity hidden in *H. mustelinus*.

Regardless the overall similarity between *H. mustelinus*, *Heptapterus* sp.n.A and *Heptapterus* sp.n.B both morphological and genetic data reciprocally supports the recognition of the three separate species.

Discussion

Heptapterus belongs to the *Nemuroglanis* sub-clade together with *Acentronichthys* Eigenmann & Eigenmann, *Cetopsorhamdia* Eigenmann & Fisher, *Chasmocranus* Eigenmann, *Heptapterus* Bleeker, *Horiomyzon* Stewart, *Imparfinis* Eigenmann & Norris, *Mastiglanis* Bockmann, *Nannoglanis* Boulenger, *Nannorhamdia* Regan, *Nemuroglanis* Eigenmann & Eigenmann (including *Imparales* Schultz and *Medemichthys* Dahl - see Bockmann & Ferraris, 2005), *Pariolius* Cope, *Phenacorhamdia* Dahl, *Phreatobius*, *Rhamdioglanis* Ihering, *Rhamdiopsis*, and *Taunayia* Miranda-Ribeiro. This is a well-supported group with 16 synapomorphies (see introduction) (Ferraris, 1988; Bockmann, 1994). All of these synapomorphies have been verified and were found in *H. mustelinus*, *H. qenqo*, *Heptapterus* sp.n.A and *Heptapterus* sp.n.B.

Heptapterus sp.n.A and *Heptapterus* sp.n.B are the most similar species in general body shape to *H. mustelinus*. These two new species have less vertebrae number when compared with *H. mustelinus* (Fig. 8 A).

Heptapterus sp.n.A is distinguished from *H. mustelinus* by the type of the posterior cranial fontanel, which in the first one is narrower than anterior (Fig. 4) and in the second one the posterior and anterior fontanel have similar wide (Fig. 3). In addition, morphometric differences were found between *Heptapterus* sp.n.A and *H. mustelinus* (Fig. 9 B). Head width (M28), internal mandibular barbel length (M34) and head width at posterior nostril (M42) were the most significantly measurements to separate these two species (Fig. 9 A), and that is supported through linear regressions analysis, in which 95% confidence intervals does not overlap (Fig. 10 A–B).

Heptapterus sp.n.B and *H. mustelinus* can be distinguished by the number of unbranched anal-fin rays (Fig. 8 C), number of pores on the lateral line (Fig. 8 B), and number of rays on the ventral lobe of the caudal-fin (Fig. 8 D). The reduction of lateral line, with 8–19 pores, might be a putative synapomorphy of *Heptapterus* sp.n.B. This feature is also observed in other heptapterids like *Gladioglanis*, *H. sympterygium*, *Phreatobius*, *Taunayia* sp. and *Rhamdiopsis* (Reichel, 1927; Buckup, 1988; Ferraris & Mago-Leccia, 1989; Lundberg *et al.*, 1991; Shibatta *et al.*, 2007 and Bockmann & Castro, 2010). In *Heptapterus* sp.n.B the extension of lateral line is small, reaching the region of the posterior postotic sensory branch 3 to posterior of dorsal-fin base, like in some specimens of *H. mustelinus*, but with significant different number of lateral line

pores (Fig. 8 B). *Heptapterus mustelinus* reaches the largest body size (maximum observed SL 154.6 mm), doubling the body size of largest measured specimen of *Heptapterus* sp.n.B (SL 73.6 mm). When compared through visual analysis, *Heptapterus* sp.n.B has a slender and narrower body than *H. mustelinus*, but these differences are not reflected in discrete variations in body proportions related to body width and body depth (Table 3). Nevertheless, body shape is significantly different among these two species, as demonstrated in the scatterplot analysis of the differences of the polar coordinates obtained for each species (Fig. 11). Prepectoral distance (M3), body depth (M6) and head width (M28) is significantly different either comparing individuals measured of all range of body size (Fig. 11 A). Comparing individuals of the same range of body size of the two species the significant differences observed were on the predorsal distance (M1), head width (M28) and head width at posterior nostril (M43) (Fig. 11 B). Differences in body shape were more clearly demonstrated through linear regressions analysis, in which we could observe that the 95% confidence intervals does not overlap with compared species indicating a significant difference in head width and body depth in specimens with corresponding body size ranges (Fig. 12 A–B), regardless the lack of discrete differences in body proportions (Table 3).

Note on synonym

Heptapterus eigenmanni is a junior synonym of *H. mustelinus* according to Buckup (1988). This statement was based in analyzes of type material and freshly preserved specimens from the type locality (Maldonado, Uruguay). Buckup (1998) designated the lectotype (MCZ 7597, wrongly cited as MCZ 7579 (Bockmann & Guazzelli, 2003)) and paralectotype (MCZ 6330 also wrongly cited as MCZ 63330) of *H. eigenmanni*. The corroboration of Backup's hypothesis was the limit of this work.

Heptapterus ornaticeps is herein considered as a junior synonym of *H. mustelinus*. The analysis of the type specimen (ZMB 20933) allowed us to note that this species has all morphological characteristics of *H. mustelinus*. In his unpublished doctoral dissertation Bockmann (1998) provided detailed information about *H. ornaticeps* and also suggests that this species could be junior synonymous of *H. mustelinus*. Bockmann (1998) had done comments about the erroneous designated type locality of *H. ornaticeps* as Rio de Janeiro. This author clarified it making reference to the book “*Fremdländische Subwasserfische*” of J. Paul Arnold aquarist who provided

the description of the species and mentions the type locality as “... südliches Brasilien und die anschließenden La Plata-Staaten” [Southern Brazil and adjacent platinum countries] same locality of distribution of *H. mustelinus* (Bockmann, 1998; Bockmann, pers comm.).

Distribution patterns

Heptapterus is widely distributed through Paraguay, Paraná, Uruguay basins, and coastal streams of Uruguay and southern Brazil. This pattern of distribution suggests that this genus is restricted to the southern zone of the Neotropical region which is well reported by several authors (Ringuelet *et al.*, 1967; Buckup, 1988; Miquelarena *et al.*, 1990; Bockmann, 1998; Bockmann & Guazzelli; 2003; Butí & Cancino, 2005; Aguilera *et al.*, 2011, Azpelicueta *et al.*, 2011; Bertaco *et al.*, 2016).

H. mustelinus has wide distribution along La Plata River, Uruguay River, Laguna dos Patos system, Tramandaí system and coastal streams of Uruguay and southern Brazil. Along of the coastal streams in Brazil, the northernmost register of *H. mustelinus* is Cubatão River near Santos, São Paulo State by Eigenmann (1917). Buckup (1988) suggested that this locality could be Cubatão River in Teresópolis (currently Águas Mornas), Santa Catarina State. We registered *H. mustelinus* until rio Itapocu, Joinville, Santa Catarina State (Fig. 7). The distribution of *H. mustelinus* through the eastern slope of the Andes in Argentina provided by Ringuelet *et al.*, 1967 was updated with the description of *H. qenqo* the only species occurring in this area (Aguilera *et al.*, 2011).

Heptapterus sp.n.A is the species of most restricted range of distribution. This species is only known from some tributaries of the rio Pelotas, in the upper rio Uruguay drainage (Fig. 7). We did not find these localities occupied by *H. mustelinus*. The distribution area of *Heptapterus* sp.n.A belongs to the Araucaria forest plateau, ecoregion in southern of Brazil restricted to the upper portions of the rio Uruguay and tributaries of the upper portion of the rio Jacuí. These areas were classified by Malabarba *et al.*, (2009) as having high endemism of fish species. These authors recognized eight endemic species for this area; *Astyanax brachypterygium* Bertaco & Malabarba, 2001; *Astyanax cremnobates* Bertaco & Malabarba, 2001; *Bryconamericus patriciae* da Silva, 2004; *Cnesterodon brevirostratus* Rosa & Costa, 1993; *Eurycheilichthys pantherinus* Reis & Schaefer, 1992; *Jenynsia eirmostigma* Ghedotti & Weitzman, 1995; *Pareiorhaphis eurycephalus* Pereira & Reis, 2002; *Pareiorhaphis*

vestigipinnis (Pereira & Reis, 1992). Further these, two species are described for this region *Trichomycterus tropeiro* Ferrer & Malabarba (2011) and *Eurycheilichthys castaneus* Reis (2017) both endemics from these geographically restricted areas. The description of *Heptapterus* sp.n.A is a new record of endemic fish for this ecoregion which added to the previously endemic species highlighting the importance of conservation of the rivers and creek from Araucaria forest plateau ecoregion.

Heptapterus sp.n.B is restricted to some creek tributaries of the rio Ibicuí, in the rio Uruguay drainage. Instead, several localities with habitats similar to those where the *Heptapterus* sp.n.B is found are commonly occupied by *H. mustelinus* (Fig. 7), being registered the co-occurrence of these two species in one locality (Lajeado Quebra Dentes, Jari municipality: UFRGS 22546 – *Heptapterus* sp.n.B and UFRGS 21200 – *H. mustelinus*). Ibicuí River is one of the main sub basins of rio Uruguay and is located at the Central Depression of Rio Grande do Sul characterized by present fine sand sediment (Bertaco *et al.*, 2016) making distinct and unique environmental for some endemic fish species as *Austrolebias ibicuiensis* Costa (1999) (temporary flooding) classified as critically endangered (Brazil Red Book Threatened Species of Fauna, 2016) and *Ituglanis inusitatus* restricted range to rio Ibicuí and rio Butuí (Ferrer & Donin, 2017). Given the restricted distribution of *Heptapterus* sp.n.B in rio Ibicuí (Fig 7 C) and not found of additional population, we could considered this species as endemic of this basin. Even though the rio Uruguay drainage is densely sampled in the Rio Grande do Sul state, Brazil (Bertaco *et al.*, 2016:405, fig. 2), we have failed to find additional populations of *Heptapterus* sp.n.A and *Heptapterus* sp.n.B.

Comparative material examined

Acentronichthys leptos. All from Brazil: São Paulo: UFRGS 10170, 4, 36.5–62.2 mm SL, rio Santos, Bertioga. UFRGS 10214, 3, 51.8–57.6 mm SL, stream 500m da polícia rodoviária, Ubatuba. UFRGS 10355, 1, 46.9 mm SL, Baía dos Santos, Cubatão.

Acentronichthys sp.n.A: UFRGS 18301, 7, 45.14.9–86.1 mm SL, Brazil, Paraná, Pontal do Paraná.

Heptapterus sympterygium. All from Brazil, Rio Grande do Sul: Rio Grande: Estação Ecológica do TAIM: UFRGS 698, 2, 26.6–29.8 mm SL. UFRGS 1201, 1, 25.5 mm SL. UFRGS 1202, 1, 23.1 mm SL. UFRGS 1203, 1, 25.7 mm SL. UFRGS 1204, 1, 24.7 mm SL. UFRGS 1200, 1, 32.9 mm SL. UFRGS 1205, 1, 31.8 mm SL. UFRGS 1206, 1, 16.0 mm SL. UFRGS 1207, 1,

33.3 mm SL. UFRGS 1208, 1, 30.6 mm SL. UFRGS 1209, 1, 38.4 mm SL. UFRGS 1210, 1, 25.7 mm SL. UFRGS 1211, 1, 31.7 mm SL. UFRGS 1212, 1, 29.6 mm SL. UFRGS 1213, 1, 25.6 mm SL. UFRGS 1214, 1, 21.2 mm SL. UFRGS 1216, 1, 17.3 mm SL. UFRGS 16251, 1, 31.6 mm SL. UFRGS 16877, 2, 33.3–50.5 mm SL. UFRGS 22365, 1, 65.4 mm SL, Viamão, Capão da Porteira. UFRGS 853, 1, 23.62 mm SL, Guaíba.

Heptapterus qenko: rio Paraná basin: Argentina: Sali-Dulce drainage: Tucumán: CI-FML 1098, 40, 81.8–146.7 mm SL, rio Tapia, Trancas. CI-FML 965, 11, 110.0–200.7 mm SL, Hualinchai, San Pedro de Colalao, Trancas. CI-FML 7109, 4, 84.5–138.7 mm SL, rio Rearte, Trancas. Salta: CI-FML 1356, 25, 121.4–200.2 mm SL, rio Sauzalito, Candelaria. MACN 3500, 5, 24.7–124.4 mm SL, río San Lorenzo. MACN 7911, 1, 141.4 mm SL, Porongal, Parque Nacional Baritú. MACN 11214, 3, 71.7–81.5 mm SL, río Calchaquí, Payogasta, Cachi. MACN 11519, 4, property El Duraznito, Rosario de la Frontera. Catamarca: MACN 5144, 1, 103.5 mm SL, dam El Lumeal.

References

- Aguilera, G., Mirande, J. M., & Azpelicueta, M. de las M. (2011). A new species of *Heptapterus* Bleeker 1858 (Siluriformes: Heptapteridae) from the Río Salí basin, north-western Argentina. *Journal of Fish Biology*, 78 (1), 240–250.
- Arratia, G., & Huaquin, L. (1995). Morphology of the lateral line system and of the skin of diplomystid and certain primitive loricarioid catfishes and systematic and ecological considerations. *Bonner Zoologische Monographien*, 36, 1–110.
- Azpelicueta, M. de las M., Aguilera. G., & Mirande, J. M. (2011). *Heptapterus mbya* (Siluriformes: Heptapteridae), a new species of catfish from the Paraná River basin, in Argentina. *Revue Suisse de Zoologie*, 118 (2): 319–327.
- Bandelt, H. J., Forster, P., & Rohl, A. (1999). Median-joining networks for inferring intraspecific phylogenies. *Molecular Biology and Evolution*, 16, 37–48.
- Bertaco, V. A., Ferrer, J., Carvalho, F. R., & Malabarba, L. R. (2016). Inventory of the freshwater fishes from a densely collected area in South America—a case study of the current knowledge of Neotropical fish diversity. *Zootaxa*, 4138(3), 401-440.
- Bleeker, P. (1858). Ichthyologiae Archipelagi Indici Prodromus.(De Vischen van den Indischen Archipel beschreven en toegelicht). Volumen I. Siluri. Batavia, Lange & Co. 370 p.
- Bockmann, F.A. (1994) Description of *Mastiglanis asopos*, a new pimelodid catfish from northern Brazil, with comments on phylogenetic relationships inside the subfamily Rhamdiinae (Siluriformes: Pimelodidae). *Proc. Biol. Soc. Wash.*, 107 (4), 760–777.
- Bockmann, F.A. (1998). Análise filogenética da família Heptapteridae (Teleostei: Ostariophysi: Siluriformes) e redefinição de seus gêneros. Unpublished Doctoral Dissertation. São Paulo, Universidade de São Paulo, 599.
- Bockmann, F. A., & Castro, R. (2010). The blind catfish from the caves of Chapada Diamantina, Bahia, Brazil (Siluriformes: Heptapteridae): description, anatomy, phylogenetic relationships, natural history, and biogeography. *Neotropical Ichthyology*, 8(4), 673-706.
- Bockmann, F. A., & de Pinna, M. C. C. (2004). *Heptapterus colletti* Steindachner, 1881: a member of the Asian bagrid genus *Olyra* erroneously assigned to the neotropical fauna. *Copeia*, 2004 (3), 665–675.

- Bockmann, F. A., & Guazzelli, G. M. (2003). Family Heptapteridae (Heptapterids). In: Reis, R. E., Kullander, S. O., & Ferraris, Jr, C. J. *Check list of the freshwater fishes of South and Central America*. Porto Alegre: Editora da Pontifícia Universidade Católica do Rio Grande do Sul-EDIPUCRS, pp. 406-431.
- Buckup, P.A. (1988). The genus *Heptapterus* (Teleostei: Pimelodidae) in southern Brazil and Uruguay, with the description of a new species. *Copeia*, 1988 (3), 641–653.
- Butí, C., & Cancino, F. (2005). Ictiofauna de la cuenca endorreica del río Salí-Dulce, Argentina. *acta Zoológica lilloana*, 49, 9-33.
- Chakrabarty, P., Warren, M., Page, L. M., & Baldwin, C. C. (2013). GenSeq: An updated nomenclature and ranking for genetic sequences from type and non-type sources. *Zookeys* 2013(346): 29-41.
- de Pinna, M. C. C. (1993). Higher-level phylogeny of Siluriformes, with a new classification of the order (Teleostei, Ostariophysi). New York, The City University of New York. 482 p. Unpublished Doctoral Dissertation
- Doyle, J. J., & Doyle, J. L. (1987). A rapid DNA isolation procedure for small quantities of fresh leaf tissue. *Phytochemical Bulletin*, 19: 11–15.
- Drummond, A.J., Suchard, M.A., Xie, D., & Rambaut, A. (2012). Bayesian phylogenetics with BEAUTi and the BEAST 1.7. *Molecular Biology and Evolution*, 29:1969–1973.
- Edgar, R.C., (2004). MUSCLE: multiple sequence alignment with high accuracy and high throughput. *Nucleic Acids Research*, 32:1792–7.
- Eschmeyer, W. N., & Fong, J. (2017). Species by family/subfamily in the Catalog of fishes, electronic version (June 2017). San Francisco (California Academy of Sciences).
- Excoffier, L., Laval, G. & Schneider, S. (2005). Arlequin ver. 3.0: an integrated software package for population genetics data analysis. *Evolutionary Bioinformatics Online*, 1, 47–50.
- Ferraris Jr, C. J. (1988). Relationships of the neotropical catfish genus Nemuroglanis, with a description of a new species (Osteichthys: Siluriformes: Pimelodidae). *Proceedings of the Biological Society of Washington*, 101(3), 509-516.

- Ferraris Jr, C. J., & Mago-Leccia, F. (1989). A new genus and species of pimelodid catfish from the Río Negro and Río Orinoco drainages of Venezuela (Siluriformes: Pimelodidae). *Copeia*, 166-171.
- Ferrer, J., & Malabarba, L. R. (2011). A new *Trichomycterus* lacking pelvic fins and pelvic girdle with a very restricted range in southern Brazil (Siluriformes: Trichomycteridae). *Zootaxa*, 2912, 59-67.
- Guisande, C., Vari, P. R., Heine, J., García-Roselló, E., González-Dacosta, J., Perez-Schofield, G. J. B., González-Vilas, L., & Pelayo-Villamil, P. (2016). VARSEDIG: an algorithm for morphometric characters selection and statistical validation in morphological taxonomy *Zootaxa*, 4162 (3), 571–580.
- Lanfear, R., Calcott, B., Ho, S. Y. W., & Guindon, S. (2012). PartitionFinder: combined selection of partitioning schemes and substitution models for phylogenetic analyses. *Molecular Biology and Evolution*, 29, 1695–1701.
- Leigh, J.W., & Bryant, D. (2015). Monte Carlo strategies for selecting parameter values in simulation experiments. *Systematic Biology*, 64 (5), 741–751.
<http://dx.doi.org/10.1093/sysbio/syv030>
- Librado, P., & Rozas, J. (2009), DnaSP v5: a software for comprehensive analysis of DNA polymorphism data. *Bioinformatics*, 25, 1451–1452.
- Lundberg, J.G., Bornbusch, A.H., & Mago-Leccia, F. (1991). *Gladioglanis conquistador* n. sp., from Ecuador with diagnoses of the subfamilies Rhamdiinae Bleeker and Pseudopimelodinae n. subf. (Siluriformes, Pimelodidae). *Copeia*, 1991(1), 190–209.
- Lundberg, J. G., & L. A. McDade. (1986). On the South American catfish *Brachyrhamdia imitator* Myers (Siluriformes, Pimelodidae), with phylogenetic evidence for a large intrafamilial lineage. *Notulae Naturae*, 463: 1-24.
- Malabarba, L.R., Fialho, C.B., Anza, J.A., Santos, J.F. & Mendes, G.N. (2009). Peixes. In: Boldrini, I.I. (Org.), Biodiversidade dos Campos do Planalto das Araucárias. Ministério do Meio Ambiente, Brasília, pp. 131–156.
- Mees, G.F. (1974). The Auchenipteridae and Pimelodidae of Suriname (Pisces, Nematognathi). *Zoologische Verhandelingen (Leiden)*, 132, 1-256, Pls. 1-15.

- Miller, M. A., Pfeiffer, W., & Schwartz, T. (2010). Creating the CIPRES Science Gateway for inference of large phylogenetic trees. In *Gateway Computing Environments Workshop (GCE), 2010* (pp. 1-8).
- Miquelarena, A. M., Menni, R. C., Lopez, H. L., & Casciotta, J. R. (1990). Ichthyological and limnological observations on the Sali river basin(Tucuman, Argentina). *Ichthyological exploration of freshwaters. Munchen*, 1(3), 269-278.
- Pons, J., Barraclough, T. G., Gomez-Zurita, J., Cardoso, A., Duran, D. P., Hazell, S., Kamoun, S., Sumlin, W. D. & Vogler, A. P. (2006). Sequence-based species delimitation for the DNA taxonomy of undescribed insects. *Systematic Biology*, 55, 595–609.
- Rambaut, A., Suchard, M.A., Xie, D., & Drummond, A.J. (2013). Tracer v1.6.
- Rambaut, A., & Drummond, A.J. (2013). Tree Annotator, Version 1.7.5.
- Reis, R. E., Lucena, Z. M. S., Lucena, C. A., & Malabarba, L. R. (2003). Peixes. In: Fontana, C. S., Bencke, G. A., & Reis, R. E (Eds.). *Livro Vermelho da Fauna Ameaçada de Extinção no Rio Grande do Sul. Porto Alegre*, Edipucrs, pp. 117–145.
- Reis, R. E., (2017). Unexpectedly high diversity in a small basin: A taxonomic revision of *Eurycheilichthys* (Siluriformes: Loricariidae), with descriptions of seven new species. *Neotropical Ichthyology*, 15(1).
- Reichel, M. (1927). Étude anatomique du *Phreatobius cisternarum* Goeldi, silure aveugle du Brésil. *Revue Suisse de Zoologie*, 34(16), 285-403.
- Ringuelet, R. A., de Aramburu, A. A., & Aramburu, R. H. (1967). *Los peces argentinos de agua dulce*. La Plata: Comisión de investigación Científica.
- Ronquist, F., & Huelsenbeck, J. P. (2003). MrBayes 3: Bayesian phylogenetic inference under mixed models. *Bioinformatics*, 19(12), 1572-1574.
- Sabaj, M. H. (2016). Standard symbolic codes for institutional resource collections in herpetology and ichthyology: an Online Reference. Version 6.5 (16 August 2016). Electronically accessible at <http://www.asih.org/>, American Society of Ichthyologists and Herpetologists, Washington, DC.
- Schaefer, S. A., & Aquino, A.E. (2000). Postotic laterosensory canal and pterotic branch homology in catfishes. *Journal of Morphology*, 246, 212–227.

- Sherman, G.E., Sutton, T., Blazek, R., Holl, S., Dassau, O., Morely, B., Mitchell, T., & Luthman, L. (2012). Quantum GIS User Guide - Version 1.8 “Wroclaw”. Available from: http://download.osgeo.org/qgis/doc/manual/qgis-1.8.0_user_guide_en.pdf (accessed June 2017).
- Shibatta, O.A., Muriel-Cunha J. & de Pinna M.C.C. (2007). A new subterranean species of *Phreatobius* Goeldi, 1905 (Siluriformes, Incertae sedis) from the Southwestern Amazon basin. *Papéis Avulsos de Zoologia*, 47(17), 191–201.
- Silvergrip, A. M. C. (1996). A systematic revision of the Neotropical catfish genus *Rhamdia* (Teleostei, Pimelodidae). Doctoral dissertation, Thesis in Zoology, Stockholm University, Stockholm).
- Stamatakis, A. (2014). RAxML version 8: a tool for phylogenetic analysis and post-analysis of large phylogenies. *Bioinformatics*, 30(9), 1312-1313.
- Swarça *et al.* (2000) Tamura, K., Stecher, G., Peterson, D., Filipski, A., & Kumar, S. (2013). MEGA6: molecular evolutionary genetics analysis version 6.0. *Molecular Biology and Evolution*, 30, 2725–2759.
- Taylor, W. R., & Van Dyke, G. C. (1985). Revised procedures for staining and clearing small fishes and other vertebrates for bone and cartilage study. *Cybium*, 9: 107-119.
- Zhang, J., Kapli, P., Pavlidis, P., & Stamatakis, A. (2013). A general species delimitation method with applications to phylogenetic placements. *Bioinformatics* 29(22), 2869-2876. DOI:<https://doi.org/10.1093/bioinformatics/btt499>

ANEXOS

Table 1. Morphometric data of *Heptapterus mustelinus*. N = 133. SD = standard deviation. Standard length (SL) is given in millimeters, and the other measurements are expressed in percentage of SL or head length (HL) for subunit of head.

	Min	Max	Mean	SD
Standard length (mm)	37.88	154.62	77.12	-
Percents of Standard Length				
M1-Predorsal distance (1-3)	28.9	38.0	35.1	1.36
M2-Preadipose distance (1-4)	46.0	56.4	52.3	1.91
M3-Prepectoral distance (1-5)	15.6	20.7	17.9	1.04
M4-Prepelvic distance (1-6)	32.3	39.7	36.5	1.33
M5-Preanal distance (1-7)	53.6	65.7	60.9	1.66
M6-Body depth (3-8)	8.9	14.3	11.2	1.12
M7-Caudal peduncle depth (9-10)	3.8	6.4	5.0	0.48
M8-Caudal peduncle length (2-11)	15.1	21.7	17.7	1.43
M9-Body width (37-38)	11.0	17.2	12.8	0.81
M10-Dorsal-fin base length (3-12)	8.2	11.2	9.9	0.63
M11-Anal-fin base length (7-11)	17.8	25.1	21.6	1.49
M12-Unbranched dorsal-fin ray length (3-15)	6.8	11.6	8.8	0.90
M13-Dorsal-fin length (16-17)	8.7	14.5	11.4	1.09
M14-Adipose-fin depth (19-20)	2.3	4.4	3.3	0.44
M15-Adipose-fin base length (4-9)	39.1	52.1	44.9	2.29
M16-Interdorsal distance (4-12)	4.4	11.1	8.4	1.60
M17-Unbranched pectoral-fin ray length (5-18)	5.7	10.3	7.6	0.93
M18-Pectoral-fin length (5-13)	8.4	15.1	11.1	0.99
M19-Pelvic-fin length (6-14)	8.7	15.3	11.4	1.17
M20-Pectoral-pelvic fins distance (5-6)	16.7	23.7	20.0	1.27
M21-Pelvic-anal fins distance (6-7)	21.1	27.9	25.1	1.38
M22-Dorsal-fin insertion-hypural plate (3-2)	61.4	69.7	66.2	1.52
M23-Pelvic-fin insertion-hypural plate (6-2)	59.5	67.6	63.7	1.36
M24-Anal-fin insertion-hypural plate (7-2)	35.8	42.1	39.1	1.56
M25-Head length (1-21)	16.6	22.4	19.3	1.03
Percents of Head Length				
M26-Snout length (1-27)	29.9	45.3	35.5	2.52
M27-Orbital diameter (26-27)	9.5	18.9	12.7	1.73
M28-Head width (39-40)	60.8	71.3	68.5	2.23
M29-Mouth width (41-42)	33.1	48.6	39.5	2.72
M30-Mandibular isthmus-lower lip distance (47-48)	20.0	35.2	23.8	2.52
M31-Mandibular isthmus-upper lip distance (47-1)	19.3	39.8	26.3	3.09
M32-Maxillary barbel length (28-29)	75.5	152.4	107.5	15.98

M33-External mandibular barbel length (43-44)	40.5	88.5	64.6	8.64
M34-Internal mandibular barbel length (45-46)	31.6	66.4	45.9	6.32
M35-Postorbital distance (21-26)	46.0	62.9	52.0	2.74
M36-Interorbital width (30-31)	15.9	29.1	22.8	2.78
M37-Snout-anterior nostril distance (1-32)	6.9	14.0	10.8	1.36
M38-Internostril distance (32-33)	7.8	15.8	10.9	1.67
M39-Posterior nostril-orbit distance (27-33)	3.1	18.2	7.1	2.27
M40-Head depth at supra occipital (22-23)	38.4	52.5	44.8	3.05
M41-Head depth at interorbital (24-25)	25.5	41.8	31.7	2.93
M42-Head width at posterior nostril (35-36)	46.2	64.6	52.1	2.83
M43-Dorsal Head length (1-34)	84.5	99.7	92.2	3.56

Table 2. Morphometric data of *Heptapterus* sp.n. A. Range includes holotype, n=30. SD=standard deviation. Standard length (SL) is given in millimeters, and the other measurements are expressed in percentage of SL or head length (HL) for subunit of head.

	Holotype	Min	Max	Mean	SD
Standard length (mm)	106.91	55.49	137.97	95.91	-
Percents of Standard Length					
M1-Predorsal distance (1-3)	38.5	33.3	39.4	36.9	1.34
M2-Preadipose distance (1-4)	55.8	50.2	56.5	52.9	1.59
M3-Prepectoral distance (1-5)	18.8	17.2	21.2	19.2	1.01
M4-Prepelvic distance (1-6)	37.4	34.7	39.7	37.7	1.21
M5-Preanal distance (1-7)	61.2	57.6	66.1	61.2	1.73
M6-Body depth (3-8)	13.8	9.5	13.9	11.9	0.99
M7-Caudal peduncle depth (9-10)	5.9	5.1	6.1	5.6	0.34
M8-Caudal peduncle length (2-11)	17.0	15.0	19.7	17.2	1.27
M9-Body width (37-38)	15.2	12.8	15.2	14.0	0.53
M10-Dorsal-fin base length (3-12)	10.9	8.6	11.3	9.6	0.63
M11-Anal-fin base length (7-11)	22.9	17.9	24.5	21.9	1.67
M12-Unbranched dorsal-fin ray length (3-15)	8.2	6.3	10.0	8.3	1.04
M13-Dorsal-fin length (16-17)	10.3	8.1	12.8	10.4	1.00
M14-Adipose-fin depth (19-20)	2.9	2.6	4.1	3.1	0.35
M15-Adipose-fin base length (4-9)	42.7	40.9	46.0	43.7	1.50
M16-Interdorsal distance (4-12)	8.2	5.6	11.3	7.7	1.30
M17-Unbranched pectoral-fin ray length (5-18)	7.1	6.1	9.5	7.4	0.87
M18-Pectoral-fin length (5-13)	9.5	8.3	13.0	10.6	1.14
M19-Pelvic-fin length (6-14)	9.9	8.7	14.6	11.2	1.32
M20-Pectoral-pelvic fins distance (5-6)	21.6	18.4	22.1	20.2	0.96
M21-Pelvic-anal fins distance (6-7)	23.2	21.4	26.6	23.8	1.19
M22-Dorsal-fin insertion-hypural plate (3-2)	66.1	63.2	68.7	65.2	1.30
M23-Pelvic-fin insertion-hypural plate (6-2)	62.3	60.1	65.2	62.4	1.12
M24-Anal-fin insertion-hypural plate (7-2)	40.3	34.9	42.7	39.2	1.63
M25-Head length (1-21)	20.5	17.9	22.5	20.5	1.16
Percents of Head Length					
M26-Snout length (1-27)	34.9	33.4	39.0	36.2	1.62
M27-Orbital diameter (26-27)	10.5	9.9	13.3	11.7	0.90
M28-Head width (39-40)	78.0	71.9	81.1	74.6	2.69
M29-Mouth width (41-42)	43.0	39.3	47.7	43.0	2.46
M30-Mandibular isthmus-lower lip distance (47-48)	22.2	20.6	25.6	22.6	1.26
M31-Mandibular isthmus-upper lip distance (47-1)	23.6	22.2	28.2	24.7	1.58
M32-Maxillary barbel length (28-29)	90.3	87.9	123.7	100.3	10.88

M33-External mandibular barbel length (43-44)	55.4	49.7	104.4	68.1	12.44
M34-Internal mandibular barbel length (45-46)	41.5	40.6	70.2	49.5	8.33
M35-Postorbital distance (21-26)	54.6	51.1	55.7	53.0	1.12
M36-Interorbital width (30-31)	21.7	17.3	25.0	21.5	1.98
M37-Snout-anterior nostril distance (1-32)	14.2	10.0	15.6	12.5	1.22
M38-Internostri distance (32-33)	9.1	8.6	11.0	9.8	0.65
M39-Posterior nostril-orbit distance (27-33)	7.1	5.9	8.7	7.2	0.71
M40-Head depth at supra occipital (22-23)	47.3	42.1	50.5	45.4	2.00
M41-Head depth at interorbital (24-25)	31.7	27.0	36.9	31.7	2.53
M42-Head width at posterior nostril (35-36)	57.4	50.3	64.4	56.3	3.76
M43-Dorsal head length (1-34)	95.8	89.6	108.3	94.6	3.80

Table 3. Morphometric data of *Heptapterus* sp.n. B. Range includes holotype (H), n=30. SD=standard deviation. Standard length (SL) is given in millimeters, and the other measurements are expressed in percentage of SL or head length (HL) for subunits of head.

	Holotype	Min	Max	Mean	SD
Standard length (mm) (1-2)	64.0	48.0	73.6	60.0	-
Percents of Standard Length					
M1-Predorsal distance (1-3)	34.9	32.5	37.7	35.1	1.4
M2-Preadipose distance (1-4)	54.0	51.0	56.3	53.5	1.6
M3-Prepectoral distance (1-5)	17.8	16.3	19.4	18.0	0.8
M4-Prepelvic distance (1-6)	35.1	34.1	38.2	36.4	1.1
M5-Preanal distance (1-7)	59.5	57.4	64.5	61.4	1.7
M6-Body depth (3-8)	8.9	7.4	10.5	8.9	0.7
M7-Caudal peduncle depth (9-10)	5.1	4.2	5.3	4.8	0.3
M8-Caudal peduncle length (2-11)	17.2	14.4	20.3	16.7	1.3
M9-Body width (37-38)	11.4	10.6	12.6	11.8	0.6
M10-Dorsal-fin base length (3-12)	10.2	9.5	11.8	10.7	0.4
M11-Anal-fin base length (7-11)	24.5	20.1	24.8	22.8	1.1
M12-Unbranched dorsal-fin ray length (3-15)	8.5	7.1	9.4	8.6	0.5
M13-Dorsal-fin length (16-17)	10.4	9.2	12.6	10.7	0.8
M14-Adipose-fin depth (19-20)	2.5	2.5	3.6	2.9	0.2
M15-Adipose-fin base length (4-9)	45.6	40.7	48.4	43.7	1.9
M16-Interdorsal distance (4-12)	8.7	6.1	10.8	8.4	0.8
M17-Unbranched pectoral-fin ray length (5-18)	8.8	7.1	9.5	8.3	0.5
M18-Pectoral-fin length (5-13)	12.1	10.3	12.9	11.9	0.5
M19-Pelvic-fin length (6-14)	12.3	10.9	13.3	12.3	0.7
M20-Pectoral-pelvic fins distance (5-6)	19.2	17.1	21.1	19.3	1.0
M21-Pelvic-anal fins distance (6-7)	25.3	23.2	26.7	25.0	0.9
M22-Dorsal-fin insertion-hypural plate (3-2)	67.8	63.1	69.2	66.3	1.4
M23-Pelvic-fin insertion-hypural plate (6-2)	66.1	61.1	66.9	64.2	1.3
M24-Anal-fin insertion-hypural plate (7-2)	39.3	37.1	42.2	39.4	1.4
M25-Head length (1-21)	18.5	17.7	21.1	19.3	0.8
Percents of Head Length					
M26-Snout length (1-27)	32.5	29.3	39.5	32.6	2.1
M27-Orbital diameter (26-27)	10.5	8.4	12.8	10.8	0.9
M28-Head width (39-40)	63.7	57.5	64.6	61.4	1.9
M29-Mouth width (41-42)	37.9	32.9	41.7	37.0	2.0
M30-Mandibular isthmus-lower lip distance (47-48)	20.7	16.2	23.5	20.2	1.7

M31-Mandibular isthmus-upper lip distance (47-1)	21.5	16.5	24.9	20.9	1.8
M32-Maxillary barbel length (28-29)	93.1	87.6	115.5	100.6	7.2
M33-External mandibular barbel length (43-44)	50.2	41.5	69.8	54.6	5.7
M34-Internal mandibular barbel length (45-46)	34.2	30.0	47.8	38.7	3.6
M35-Postorbital distance (21-26)	52.0	50.1	54.7	52.6	1.4
M36-Interorbital width (30-31)	19.3	15.5	21.0	17.9	1.7
M37-Snout-anterior nostril distance (1-32)	10.3	7.0	11.4	10.2	0.9
M38-Internostril distance (32-33)	7.5	7.3	9.4	8.4	0.7
M39-Posterior nostril-orbit distance (27-33)	4.9	3.9	7.5	5.9	1.1
M40-Head depth at supra occipital (22-23)	38.6	32.2	41.8	37.7	2.4
M41-Head depth at interorbital (24-25)	28.0	23.7	29.9	26.1	1.7
M42-Head width at posterior nostril (35-36)	52.4	44.8	53.0	47.7	2.3
M43-Dorsal Head length (1-34)	96.0	87.5	98.2	92.9	2.9

Table 4. Pairwise K2P genetic distance values for mtDNA Cytochrome Oxidase C subunit 1 gene (*COI*) sequences among *Heptapterus* sp.n. A, *Heptapterus* sp.n. B and *H. mustelinus* populations from the rio Maquiné (MAQ); rio Negro (NEG); laguna dos Patos drainage comprising the rio Camaquã (CAM), rio Jacuí (JAC), rio Jaguarão (JAG), and rio Taquari (TAQ); and rio Uruguay drainage comprising the rio Ibicuí (IBI), rio Ijuí (IJU), rio Quaraí (QUA), and upper rio Uruguai (AUR). Bold = values greater than 2%.

	1	2	3	4	5	6	7	8	9	10	11	12	13	14	15	16	17	18	19	20	21	22	23	24	25	26	27		
1- <i>H. mustelinus</i> (AUR1)	0.0																												
2- <i>H. mustelinus</i> (AUR2)	0.0	0.0																											
3- <i>H. mustelinus</i> (IJU1)	0.5	0.5	0.0																										
4- <i>H. mustelinus</i> (IBI1)	0.8	0.8	0.7	0.0																									
5- <i>H. mustelinus</i> (QUA1)	0.5	0.5	0.7	0.7	0.0																								
6- <i>H. mustelinus</i> (QUA2)	0.5	0.5	0.7	0.7	0.0	0.0																							
7- <i>H. mustelinus</i> (NEG1)	0.2	0.2	0.3	0.7	0.3	0.3	0.0	0.0																					
8- <i>H. mustelinus</i> (NEG2)	0.2	0.2	0.3	0.7	0.3	0.3	0.0	0.0	0.0																				
9- <i>H. mustelinus</i> (NEG3)	0.2	0.2	0.3	0.7	0.3	0.3	0.0	0.0	0.0	0.0																			
10- <i>H. mustelinus</i> (TAQ1)	0.3	0.3	0.5	0.8	0.5	0.5	0.2	0.2	0.2	0.2	0.0																		
11- <i>H. mustelinus</i> (JAC1)	0.3	0.3	0.5	0.8	0.5	0.5	0.2	0.2	0.2	0.2	0.3	0.0																	
12- <i>H. mustelinus</i> (JAC2)	0.3	0.3	0.5	0.8	0.5	0.5	0.2	0.2	0.2	0.2	0.3	0.0	0.0																
13- <i>H. mustelinus</i> (JAC3)	0.3	0.3	0.5	0.8	0.5	0.5	0.2	0.2	0.2	0.2	0.3	0.0	0.0	0.0															
14- <i>H. mustelinus</i> (CAM1)	0.3	0.3	0.5	0.8	0.5	0.5	0.2	0.2	0.2	0.2	0.3	0.3	0.3	0.3	0.0														
15- <i>H. mustelinus</i> (CAM2)	0.3	0.3	0.5	0.8	0.5	0.5	0.2	0.2	0.2	0.2	0.3	0.3	0.3	0.3	0.0	0.0													
16- <i>H. mustelinus</i> (JAG1)	0.5	0.5	1.0	1.4	1.0	1.0	0.7	0.7	0.7	0.8	0.8	0.8	0.8	0.8	0.5	0.5	0.0												
17- <i>H. mustelinus</i> (JAG2)	0.5	0.5	1.0	1.4	1.0	1.0	0.7	0.7	0.7	0.8	0.8	0.8	0.8	0.8	0.5	0.5	0.0	0.0											
18- <i>H. mustelinus</i> (MAQ1)	0.2	0.2	0.3	0.7	0.3	0.3	0.0	0.0	0.0	0.2	0.2	0.2	0.2	0.2	0.2	0.7	0.7	0.0	0.0										
19- <i>H. mustelinus</i> (MAQ2)	0.2	0.2	0.3	0.7	0.3	0.3	0.0	0.0	0.0	0.2	0.2	0.2	0.2	0.2	0.2	0.7	0.7	0.0	0.0										
20- <i>H. mustelinus</i> (MAM1)	1.2	1.2	1.0	0.7	1.4	1.4	1.0	1.0	1.0	1.2	1.2	1.2	1.2	1.2	1.4	1.4	1.0	1.0	0.0										
21- <i>Heptapterus</i> (MAM2)	1.0	1.0	0.8	0.5	1.2	1.2	0.8	0.8	0.8	1.0	1.0	1.0	1.0	1.0	1.0	1.2	1.2	0.8	0.8	0.2	0.0								
22- <i>Heptapterus</i> sp.n. A	2.9	2.9	2.8	2.4	3.1	3.1	2.8	2.8	2.8	2.9	2.9	2.9	2.9	2.6	2.6	3.1	3.1	2.8	2.8	2.2	2.2	0.0							
23- <i>Heptapterus</i> sp.n. A	2.9	2.9	2.8	2.4	3.1	3.1	2.8	2.8	2.8	2.9	2.9	2.9	2.9	2.6	2.6	3.1	3.1	2.8	2.8	2.2	2.2	0.0	0.0						
24- <i>Heptapterus</i> sp.n. B	4.9	4.9	4.7	4.7	5.1	5.1	4.7	4.7	4.7	4.9	4.9	4.9	4.9	4.5	4.5	4.7	4.7	4.7	4.7	4.2	4.2	4.0	4.0	0.0					
25- <i>Heptapterus</i> sp.n. B	5.1	5.1	4.9	4.9	5.3	5.3	4.9	4.9	4.9	5.1	5.1	5.1	5.1	4.7	4.7	4.9	4.9	4.9	4.9	4.3	4.3	4.2	4.2	0.5	0.0				
26- <i>Taunayia bifasciata</i>	10.2	10.2	10.0	10.0	10.4	10.4	10.0	10.0	10.0	10.2	10.2	10.2	10.2	9.8	9.8	10.0	10.0	10.0	10.0	9.8	9.6	9.6	11.4	11.5	0.0				
27- <i>Acentronichthys leptos</i>	14.5	14.5	14.3	13.9	14.7	14.7	14.3	14.3	14.3	14.1	14.5	14.5	14.5	14.5	14.5	14.7	14.7	14.3	13.9	13.7	13.9	13.9	15.1	15.3	11.0	0.0			

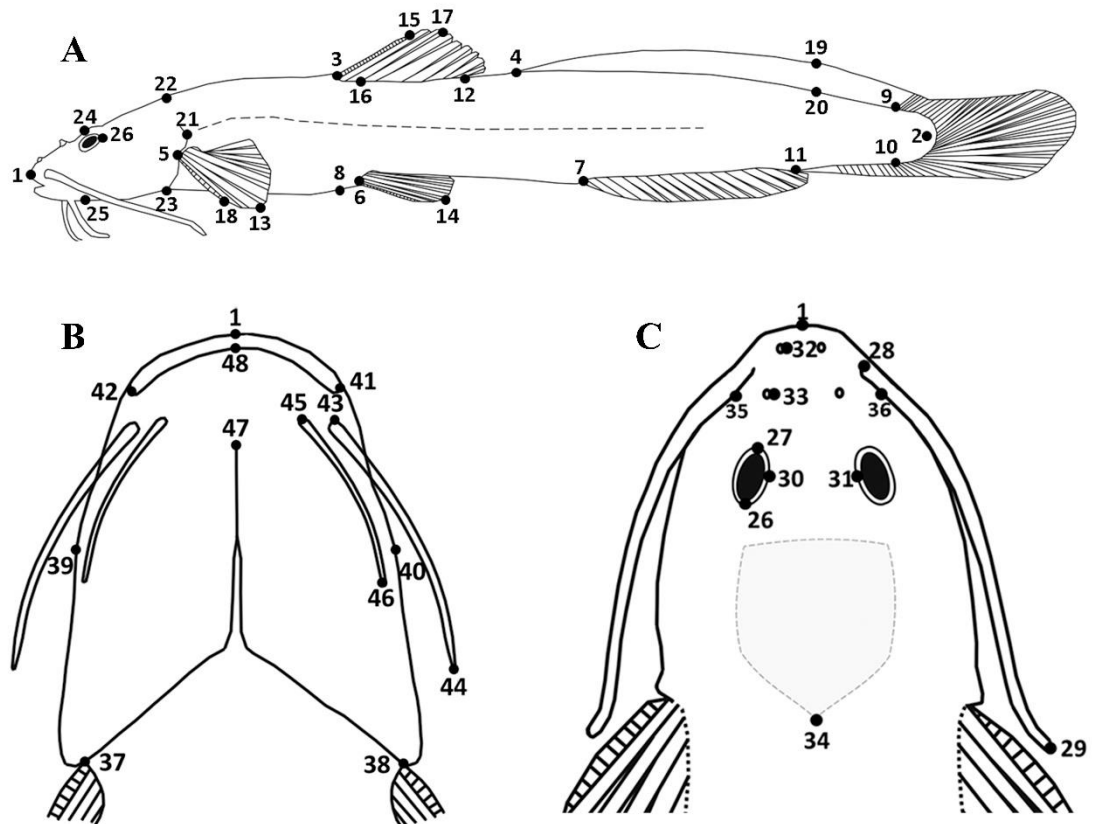


Figure 1. Diagram showing the landmarks used for the measurements described in Table 1. A - Lateral view, B - Ventral view and C - Dorsal view.



Figure 2. *Heptapterus mustelinus* UFRGS 21199, 117.6 mm SL, Brazil, Rio Grande do Sul, São Gabriel, tributary of creek Caibote-Mirim, rio Jacuí drainage, Laguna dos Patos system. **A.** Lateral view, **B.** Dorsal view and **C.** Ventral view. Scale bar = 1 cm.

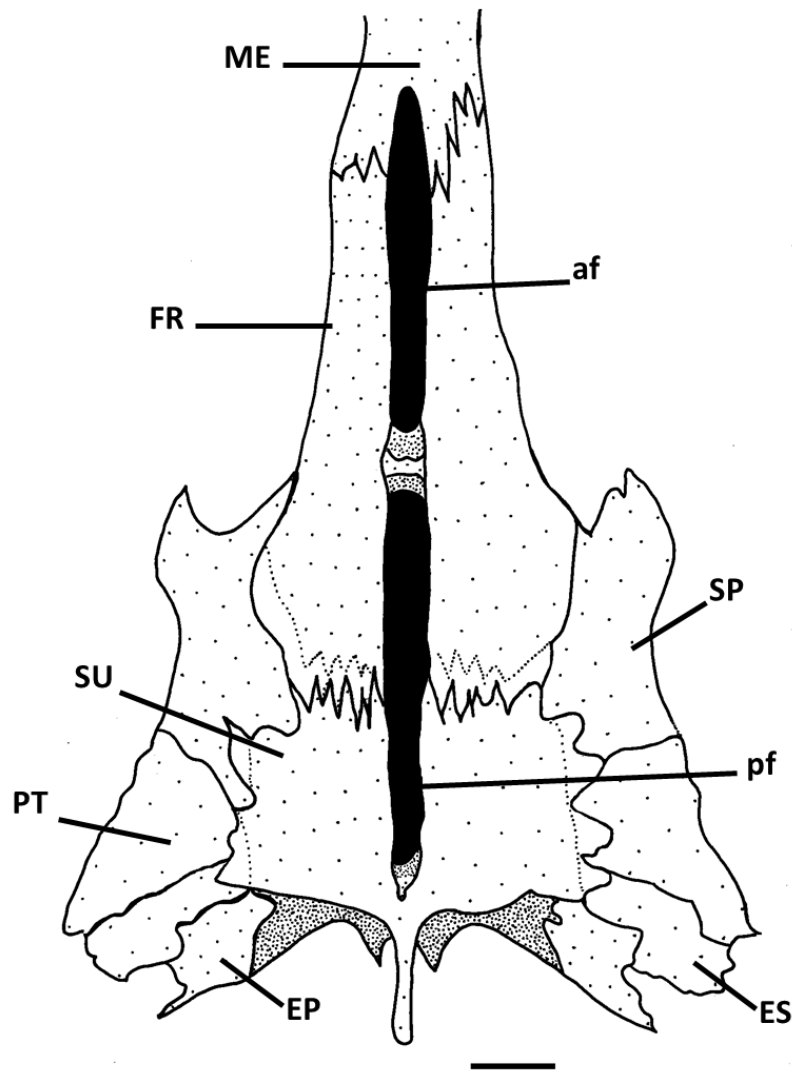


Figure 3. Dorsal view of posterior neurocranium of *Heptapterus mustelinus* UFRGS 21202, 89.2 mm SL. Abbreviations: af, anterior fontanel; FR, frontal; EP, epioccipital; ES, extra-scapular; ME, mesethmoid; pf, posterior cranial fontanel; PT, pterotic; SP, sphenotic; SU, supraoccipital. Scale bar = 1 mm.



Figure 4. *Heptapterus* sp.n. A. UFRGS 22840, holotype, 106.9 mm SL, Brazil, Rio Grande do Sul, Vacaria, creek Passo do Portão, tributary to rio Pelotas, rio Uruguay basin. **A.** Lateral view, **B.** Dorsal view and **C.** Ventral view. Scale bar = 1 cm.

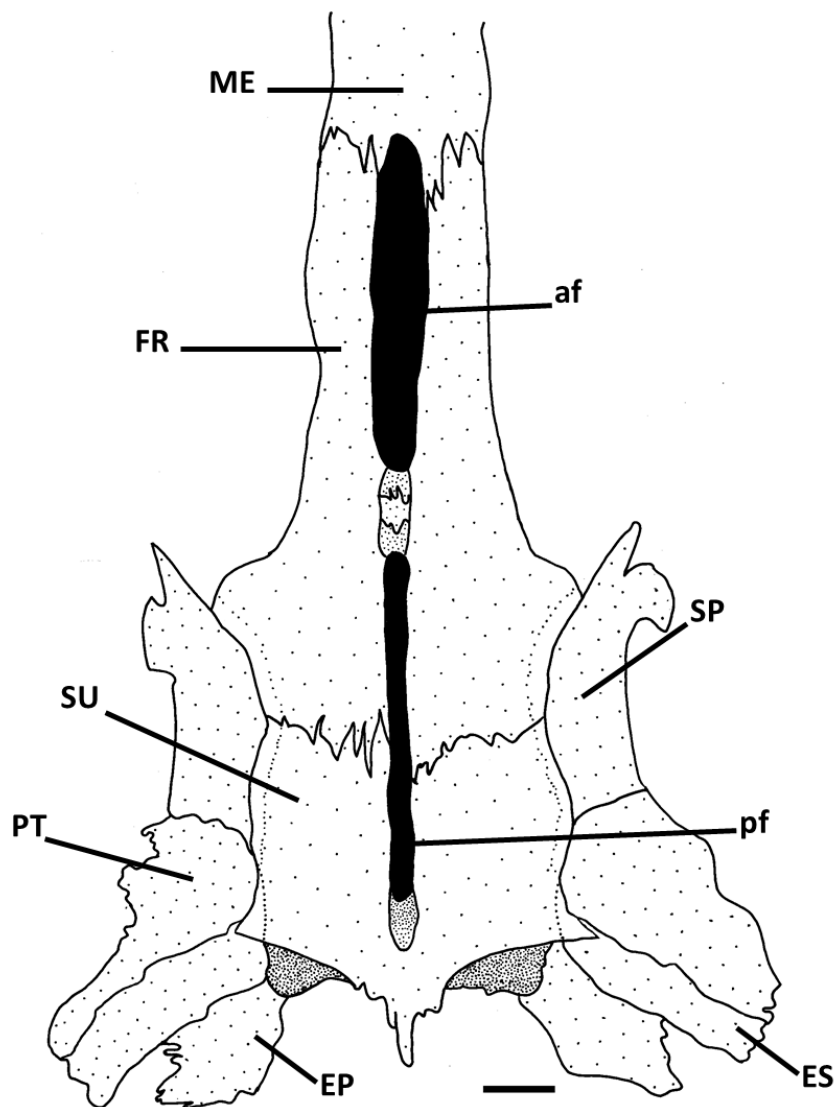


Figure 5. Dorsal view of posterior neurocranium of *Heptapterus* sp.n. A. UFRGS 21105, 114.5 mm SL, paratype. Abbreviations: af, anterior fontanel; EP, epioccipital; ES, extra-scapular; FR, frontal; ME, mesethmoid; pf, posterior cranial fontanel; PT, pterotic; SP, sphenotic; SU, supraoccipital. Scale bar = 1 mm.



Figure 6. *Heptapterus* sp.n. B, holotype, UFRGS 22500, 64.0 mm SL, Brazil, Rio Grande do Sul, Quevedos, Sanga das Tunas, tributary of rio Ibicuí, rio Uruguai drainage. **A** - Lateral view. **B** - Dorsal view and **C** - Ventral view (Scale bar = 1 cm).

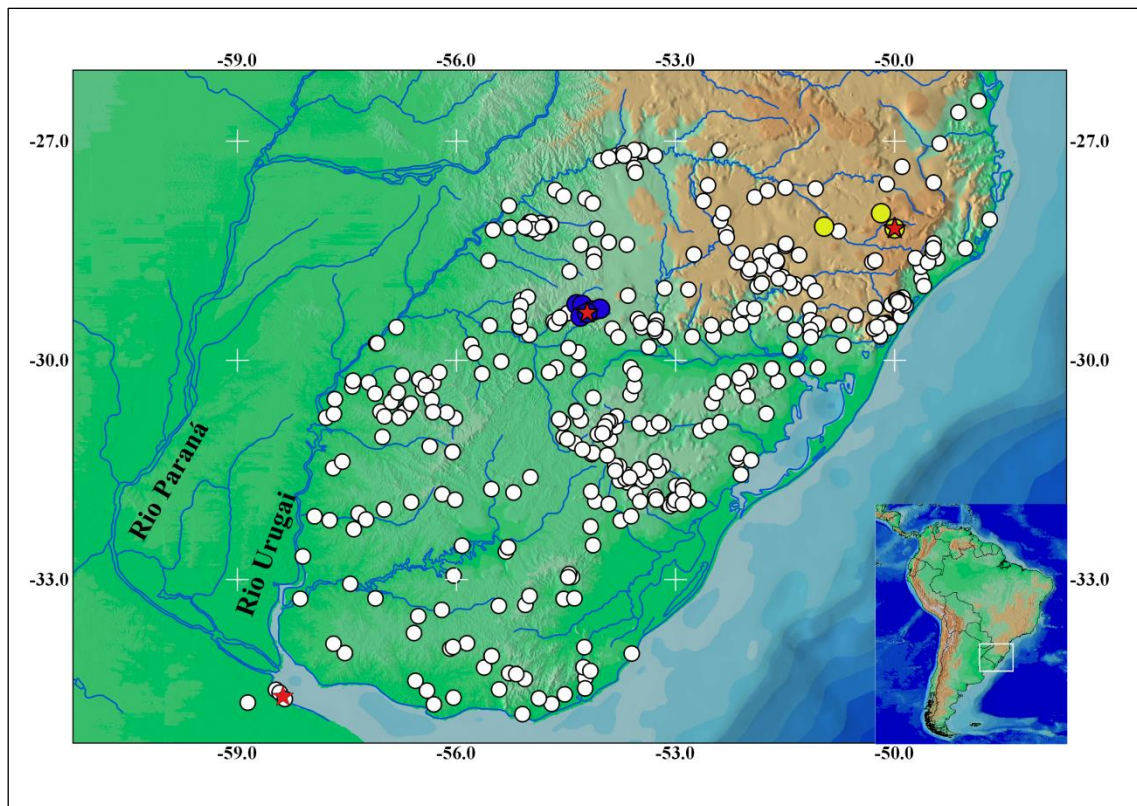


Figure 7. Distribution map of *Heptapterus mustelinus* (white dot). *Heptapterus* sp.n. A (yellow dot). *Heptapterus* sp.n. B (blue dot). Star symbol (red) represents the type locality. Each symbol may represent more than one collection lot.

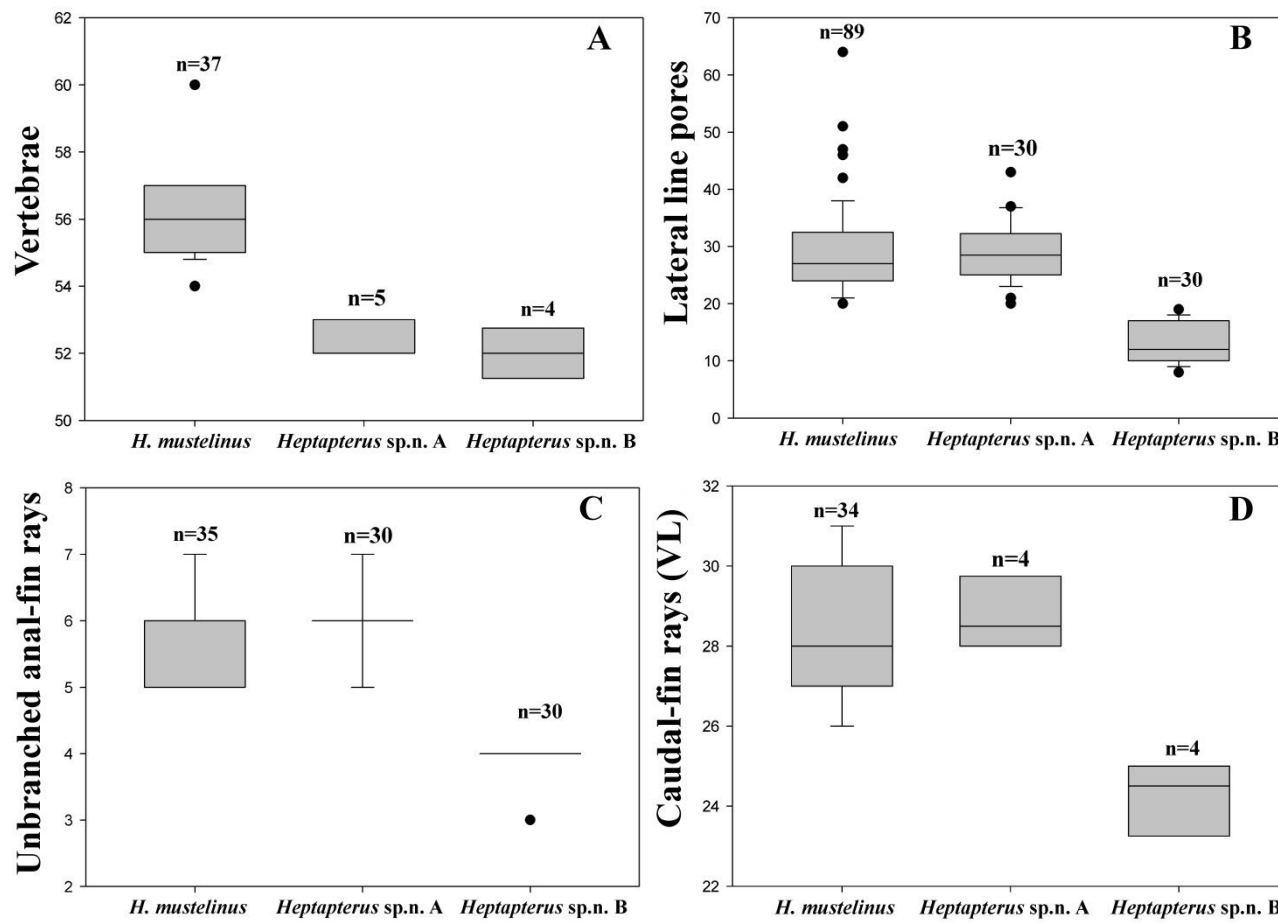


Figure 8. Variation of meristic characters of *Heptapterus mustelinus*, *Heptapterus* sp.n. A and *Heptapterus* sp.n. B. **A** - Number of vertebrae. **B** - Pores in lateral line **C** - Unbranched anal-fin rays. **D** - Caudal fin rays on ventral lobe.

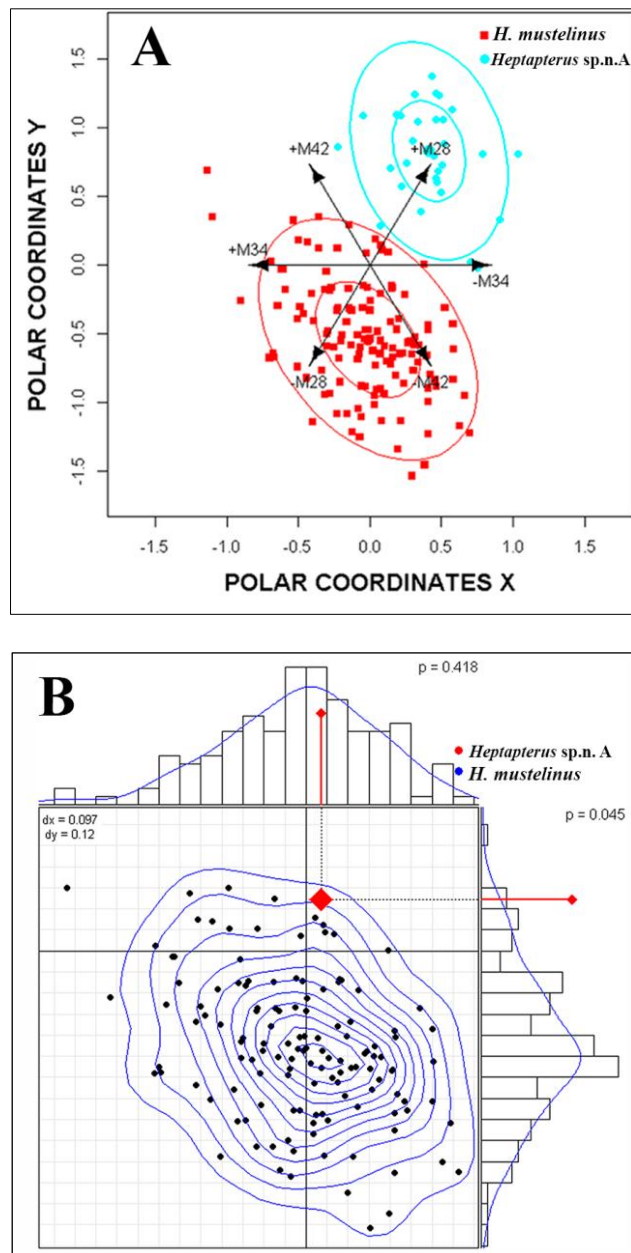


Figure 9. **A** - Scatterplot of the polar coordinates obtained for *Heptapterus mustelinus* (red square) and *Heptapterus* sp.n. A (aqua circle), arrows shows the most significantly. **B** - Bivariate randomization test shows the individual (red point) with a higher probability of belonging to *Heptapterus mustelinus* of all identified like *Heptapterus* sp.n. A.

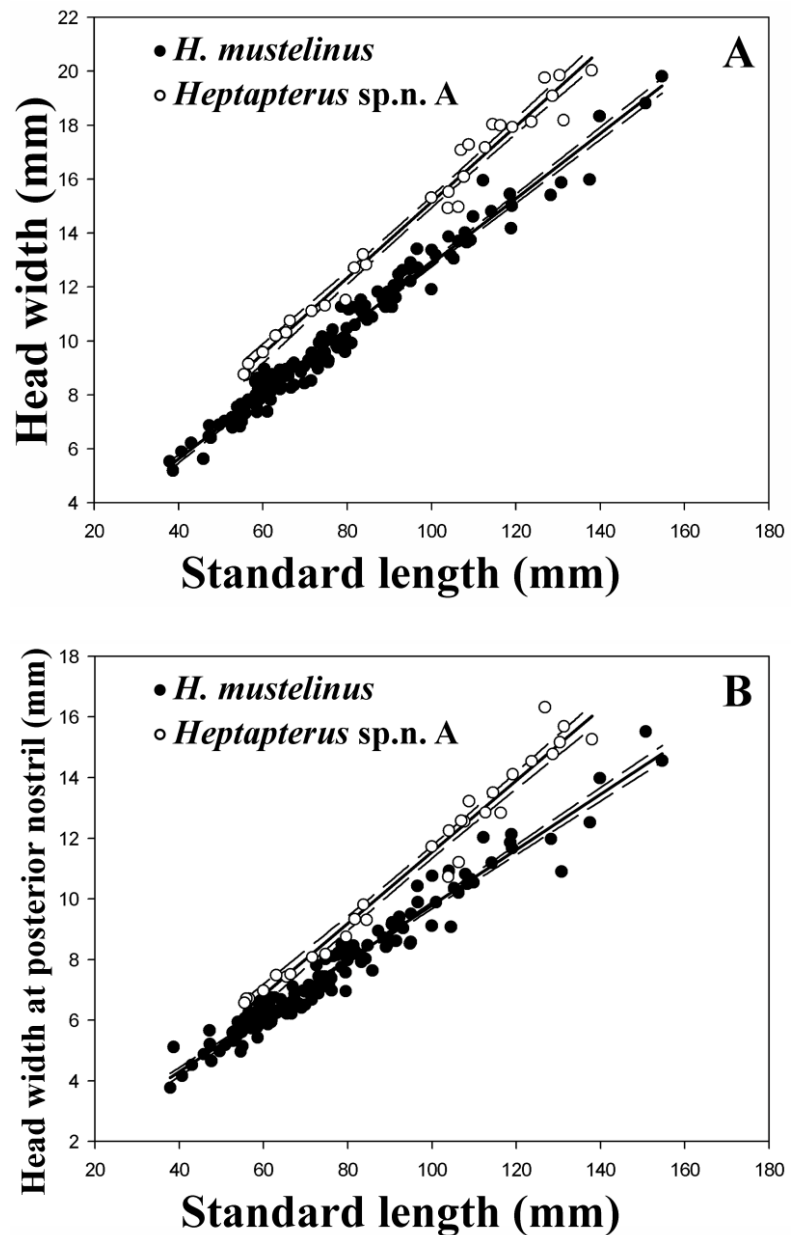


Figure 10. Linear regression of measurements between *Heptapterus mustelinus* (black circle) and *Heptapterus* sp.n. A (white circle). **A** - Head width (M28) vs. standard length **B** - Head width at posterior nostril (M42) vs. standard length Line means trend line.

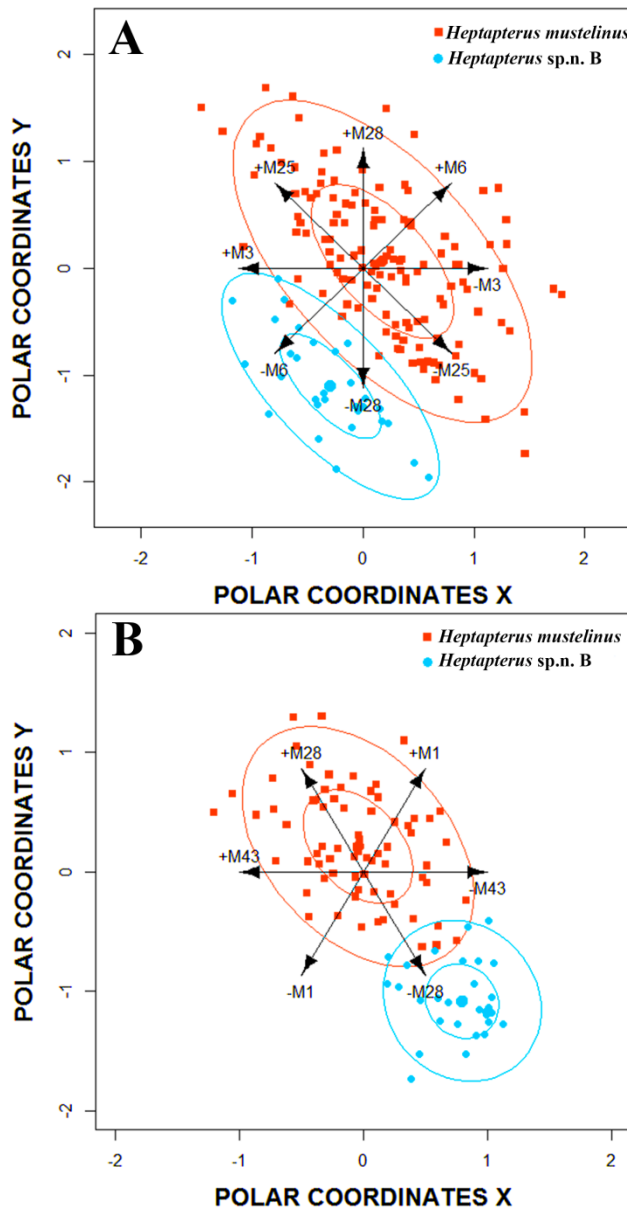


Figure 11. Scatterplot of the polar coordinates obtained for *Heptapterus mustelinus* (red square) and *Heptapterus* sp.n. B (aqua circle). **A** - Using all measured individuals (range size 48.0–73.6 mm SL in *Heptapterus* sp.n. B and 37.9–154.6 mm SL in *H. mustelinus*). **B** – Restricted to individuals of the same range size (48.0–75.0 mm SL). Arrows means most significantly measurements.

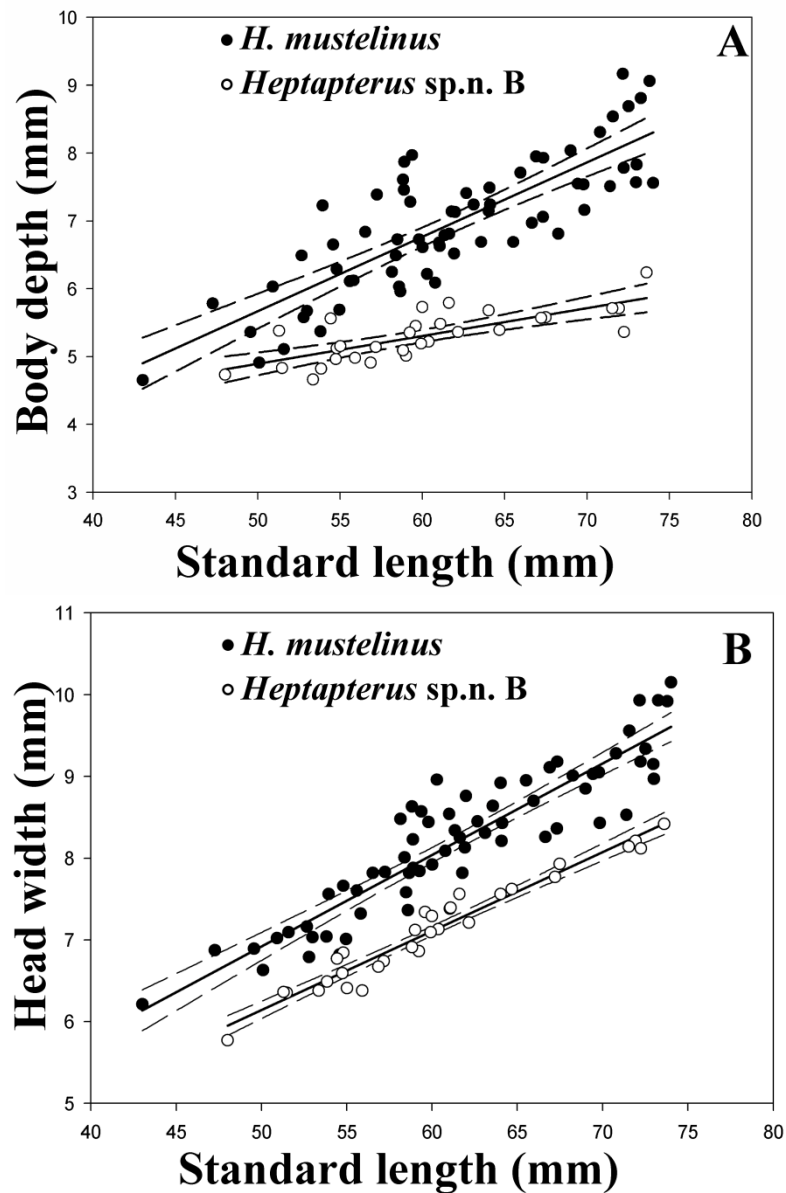


Figure 12. Linear regression of measurements between *Heptapterus mustelinus* (white circle) and *Heptapterus* sp.n. B (black circle). **A** - Body depth (M6) vs. standard length. **B** - Head width (M28) vs. standard length. Using individuals range size of 48.0–74.0mm SL. Line means trend line.

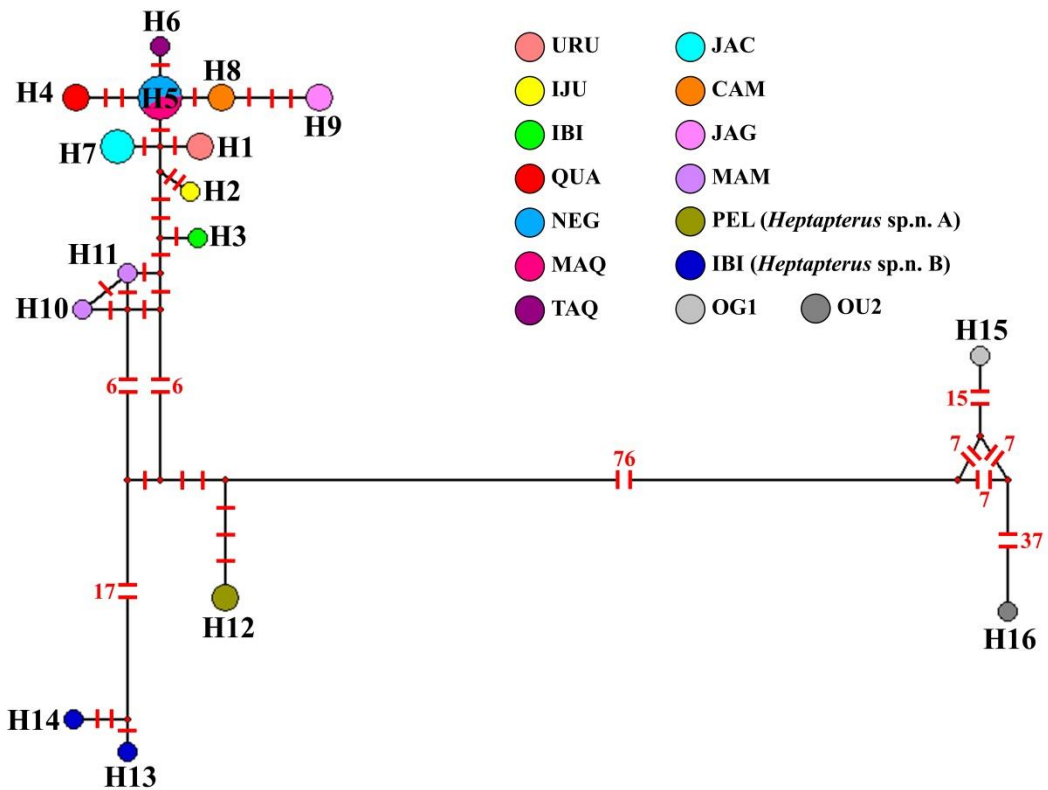


Figure 13. Haplotype network at upper left shows the genetic connectivity of *COI* haplotypes of *Heptapterus mustelinus* (H1–H11), *Heptapterus* sp.n. A (H12) and *Heptapterus* sp.n. B (H13, H14). Each circle represents a unique haplotype with its size proportional to haplotype frequency. Color corresponds to each basin.

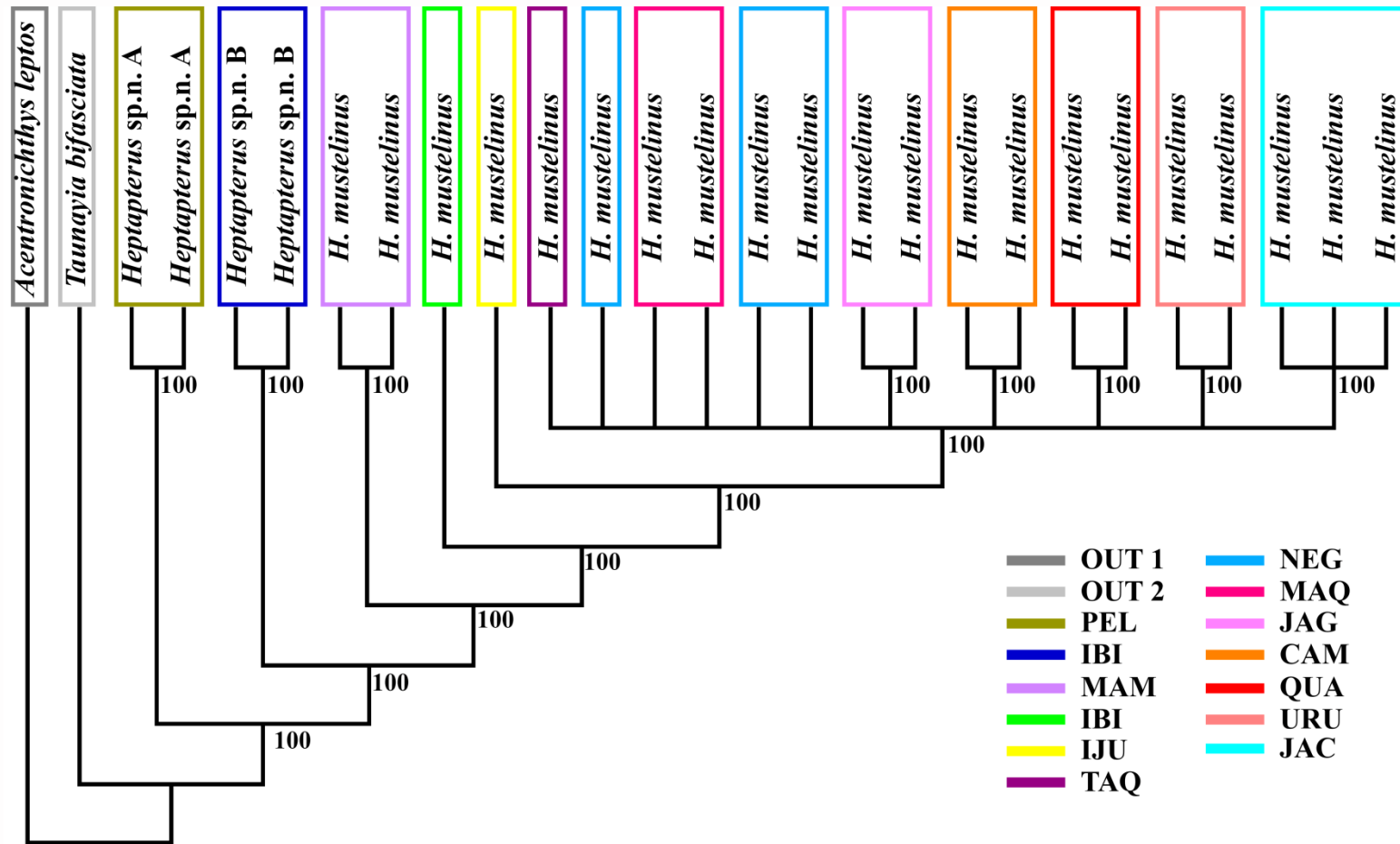


Figure 14. Phylogenetic relationships of *Heptapterus* based on Maximum likelihood analysis of a 1412 base pair alignment consisting of two mitochondrial (*COI* and *CytB*). Node numbers correspond to Maximum Likelihood (ML) support. Color corresponds to each basin.

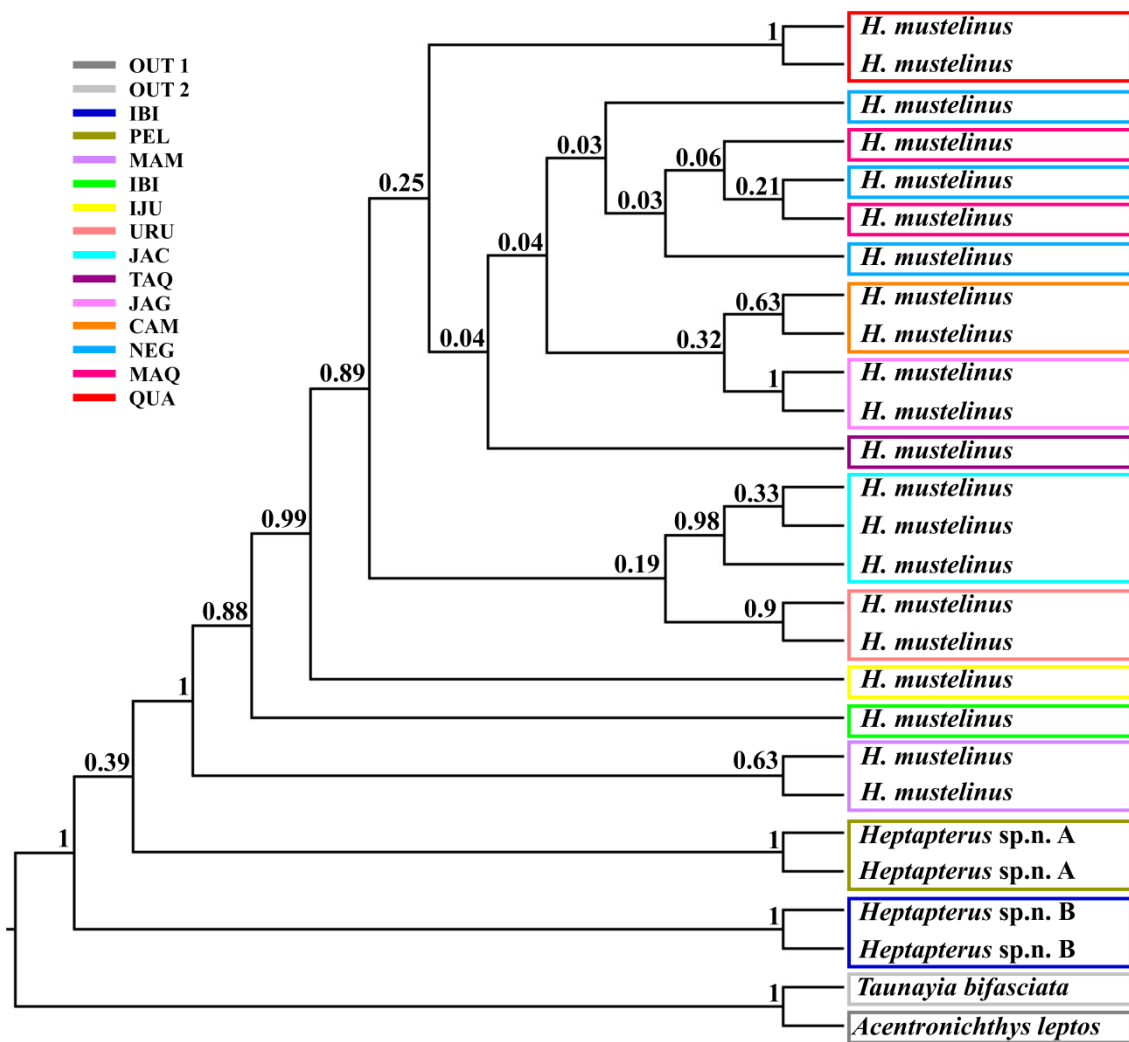


Figure 15. Phylogenetic relationships of *Heptapterus* based on Bayesian analysis of a 1412 base pair alignment consisting of two mitochondrial loci (*COI* and *CytB*). Node numbers correspond to Bayesian posterior probability (BI). Color corresponds to each basin.

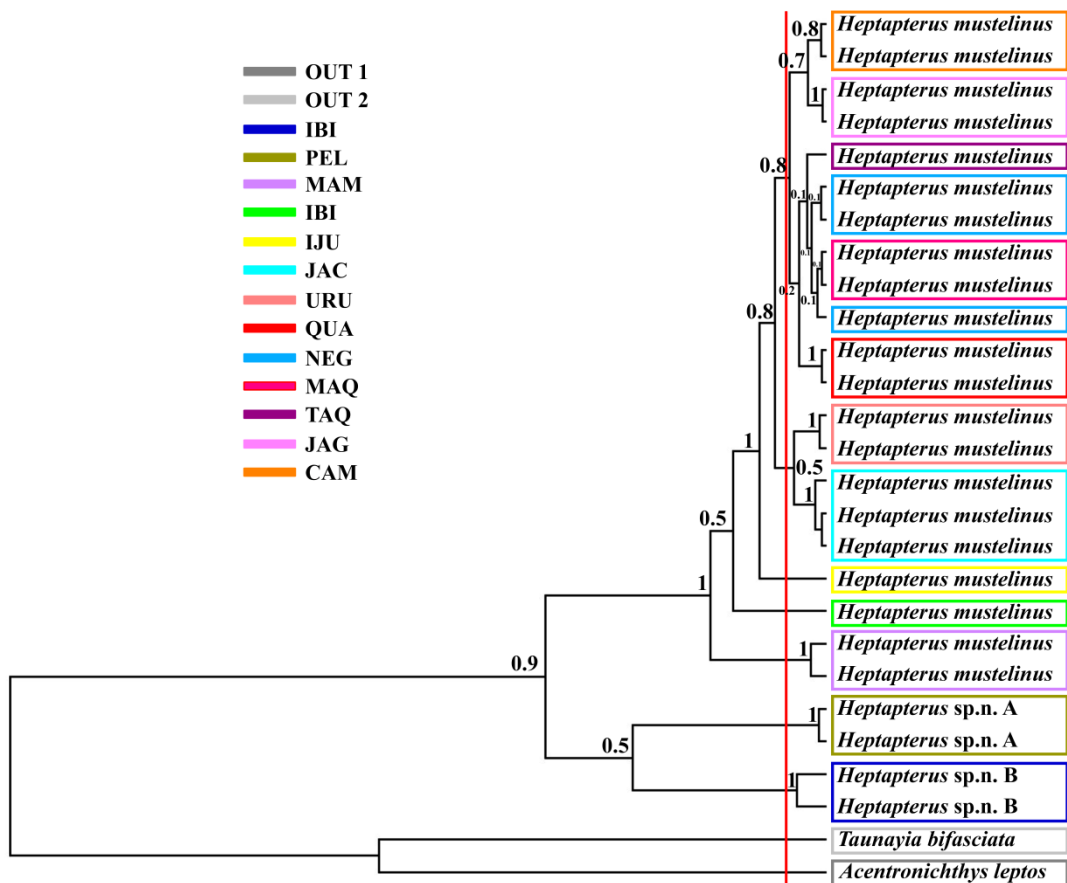


Figure 16. Bayesian phylogenetic tree of *Heptapterus* obtained with mitochondrial (*COI*) loci, rooted in *Taunayia bifasciata* and *Acentronichthys leptos*; the vertical red line shows the coalescent branching process of all sequence, estimated by using the single-threshold model in the GMYC test with Birth-Death speciation models. Color corresponds to each basin.

CONSIDERAÇÕES FINAIS

No presente trabalho foi feita a revisão taxonômica de *Heptapterus mustelinus*, uma espécie com ampla distribuição que vai do río de La Plata, rio Uruguai, Argentina até o sistema da Laguna dos Patos e rios costeiros do sul de Brasil. Duas novas espécies foram descritas, *Heptapterus* sp.n. "A" restrita para o rio Pelotas afluente da parte alta do rio Uruguai e *Heptapterus* sp.n. "B" endêmica de tributários do rio Ibicuí, afluente da parte baixa do rio Uruguai. Os dados morfológicos e moleculares corroboram a diagnose das duas espécies novas de *Heptapterus*. O número de vértebras, além de outros caracteres morfológicos, diagnosticam as espécies novas das populações de *H. mustelinus*.

A análise molecular revelou que *Heptapterus mustelinus* é um complexo de espécies, com populações que apresentam variação molecular, porém não apresentam uma variação morfológica suficiente entre as populações para serem tratados como linhagens diferentes. Estudos filogenéticos dos dados morfológicos e moleculares poderão ajudar a entender a diversidade por trás deste complexo de espécies.

A hipótese da distribuição do gênero para a região sul do Brasil será abordada a partir de uma revisão taxonômica das espécies válidas para o gênero *Heptapterus* mediante análises filogenéticas. Assim como a designação do neótipo para *Heptapterus mustelinus*.

